Spring 2017

Low Temperature Plasma for the Treatment of Epithelial Cancer Cells

Soheila Mohades
Old Dominion University

LOW TEMPERATURE PLASMA FOR THE TREATMENT OF

EPITHELIAL CANCER CELLS

by

Soheila Mohades
B.A. November 2008, University of Shahid Beheshti, Iran
M.S. February 2012, University of Shahid Beheshti, Iran

A Dissertation Submitted to the Faculty of
Old Dominion University in Partial Fulfillment of the
Requirements for the Degree of

DOCTOR OF PHILOSOPHY

ELECTRICAL AND COMPUTER ENGINEERING

OLD DOMINION UNIVERSITY
May 2017

Approved by:

Mounir Laroussi (Director)

Wayne Hynes (Member)

Frederic D. McKenzie (Member)

Sylvain Marsillac (Member)

ABSTRACT

LOW TEMPERATURE PLASMA FOR THE TREATMENT OF EPITHELIAL CANCER CELLS

Soheila Mohades
Old Dominion University, 2017
Director: Dr. Mounir Laroussi

Biomedical applications of low temperature plasmas (LTP) may lead to a paradigm shift in treating various diseases by conducting fundamental research on the effects of LTP on cells, tissues, organisms (plants, insects, and microorganisms). This is a rapidly growing interdisciplinary research field that involves engineering, physics, life sciences, and chemistry to find novel solutions for urgent medical needs. Effects of different LTP sources have shown the anti-tumor properties of plasma exposure; however, there are still many unknowns about the interaction of plasma with eukaryotic cells which must be elucidated in order to evaluate the practical potential of plasma in cancer treatment.

Plasma, the fourth state of matter, is composed of electrons, ions, reactive molecules (radicals and non-radicals), excited species, radiation, and heat. A sufficient dose (time) of plasma exposure can induce death in cancer cells. The plasma pencil is employed to study the anti-tumor properties of this treatment on epithelial cells. The plasma pencil has been previously used for the inactivation of bacteria, destroying amyloid fibrils, and the killing of various cancer cells. Bladder cancer is the 9th leading cause of cancer. In this dissertation, human urinary bladder tissue with the squamous cell carcinoma disease (SCaBER cells) is treated with LTP utilizing two different approaches: direct plasma exposure and Plasma Activated Media (PAM) as an advancement to the treatment. PAM is produced by exposing a liquid cell culture medium to the plasma pencil. Direct LTP treatment of cancer cells indicates a dose-dependent killing effect at post-treatment times. Similarly, PAM treatment shows an anti-cancer effect by inducing substantial cell death. Reactive oxygen species (ROS) and reactive nitrogen species (RNS) have an important role in the biomedical effects of LTP treatment. This study demonstrates the capability of the plasma pencil to transport ROS/RNS into cell culture media leading to their activation. The effectiveness of PAM against SCaBER cells is the highest when it is used immediately after preparation. It is found that

the killing effect of PAM decreases gradually over time, depending on the dose of plasma exposure. Hydrogen peroxide is known as one of the most stable and impactful ROS in biological systems. Measurements show that the plasma pencil generates a significant amount of hydrogen peroxide in PAM. Interestingly, the concentration of hydrogen peroxide in PAM decreases gradually over time, which correlates well with the decrease of PAM effectiveness with storage time. While the effects of PAM treatment on cancerous epithelial cell lines have been studied, much less is known about the interaction of PAM with normal epithelial cells. Effects of PAM on non-cancerous Madin-Darby Canine kidney (MDCK) epithelial cells indicates that MDCK cells are much more robust than SCaBER cells against PAM treatment. The dose of PAM, which causes a widespread death in SCaBER cells, does not significantly impact viability and morphology of MDCK cells. Time-lapse imaging of normal cells shows that PAM treatment inhibits cell proliferation and random migration. In addition, immunofluorescence staining shows that PAM treatment causes a significant reduction in the nuclear localization of proliferation marker, Ki-67, without any damage to the morphological properties of cells including adhesions and cytoskeleton function. This dissertation clearly demonstrates the capability of PAM treatment in inducing death in cancerous cells that can be important for cancer therapy. Hydrogen peroxide is identified as an important ROS responsible for the anti-tumor properties of PAM, although much additional work remains to comprehensively understand all the involved ROS/RNS and their role in PAM treatment.

In loving memory of my grandmother, Delshad Shekarriz (1938-2014).

ACKNOWLEDGMENTS

This dissertation would not have been possible without the guidance and support of many individuals who helped me to the completion of my Ph.D.

First and foremost, I would like to express my deepest gratitude to my advisor, Professor Mounir Laroussi, for his excellent guidance, patience, encouragement throughout this research and writing of this dissertation. I appreciate all his contributions of time, immense knowledge, and support to make my Ph.D. experience productive.

I would like to thank Prof. Wayne Hynes, Prof. Frederic D. McKenzie, and Prof. Sylvain Marsillac for their encouragement and insightful comments as my thesis committee members.

My sincere thanks to Dr. Nazir Barekzi for helping me to develop my background in cell biology and for his generous assistance. I would like to thank Dr. Venkat Maruthamuthu for providing me the opportunity to use the facilities in the Cellular and Multi-cellular Mechanobiology and for his best suggestions and patience.

I would also like to acknowledge the help of past and present colleagues and friends, in particular, Hamid Razavi, for all his kind help, Jessica Sears, Sandeep Dumbali, Mehmet Arda Akman, Yashar Bashirzadeh, Turaj Vazifehdan, Delaram Asadzadeh Totonchi, and Lucas Van Way. Also, I would also like to acknowledge staff in the Biological Sciences Support Facilities at Old Dominion University.

I would like to convey my warmest appreciation to my family for their unfailing love, encouragements, and support throughout my life, to my father, Mahmoud, my mother, Roshanak, and my brothers, Nima and Saman. My deepest appreciation to my colleague and my husband, Hamid, for all his kind help throughout my Ph.D. and for standing by me during the hard times. This dissertation would not have been possible without his support. I dedicate this thesis to the memory of my grandmother, Delshad Shekarriz, for inspiring me to dream big.

TABLE OF CONTENTS

Page

LIST OF TABLES

LIST OF FIGURES

CHAPTER I

INTRODUCTION

I.1   NON-EQUILIBRIUM LOW TEMPERATURE PLASMA

Plasma is known as the fourth state of matter. It is composed of electrons, ions, reactive molecules (radicals and non-radicals), excited species, radiation, and heat. In terms of temperature, plasma can be divided into two regimes: 1. Cold or non-equilibrium and 2. Hot or thermal. In non-equilibrium plasmas, the temperatures of ions and neutrals are close to room temperature while the energy of the electrons is very high. The collisions of the energetic electrons with the molecules of the background gas lead to atomic and molecular dissociation, excitation, and ionization. Since these plasmas are weakly ionized, the gas phase chemistry is maintained without an increase in the gas temperature. Non-equilibrium plasma is often referred to as low-temperature plasma (LTP), or cold plasma, where the gas temperature is close to room temperature. This feature makes non-equilibrium plasma sources attractive for many industrial applications. Material processing, etching, and surface deposition are well-known examples of such applications. Operating at atmospheric pressure and having biologically tolerable temperatures make LTP sources safe to apply to thermally sensitive targets such as cells and tissues. Charged particles, reactive species (radicals and non-radicals), and UV radiations may be implicated in many of the observed biological effects when plasma comes in contact with microorganisms and living tissues. However, mounting experimental evidence has shown that oxygen and nitrogen reactive species play a major role [1-3]. Table 1 shows a list of reactive oxygen species (ROS) and reactive nitrogen species (RNS) [1].

Table 1, A list of various reactive oxygen and nitrogen species [1].

Reactive Oxygen Species (ROS)		Reactive Nitrogen Species (RNS)	
Radicals	**Non-radicals**	**Radicals**	**Non-radicals**
Superoxide, O_2^-	Hydrogen Peroxide, H_2O_2	Nitric oxide, NO	Nitrous acid, HNO_2
Hydroxyl, OH	Ozone, O_3	Nitrogen dioxide, NO_2	Nitrosyl cation, NO^+
Hydroperoxyl, HO_2	Singlet Oxygen, (O_2 1 Dg)	Nitrate radical, NO_3	Nitroxyl anion, NO^-
Singlet, ($^1O_2$)	Organic peroxides, ROOH		Alkyl peroxynitrates, RO_2ONO
Carbon dioxide radical, CO_2^-	Peroxynitrite, $ONOO^-$		Alkyl peroxynitrites, ROONO
Carbonate, CO_3^-	Peroxynitrate, O_2NOO^-		
Peroxyl, RO_2	Peroxynitrous acid, ONOOH		
Alkoxyl, RO	Peroxomonocarbonate, $HOOCO_2^-$		

I.2 BIOMEDICAL APPLICATIONS OF LOW TEMPERATURE PLASMA

I.2.1 Cold Plasma Devices in Biomedical Applications

In the last two decades low temperature plasma has been used in various biological and medical applications ranging from the inactivation of bacteria to wound healing and, more recently, in cancer therapy [4-7]. Many LTP sources have been developed to date and each is utilized for a specific biomedical application [8]. Depending on the desired application the plasma power density, working gas mixture, and configuration of the plasma device can be modified. Following is a brief introduction of some major plasma devices and their applications.

Generally, low temperature plasma devices are categorized into three groups as direct, indirect, and hybrid plasma sources. Dielectric barrier discharge (DBD) and floating electrode dielectric barrier discharge (FE-DBD) are examples of direct plasma sources. FE-DBD device [9] has a similar operation to DBD, except the secondary electrode is the surface of a target tissue or skin. This device was used in some *in vitro* experiments (sterilization) and *in vivo* experiments on animals (wound healing and blood coagulation) [9-11].

Plasma jets, plasma needles, and plasma torches are examples of indirect plasma sources. In such devices plasma is generated inside a chamber and a plume of plasma drifts out of a nozzle through the flow of a feeding gas [12, 13]. The volume of the treated area is small but can be increased by multiplying the number of jets. The concentrations of plasma-generated species in indirect devices are much smaller than in DBDs.

The MicroPlaSter is a microwave driven plasma torch that was used in clinical trials for wound healing. It works with argon gas and an input power of 80-110 W [14]. Experimental results showed the effectiveness of the MicroPlaSter in the inactivation of drug-resistant bacteria and fungi [15, 16].

Another example of indirect plasma devices is atmospheric pressure plasma jets (APPJ). In these devices, plasma can be generated by either one or two electrodes and the working gas is usually helium or argon. The first LTP jet used in biomedical applications was developed by Laroussi and colleagues. This jet device is known as the plasma pencil [17, 18]. The plasma pencil has been used for the inactivation of bacteria and the killing of various cancer cells [17, 19, 20]. Figure 1 shows a photograph of the plasma pencil in operation. In addition to bacterial inactivation, plasma pencil was used in a research to destroy amyloid fibrils. Amyloid fibrils are proteins which are associated with some neurodegenerative diseases such as Alzheimer's and Parkinson's. Results of this research indicated that the plasma treatment induces severe damage to the fibril and causes extensive breakage in the treated proteins [21].

kINPen 09 (INP Greifswald, Germany) is a single electrode APPJ driven by radio-frequency which was applied *in vitro* for skin decontamination [22].
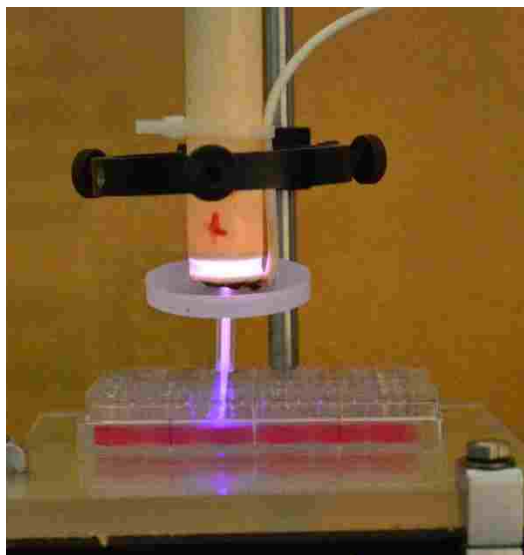
Figure 1. Plasma plume of helium gas launched out of the plasma pencil is in contact with a liquid sample.

One of the most recent designs of LTP sources is a combination of direct and indirect plasma called Surface Micro-Discharge (SMD) or hybrid plasma. It is made of three layers: a dielectric material that is sandwiched between a high voltage electrode and a grounded mesh electrode [23, 24]. The ignited corona discharge surrounds the mesh and gaps between electrodes. This plasma source has advantages of both direct and indirect plasma. Experimental results have demonstrated the effectiveness of this device against highly resistive bacteria and microorganisms. Another example of SMD devices is called self-sterilizing surface (SSS) electrode which is shown in Figure 2 [25].
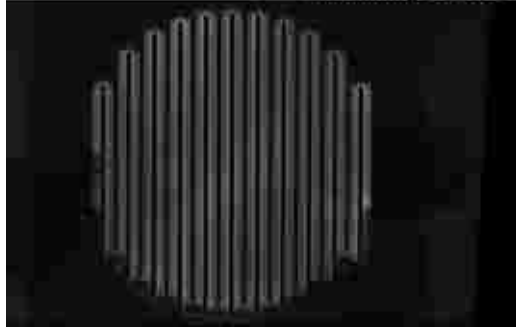
Figure 2. Arrangement of the self-sterilizing surface discharge (Reprint with the permission from the publisher John Wiley and Sons) [25].

Different areas of plasma medicine

The scientific discipline that deals with the biological and medical applications of low temperature plasma is known as Plasma Medicine. Plasma medicine is a novel discipline which includes the following major areas of applications:

- Inactivation of microorganism/pathogens: surface and liquid sterilization, destruction of biofilms, and disinfection of biological tissues
- Dental applications: oral plaque biofilm control, disinfection of root canal, and tooth bleaching.
- Wound healing: stimulation of cell proliferation, angiogenesis, and blood coagulation.
- Cancer therapy

I.3   LOW TEMPERATURE PLASMA FOR CANCER THERAPY

I.3.1   Previous Research on Plasma for Cancer Treatment

Recent investigations showed that low temperature plasma exhibits anti-cancer effects [26]. LTP has been shown to induce cell death in vitro and cell growth arrest leading to tumor reduction in vivo. Several studies showed the capability of LTP treatment to modulate oxidative stress in cancer cells via direct plasma exposure or Plasma Activated Media (PAM).

Stoffel and colleagues studied the effects of cold plasma on eukaryotic cells using what is called the plasma needle [27, 28]. They studied cellular morphology, attachment, and viability at different exposure times and plasma doses. The results on normal vascular and fibroblast cells showed a dose-dependent cell death which is manifested by apoptosis at shorter treatment time and necrosis at longer treatment time. Similar results were reported on non-small cells lung cancer (NSCLC) [29]. According to this research, cell detachment occurred at the area of the direct impact of plasma needle even after a short exposure time but the cells that remained alive could reattached to the surface. Also, the presence of a thin layer of culture media inhibited the cell detachment. They concluded that cell detachment by the plasma needle was the result of a physical process on the cells [30].

Keidar and colleagues [31] treated normal mice fibroblast cells directly by plasma jet while cells were covered with a thin layer of growth media. The results showed that plasma treatment affects cell-surface attachment and cell migration rate depending on the intensity of the plasma treatment [31]. Work on human liver cancer cells showed that the viable cells were detached after plasma jet treatment and were reattached again to the surface after a short period of time [32].

The efficiency of cold plasma treatment against tumor cells grown *in vitro* has been reported on human melanoma [33, 34], breast cancer [35-38], colon/rectum cancer [39-41], liver cancer [42], leukemia [43], brain cancer [44, 45], prostate cancer, [20, 46] and other cancerous cells [18, 26, 47]. Most of the results show a dose-dependent effectiveness of plasma treatment. The cell death mechanism investigations on many cell lines indicated that a lower dose of plasma exposure or shorter time of treatment leads to apoptosis in some types of tumor cells; however, a longer exposure time results in necrosis [34, 48].

Apoptosis or "programmed cell death" is a genetically determined elimination of cells. It is considered as a vital component of various processes such as "normal cell turnover, proper development and functioning of the immune system, hormone-dependent atrophy, embryonic development and chemical-induced cell death" [49]. Necrosis is the alternative to apoptotic cell death and is considered to be a toxic process. In fact, necrosis refers to a degradative process which is associated with inflammation and is usually considered to be a non-desirable mechanism of cell death [49].

In addition to the *in vitro* research, progress in the field continued through *in vivo* experimental trials and the treatment of solid tumors [44, 50]. The first reports were published by [51, 52] on

U87 glioblastoma tumor implanted in mice. This tumor is one of the most aggressive and resistant to radio-therapy and chemotherapy. The results of LTP treatment after five consecutive days showed a significant reduction in the size of the treated tumor and the extension of survival time of mice. Similar results in the size reduction of tumors were reported in [50, 53-55] which were mainly mediated by apoptosis. All *in vivo* experiments indicated that effectiveness of low temperature plasma treatment on destroying cancer cells from different tumor types and implicated that ROS generated by plasma as one of the main active agents in the process. [44].

Plasma Pencil Treatment of Non-adherent Cells

The first study on anti-cancerous effects of the plasma pencil in Laroussi's group was on non-adherent cells. Barekzi and Laroussi studied the effect of direct plasma treatment on the viability of the non-adherent leukemia cancer cells [43]. In this research, the human T-cells (CCL-119; aka CCRF-CEM) with acute lymphoblastic leukemia was used. The cell culture media was RPMI-1640 at neutral balanced pH. A sample of CCRF-CEM cells with a concentration of 1×10^6 cells ml^{-1} was exposed to the plasma pencil and was incubated for subsequent cell viability measurements using trypan blue exclusion assay. The results of cell viability immediately after LTP treatment showed no killing of leukemia cells except for the 10 min treatment time which suggests that a high dose of plasma could cause immediate killing of leukemia cells. However, the results at longer post-treatment time at 12, 36, and 60 h indicated that as the exposure time of plasma increases, the number of dead cells significantly increases. For example, 4 min exposure time had an average percent viability of 22.3% after 12 h post treatment.

A further step towards the understanding of the anti-cancer effect of plasma is to evaluate different cell types and cell lines. Different cells respond differently to the LTP treatment due to their unique morphology, phenotype, function, cell resources, and organ of origin. This research concerns the study of the effects of LTP treatment on the adherent epithelial cells.

Epithelial cells are adherent ones that cover flat surfaces and fill most of the cavities of many organs of the body. Epithelial cells are different in size and shape but all are tightly packed together with almost no intercellular spaces.

I.3.2   Biological Roles of Reactive Oxygen and Nitrogen Species

ROS/RNS or RONS (reactive oxygen and nitrogen species) are well known as disease-associated agents, which interrupt the biochemistry of cells. An increase in the oxidative stress can cause

DNA damage or mutation, lipid peroxidation, and protein oxidation [56]. In nature, ROS and RNS are weapons of the immune system of plants and animals to fight against invasive bacteria, microorganisms, and cancer cells. In particular, ROS are known as mediators of intracellular signaling cascades and its excessive production can lead to oxidative stress, interruption in cell function, and finally cell apoptosis or necrosis [57, 58]. As a result, a balance between oxidant agents and intracellular antioxidant resources is critically important for a proper cell function and regulation [1, 59]. An introduction of most known ROS and RNS and their properties will be discussed in detail in Chapter II.

I.3.3   Conventional Methods in Cancer Therapy

Cancerous tumors are malignant tumors. They are results of abnormal cell division which are invasive and can spread into surrounding tissues or travel to organs far from the original location. Normal cells can stop dividing when they come into contact with the same cell type or go through apoptosis when they are old. This mechanism prevents the abnormal growth in normal cells. In contrast, cancerous cells fail to check and balance such steps to limit cell division. For instance, cancer cells are able to ignore signals of the apoptosis process, which body uses it as a mechanism to discard unneeded cells [60].

There are several types of cancer treatment including chemotherapy, radiation therapy, immunotherapy, and targeted therapy [61]. Radiation therapy is an expensive treatment in which a high dose of x-ray radiation is used to kill cancer cells or to slow down the growth [62]. Radiation therapy not only kills cancer cells but also affects healthy surrounding cells which leads to side effects like fatigue.

Chemotherapy is the use of drugs to stop or to slow growth of cancer cells which proliferate quickly [62]. It not only kills fast-growing cancer cells but also kill normal healthy cells which grow and divide fast such as skin, hair, bone marrow, and blood cells. Damages to healthy cells are the main side effects of chemotherapy such as mouth sores, nausea, and hair loss.

Immunotherapy is a relatively newer type of cancer treatment which is not as widely used as surgery, chemotherapy, and radiation therapy. In this method substances from the immune system such as white blood cells are used to fight against cancer. Immunotherapy drugs are the small molecule or monoclonal antibodies that are designed to mark cancer cells so the immune system will be able to identify and destroy them [63]. The most common side effect of this method is the

skin reaction to the injection area. However, in rare cases, it may cause severe, or even fatal, allergic reactions.

Each therapy method is applicable for a specific type of cancer and it can be combined with one or more methods. Almost all conventional cancer therapies are associated with serious side effects to the patients and can reach a saturation level of their efficacy [61, 64]. More importantly, cancer cells build resistance to these treatments methods leading them to fail to help the patient after an initial benefit. Therefore, new cancer therapies are urgently needed in the fight to cure cancer.

I.4   OUTLINE OF PRESENT RESEARCH

This dissertation is organized as follows. Experimental setup, cell lines, cell cultures, and experiment protocols will be explained in Chapter II. This chapter includes an introduction of direct treatment as the initial approach to treating cancer cells and Plasma Activated Media as advancement to the *in vitro* treatment. PAM is produced by exposing liquid cell culture media to the plasma pencil and it can be as effective as direct plasma treatment in killing cancer cells. PAM protocol is more amenable to characterize the plasma-generated chemical species in media and it widens the scope of our investigations. Therefore, PAM protocol was followed in the experiments presented in this document. To evaluate the effectiveness of PAM over time, aged-PAM will be introduced and its effect on cancer cells will be examined. The concentrations of hydrogen peroxide as an important ROS will be measured at different times after plasma exposure. The relation between the effectiveness of PAM and the concentration of hydrogen peroxide will be analyzed. To understand how plasma treatment affects non-cancerous cells, a normal cell line will be examined. Time-lapse microscopy and immunofluorescence assay will be employed in order to achieve a further characterization of PAM effects on normal cells. Results of the treatment of the cancer cells will be shown in Chapter III. In this chapter, the results of measurement of hydrogen peroxide concentration, apoptosis or necrosis identification, and the effect of plasma treatment on DNA will be shown. In Chapter IV, the effects of PAM treatment on the normal cells will be presented. Moreover, characterization studies on cell motility, proliferation, and morphology of normal cells will be shown. The conclusion and suggestions for future investigations are presented in the last chapter. This research received the Institutional Biosafety Committee (IBC) approval under the title of "Biomedical Use of Cold Plasma".

I.5   CONTRIBUTION OF THIS DISSERTATION

This dissertation explores the anti-cancer properties of plasma activated media and the response of normal epithelial cells to this treatment. A temporal evaluation is conducted on the effectiveness of PAM in the treatment of urinary bladder cancer cells. Mechanisms of cell injury induced by PAM treatment in cancer cells are identified. A correlation between the concentration of hydrogen peroxide in PAM and the anti-cancer effects of PAM is elucidated. Finally, effects of PAM treatment on cell viability, proliferation, and morphology of normal non-cancerous cells are investigated. The data produced in this work and its interpretation are novel and contribute new knowledge to the field of plasma biomedicine.

CHAPTER II

MATERIALS AND EXPERIMENTAL METHODS

II.1 MATERIALS

II.1.1 Plasma Source

The source of plasma used in this research is the plasma pencil. As it is already mentioned, the plasma pencil is a handheld plasma jet device which was developed by Laroussi and colleagues for biomedical applications. It generates plasma moderately low temperature at atmospheric pressure. In this context low temperature, refers to temperatures that are not harmful to biological organisms and tissues. The rotational temperatures of $N_2C\,^3\Pi_u$ derived from optical emission spectroscopy measurement of nitrogen (N_2) at SPS 0-0 band and $\Delta v = -2$ bands was used to determine the gas temperature of the plasma pencil. Depending on the experimental parameters the gas temperature was found to be below 400 K in most cases, which is tolerable for biological cells and tissues [65, 66]. The plasma pencil is made of two ring-shaped copper electrodes embedded in a dielectric cylindrical tube. Each electrode is attached to a surface of centrally perforated alumina (Al_2O_3) disk. The diameter of the disk is 2.5 cm and diameter of the hole at the center is 3 mm. The two disks are set parallel to each other. The gap distance between the two disks varies from 0.3 to 1 cm. The working gas is introduced through a gas inlet at a desired flow rate. Plasma is ignited in the gap by applying repetitive high voltage pulses to one of the electrodes while the second one is grounded and the plasma plume emerges out of the nozzle. Figure 3 shows the schematic of the plasma pencil and the experimental setup.

The high voltage pulse generating system is composed of a high voltage DC power supply (Spellman SL, 1200 Watt maximum power), a high voltage pulse generator (DEI PVX-41, maximum output voltage: 10 kV), and a single channel arbitrary function generator (Tektronix AFG 3021). The flow of the working gas is controlled by a mass flow meter (Bronkhorst High-Tech).

A high voltage pulse generator converts a high voltage DC input into a pulsed output. The function generator controls the width and repetition rate of the pulses. The pulse generator in this setup is capable of producing high voltage pulses up to 10 kV with a repetition rate up to 10 kHz and pulse

width varying from 200 ns to DC. The rise and fall time of the voltage pulse is about 60 ns. The electrical and chemical characterizations of the plasma pencil have been published previously showing the identification of the various reactive species generated in the gas phase by means of optical emission spectroscopy [65, 67-70].

For all experiments in this research, plasma was ignited with the following conditions unless otherwise mentioned: voltage pulse amplitude of 7 kV, frequency of 5.00 kHz, and pulse width of 800 ns. The flow rate of He was 5.0 ± 0.1 slm (the gas velocity was around 3 m s^{-1}). The distance between the nozzle tip and media surface was ~22 mm while the depth of media was ~3 to 4 mm.
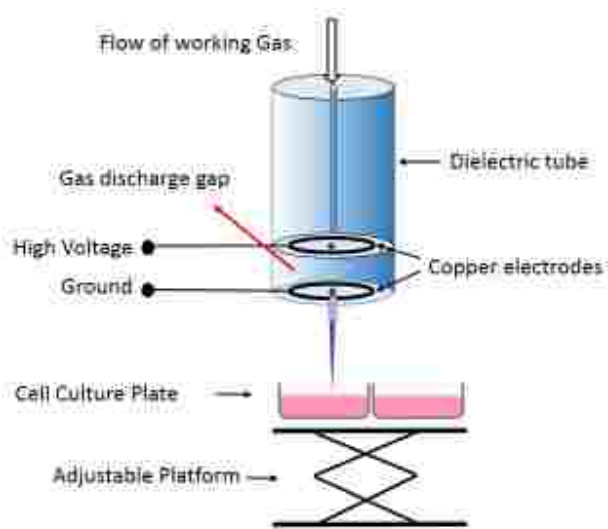
Figure 3. Schematic of the plasma pencil and the experiment setup.

II.1.2 Cell Lines and Cell Culture

Two adherent epithelial cell lines were used in this study: SCaBER (ATCC® HTB3™) cells from urinary bladder tissue with the squamous cell carcinoma disease was purchased from ATCC (Manassas, VA). SCaBER cells were cultured in MEM (Minimum Essential Medium) with 10%

Bovine Calf Serum and 1% Penicillin/Streptomycin/Glutamine, all purchased from HyClone (Logan, UT, USA). MDCK (Madin-Darby Canine Kidney, ATCC® CCL-34™) cells are normal (non-cancerous) epithelial cells originally derived from a canine kidney which was generously provided by Dr. Venkat Maruthamuthu (Department of Mechanical & Aerospace Engineering, Old Dominion University, Norfolk, VA). MDCK cells were grown in EMEM (Eagle's Minimum Essential Medium, ATCC, Manassas VA) supplemented with 10% Bovine Calf Serum and 1% Penicillin/Streptomycin/Glutamine. Cells were seeded in a 75 cm^2 vented cell culture flask and maintained at 37 ºC in a humidified incubator with 5% CO_2. The media was replaced twice a week. To harvest cells, 1 ml of trypsin-EDTA 0.25% (HyColne, Logan, UT) was used following standard cell culture protocol [71]. Once a flask had reached a high confluence, it was used to make a cell suspension with a desired density. A specific amount of the cell suspension was seeded into either a 96-well, 24-well, or 6-well plate depending on the experimental protocol and the details will be explained more in the experimental methods (section II.2). After seeding, cell culture plates were incubated overnight at 37 ºC in a humidified incubator with 5% CO_2 to provide a complete cell adhesion to the cell culture plate. Figure 4 shows bright field images of a SCaBER cells and MDCK cells acquired at 10X magnification. This research received the Institutional Biosafety Committee (IBC) approval under the title of "Biomedical Use of Cold Plasma".
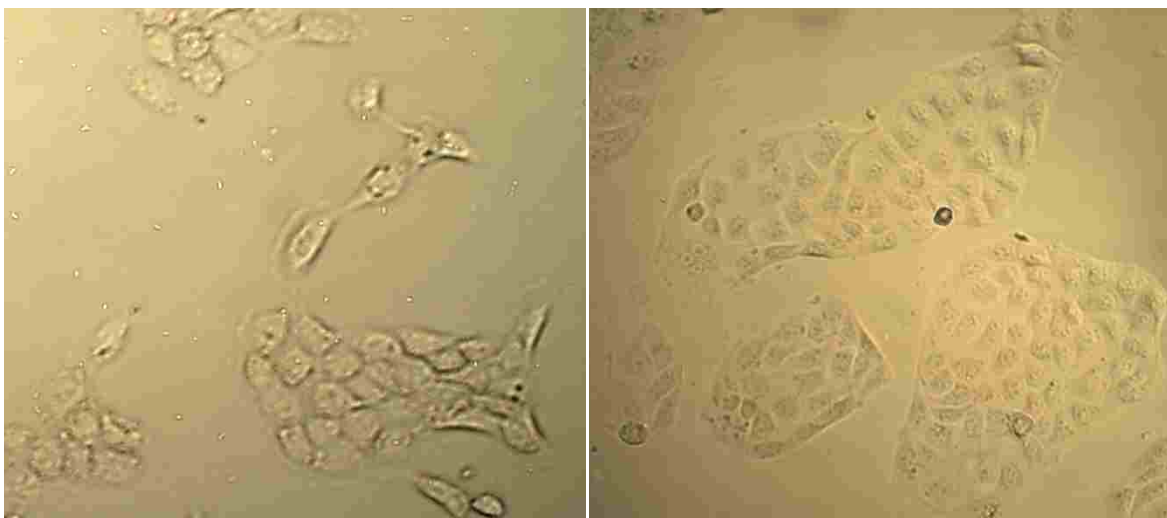
Figure 4. Bright field images of SCaBER cells (left) and MDCK cells (right) at 10x magnification.

II.1.3   Cell Viability Assays

Dye exclusion is a traditional method to assess the viability of cells and trypan blue dye exclusion staining is one of the most common and standard methodologies. Nonviable cells take the dye in and turn into a blue color while viable cells remain unstained due to their intact cell membrane which prevents dye penetration. Therefore, viable cells are easily distinguishable from dead cells. A 1:1 ratio of trypan blue dye (0.4%) and cells suspended solution was used. The number of live and dead cells were counted using a hemocytometer under a bright field microscope (ACCU-SCOPE® 3020). Figure 5 shows an image of SCaBER cells assayed by trypan blue exclusion assay in which dead cells are differentiated from live cells by their color i.e. bright and colorless cells are live and dead cells (arrow) are blue.
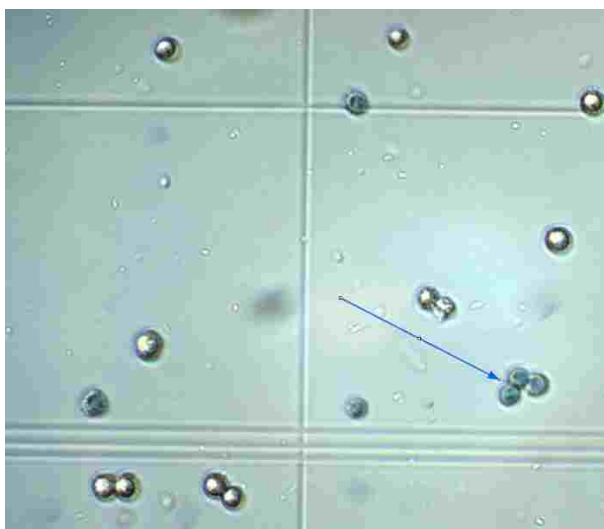
Figure 5. An image of SCaBER cells treated by plasma for 2 min after the trypan blue exclusion assay. Live cells are bright as the dye cannot penetrate into an intact cell membrane while dead cells are stained (arrow). The image is at 10x magnification.

The second method to assess metabolically active cells was the MTS assay which is a fast and convenient colorimetric method. Cell viability was measured using The CellTiter 96® AQueous

One Solution Cell Proliferation Assay (MTS) (Cat#G5421 Promega) following the manufacturer's protocol. The solution reagent contains a tetrazolium compound [3-(4, 5-imethylthiazol-2-yl)-5-(3-carboxymethoxyphenyl)-2-(4-sulfophenyl)-2H-tetrazolium, inner salt; MTS] and an electron coupling reagent (phenazine ethosulfate; PES). PES is a chemical stabilizer to enhance MTS solution stability. Metabolically active cells (presumably by NADPH or NADH) reduces the MTS tetrazolium compound into a colored formazan product that is soluble in cell culture medium.

In this assay, media in each well of a 96 well plate was replaced by 100 µl of fresh complete cell culture media and, 20 µl/ well of the MTS solution was added. Cells were placed in an incubator at 37 ºC in a humidified incubator with 5% CO_2 for 1 hour. Absorbance was recorded at 490 nm using a microplate reader (AgileReader, ACTGene, Inc.). To quantify the absorbance intensity acquired from MTS assay, the number of live cells in control samples was counted using a trypan blue exclusion assay and it was used to calculate cell number densities in PAM treated samples.

II.2   EXPERIMENTAL METHODS

II.2.1   Direct Treatment

In this experiment, cells were cultured in a 24-well plate and were exposed directly to the plasma pencil. Cells were covered with a layer of liquid media during plasma exposure. The schematic of the setup is shown in Figure 6. SCaBER cells were prepared at a concentration of 5×10^5 cells/ ml. One milliliter of the cell solution was seeded in individual wells and the plate was incubated overnight at 37 ºC in a humidified incubator with 5% CO_2 while cells adherence was monitored. Before plasma exposure, media in each well was replaced with 1 ml of fresh complete cell culture media. Each well was treated by the plasma pencil for 2, 3, 4, and 6 min, then samples were returned to the incubator for later viability analysis. The number of live/dead cells were counted at 12 and 24 h post-treatment time using the trypan blue exclusion assay. To examine whether the plasma pencil induces any cell damage immediately after treatment, the viability of SCaBER cells was measured immediately after direct plasma treatment (0 h). In addition, the effect of helium gas on cell viability was examined by treating SCaBER cells with a helium gas flow (flow rate of 5 slm) for up to 6 min without plasma ignition. Since no changes occurred in the viability of helium treated cells compared to the control, it is concluded that helium gas does not impact cells viability.

Cells grown in a 24-well plate
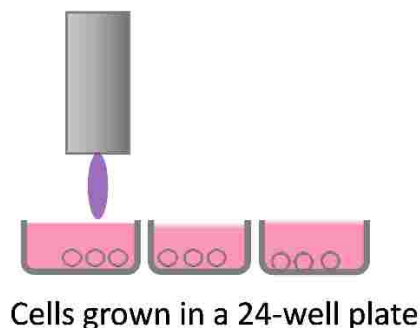
Figure 6. Direct plasma pencil treatment of cells seeded in a 24-well plate.

II.2.2   PAM Treatment

Another method to treat cells was investigated by using plasma activated media which was produced by exposing cell culture media to LTP. This protocol provides an indirect treatment of a sample and allows for later application. PAM protocol has an advantage compared to the direct treatment protocol in which a cell culture plate remains in an incubator during the PAM preparation time. This can minimize possible temperature-related stress (below 37 ºC) in cells. In addition, in direct plasma treatment one cannot measure the concentration of chemical reactive species in plasma treated media without considering their mutual interaction with cells.

To make PAM, in all experiments 1 ml of a fresh complete cell culture media in an individual well of a 24-well plate was exposed to the plasma pencil for the designated exposure time. In PAM treatment protocol, a suspension of SCaBER cells with a concentration of 4×10^5 cells/ ml were prepared and 100 µl of the cell solution was seeded in each well of a 96-well plate.

The plate was incubated at 37 ºC in a humidified incubator with 5% CO_2 overnight for eventual PAM treatment at a later time. Once the media was exposed to LTP to create PAM, the old media (which was used to grow cells overnight) on top of cells in a 96-well plate was replaced by 100 µl of PAM. Cells were then stored in an incubator for MTS assay at 12, 24, and 48 h post PAM treatment. In the control sample, the older media was replaced with fresh non-plasma treated media. Figure 7 represents a schematic of PAM treatment procedure.
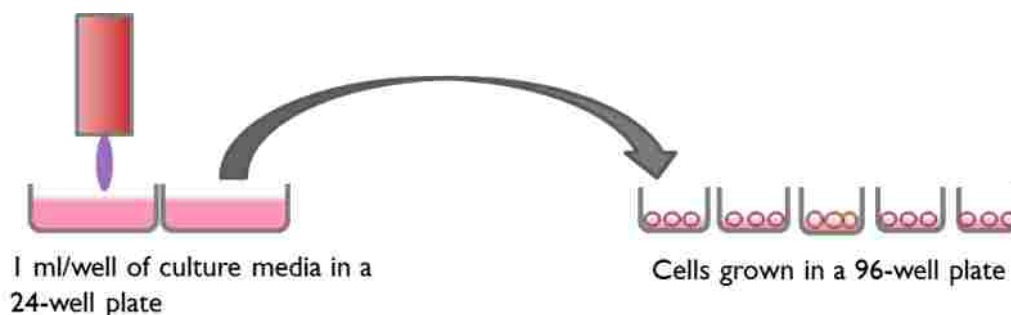
Figure 7. Schematic of PAM preparation and cell treatment.

Most conventional cancer treatment methods harm or kill normal cells as well as cancer cells which engender mild to severe side effects. To understand the practical therapeutic potential of plasma in cancer treatment, it is crucial to investigate its effects on normal healthy cells.

To evaluate effects of plasma treatment on normal epithelial cells, MDCK (non-cancerous) cells were studied. Similar to PAM treatment of SCaBER cells, a cell suspension of MDCK cells with a concentration around 2×10^5 cells/ ml were seeded in each well of a 96-well plate and were incubated at 37 ºC in a humidified incubator with 5% CO_2 overnight. The viability of MDCK cells was monitored at 12, 24, and 48 h post PAM treatment using the MTS assay.

The same media with the same chemical composition which was used to grow the cells was also used to make PAM i.e. MEM PAM for SCaBER cells and EMEM PAM for MDCK cells. EMEM PAM was used for treating MDCK cells because this cell line was found to grow better in this type of culture media and therefore provided the best-growing condition for the control sample. The chemical formula of MEM and EMEM are slightly different. EMEM contains more amino acid compounds and 1 mM Sodium Pyruvate while MEM contains 2.2 g/L Sodium Bicarbonate according to the manufacturer data sheet. It was assumed that the difference in the composition does not have a significant effect on the final results and to validate our assumption the H_2O_2 was measured in both plasma treated media. In addition, Kaushik *et al.* [72] reported that addition of 10mM Sodium Pyruvate in their investigated media resulted in 20% reduction in the effectiveness of the PAM. However, 1mM sodium pyruvate in the EMEM media is 10 times lower than what

was used in Kaushik *et al.* [72] experiment and accordingly its scavenging effect should be negligible.

The pH of the cell culture media was measured with an Orion star A216 pH meter (Thermo scientific, Beverly, MA, USA) before and after plasma exposure. The exposure time was from 1 to 10 minutes. The pH of the untreated media was around 7.4 while the pH of 10 min PAM was 7.4 ± 0.4 indicating that PAM remains at buffered pH even after 10 min treatment eliminating the possibility of acidic side effect on treated cells. In addition, the temperature of the media was measured before and after plasma exposure with a thermometer and no temperature increase was observed.

In prior work, it was observed that PAM treatment has a dose-dependent cytotoxic effect on cell viability which was measured at different plasma exposure time. Similarly, diluting PAM with non-treated media may reduce the concentration of LTP-generated reactive species and the effectiveness of PAM against cells. To evaluate the validity of this hypothesis, effects of diluted PAM on SCaBER cells viability were measured. Because of its pronounced killing effect 4 min PAM was selected for making aliquoted PAM. MEM PAM was prepared by 4 min plasma exposure and it was diluted with the untreated media to make the following dilutions: 1:1 (the portion of PAM to the total volume), 1:2, 1:4, and 1:8. In fact, 1:1 is just 4 min PAM, 1:2 is 1 part PAM and 1 part media, etc. The Aliquoted PAM was immediately used to treat SCaBER cells following the same procedure used in PAM treatment and the viability was measured at 12 and 24 h post treatment using MTS assay.

In the next experiment, the potency of PAM against SCaBER cancer cells was compared to that of an apoptosis-inducing drug, staurosporine (cat# 569397, EMD Millipore Corporation). To accomplish this, 5×10^5 cells per ml of SCaBER cells were grown overnight in a 24-well plate. Then, cells were treated with 1 ml of media that contained 1 μM staurosporine and 1 ml of 4 min PAM while the control sample did not receive any treatment. Cell viability was analyzed at 10 and 24 h post treatment using the trypan blue exclusion assay.

II.2.3   Aged-PAM Treatment

Reactive oxygen species and reactive nitrogen species generated by the LTP in the gaseous state or liquid state have specific but different lifetimes. In liquids, some species have very short lifetimes as low as micro to nanoseconds. These include molecules such as OH radical, superoxide anion (O_2^-), singlet oxygen, and nitrite (NO_2^-) while others have relatively longer lifetime such as

hydrogen peroxide and nitric oxide (NO) [73]. Since the anti-tumor effect of plasma is highly linked to the concentrations and lifetimes of RONS, knowledge of these quantities in PAM is important as they directly correlate to its efficacy. Therefore, two questions arise: Will PAM retain its anti-tumor property over time? How long after plasma exposure does PAM remain effective against cancer cells? Measuring the efficiency of PAM at various times after preparation allows for an insight into the temporal presence and stability of RONS in PAM.

To investigate the effects of aged-PAM, the MEM PAM was maintained in the dark at room temperature for a designated time before using it to treat SCaBER cells. In this experiment, SCaBER cells were prepared similarly to the application of immediate PAM. However, in this case PAM was stored (or aged) 1, 8, and 12 h before application. The viability of cells was measured at 12, 24, and 48 h post aged-PAM treatment using MTS assay. Figure 8 shows a schematic of the aged-PAM protocol.
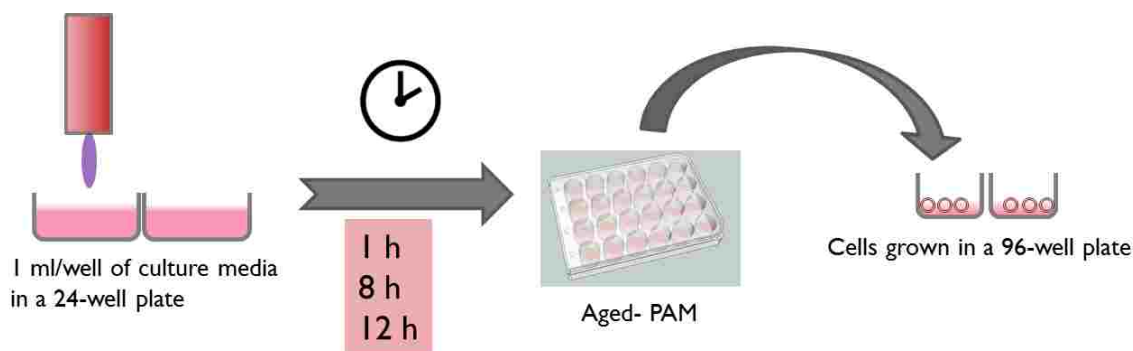
Figure 8. Aged-PAM preparation: PAM was stored at room temperature for a designated time before applying in cell treatment.

II.3   REACTIVE OXYGEN SPECIES IN PAM

II.3.1   Types of Reactive Species

Reactive oxygen species are radical or non-radical reactive molecules containing oxygen. ROS are strong oxidants which react with most biomolecules and could produce a chain of secondary reactions. Interaction of plasma with cells causes an oxidative stress which is associated with damage to macromolecules such protein, nucleic acids, and lipids [74]. For instance, hydrogen peroxide, H_2O_2, and superoxide, $O_2^{\bullet-}$, can cause hundreds of modification to proteins. On the other hand, reactive species are natural byproducts of intercellular reactions such as in metabolic processes [74]. The two-edged sword role of ROS was revealed by two discoveries in the 1970s and 1980s; first, the toxic role of superoxide released from phagocytes via NOX enzyme (NADPH (Nicotinamide adenine dinucleotide phosphate oxidase) and second, the beneficial messenger role of ROS in peptide signaling [75]. A low concentration of ROS is beneficial for cells and has an important role in regulating cell signaling pathways and affect cellular processes such as metabolism, proliferation, differentiation, survival processes (like apoptosis), antioxidant response, and DNA damage response [42, 74]. However, at higher concentration and when ROS level overwhelms the cells' antioxidant capacity, irreversible cell injury or death occurs, depending on the cell type and environmental conditions. A cell type with a higher antioxidant capacity can overcome a specific level of ROS that is harmful for another cell type. What is important is the balance between antioxidant capacity and ROS level and accordingly, one can determine the consequence of an "oxidative stress" in cells [76]. The followings are the most important ROS in biological systems: O_2^-, H_2O_2, hydroxyl radical ($^\bullet OH$), and singlet oxygen $O_2\,(^1\Delta_g)$.

The existence of the superoxide radical was proposed in 1933 according to quantum mechanics theory [77]. The superoxide anion is the precursor of the majority of reactions due to its high oxidation-reduction ability. One of the most famous reactions of superoxide anion is dismutation reaction in which $O_2^{\bullet-}$ dismutate to hydrogen peroxide:

$$2O_2^{\bullet-} + 2H^+ \rightarrow H_2O_2 + O_2 \tag{1}$$

Superoxide dismutase (SOD) is an enzyme that catalyzes this reaction in cells. It is an antioxidant defense mechanism which converts the highly toxic $O_2^{\bullet-}$ into the less toxic H_2O_2 [59]. The discovery of SOD led to the recognition of ROS biological functions [78].

Hydrogen peroxide was produced as a disinfectant for the first time in early 1800 and because of its oxidative properties, it was not considered to have a role in normal cell signaling [78]. Hydrogen peroxide is commonly used in household products such as bleach-free cleaners, toothpaste, and hair products. It is an important ROS by being able to penetrate the cell membrane. It is not a radical species but it intermediates in many reactions and results in more ROS production such as $OH^{\bullet}$ [59]. Hydrogen peroxide with an oxidation potential of 1.8 V has a relatively higher stability than other ROS species [73]. There are four known pathways to detoxify hydrogen peroxide in cells including glutathione peroxidase, catalase, peroxiredoxin enzymes, and non-enzymatic method by reacting with thiol proteins [73, 79].

Hydroxyl radical is probably the most reactive ROS. Having the half-life of 10^{-9} s in comparison with the 10^{-5} s for superoxide anion and ~60 s for hydrogen peroxide, $OH^{\bullet}$ is probably the most short-lived ROS [73].

$OH^{\bullet}$ causes significant damage to biological macromolecules. Hydroxyl radical is a powerful and non-selective oxidant which can react with almost every organic compound [73]. Formation of hydrogen peroxide from two hydroxyls occurs as follows:

$$OH + OH + M \rightarrow H_2O_2 + M \qquad (2)$$

Singlet delta oxygen in liquid media has a lifetime in the range of 10^{-3} to 10^{-6} s, depending on the solvent composition. Singlet oxygen is less stable than the ground state oxygen as it is in the excited state of the oxygen molecule in which two electrons occupy the same orbital with the antiparallel spins [73]. Singlet oxygen is considered to be cytotoxic to eukaryotic cells, bacteria, and viruses by its adverse effects on biomolecules such as DNA, proteins, and lipids [80]. Usually, its generation in biological systems is via photo-excitation in which specific organic molecules absorb a particular wavelength and produce singlet oxygen [73].

The second important category of biologically reactive species are the reactive nitrogen species (RNS) such as nitric oxide (NO or $NO^{\bullet}$), nitrite (NO_2^-), nitrate (NO_3^-), and peroxynitrite ($ONOO^-$). Reactive nitrogen species react to form different products containing nitrogen oxides such as nitrated fatty acids. Other than oxidizing of macromolecules, RNS play roles as signal transduction mediators. These products can then react to make a cascade effect in biochemical cycles. For instance, a presence of nitrite in human perspiration in a slightly acidic environment of skin will create NO which acts as an antibacterial [81]. NO is an important reactive species in cell signaling

pathways. NO is a diffusible radical which is involved in the circulatory system and results in widening of blood vessels (vasodilation) and also its by-products play role in the nervous system functions [82]. It is also the precursor of many reactions such as the formation of $NO_2^\bullet$ and $ONOO^-$ [73]. Peroxynitrite protects organisms from pathogens; however, its overproduction is harmful and leads to oxidation of proteins, lipid peroxidation, and DNA and mitochondrial damage [82].

As it is described above, some of the LTP-generated species have short lifetimes and cannot penetrate deep into liquid media. However, due to their high reactivity, they interact with the liquid and generate relatively stable long-lived species in the bulk of the liquid. These include hydrogen peroxide, nitrites, nitrates, and organic peroxides. In particular, hydrogen peroxide is known to cause various oxidizing reactions in biological cells, including the peroxidation of lipids and induction of DNA damage. Hydrogen peroxide is also known to play a role in mitogenic stimulation and cell cycle regulation [83, 84]. Because of the ability of hydrogen peroxide to penetrate the cell membrane and its relatively long lifetime, its concentration was measured over time in PAM.

II.3.2   Measurements of Hydrogen Peroxide in PAM

To measure the concentration of hydrogen peroxide generated in PAM, an Amplex red hydrogen peroxide assay kit was used (Molecular Probes, Invitrogen, Burlington, Ontario, Canada). This kit contains an Amplex red reagent, dimethylsulfoxide (DMSO), 5X reaction buffer, horseradish peroxidase, and hydrogen peroxide. This kit must be stored at -20 ℃ and protected from light for optimal use. The Amplex red reagent is one of the most commonly used to measure concentrations of hydrogen peroxide. The reaction of Amplex red reagent with hydrogen peroxide in the presence of horseradish peroxide (HRP), which plays the role of a catalyzer in this reaction, results in the production of resorufin. Resorufin is a colored compound that can be detected fluorometrically or spectrophotometrically.

In all experiments, each plasma treated sample was diluted 1:10 with a fresh complete media to be within the acceptable range of the assay. The control sample was a complete media with no plasma treatment. A standard curve of known H_2O_2 concentration was prepared from a 3% hydrogen peroxide stock solution (in complete cell culture media) within the range of 0 to 50 µM. The standard curve was used to convert the acquired absorbance into concentration (µM). 50 µL of all samples including PAM, control, and standard curve were transferred into individual wells of a 96-well plate. 50 µL of the working solution composed of 100 µM Amplex red reagent and 0.2

U/mL HRP was loaded in each well. Then, the 96-well plate was incubated in a dark place at room temperature for 30 min. The absorption of samples was measured at 570 nm using a microplate reader (AgileReader, ACTGene). Moreover, to record the fluorescent light intensity, a fluorescence microplate reader (BMG Labtech FLUOstar) was used with an excitation wavelength of 570 nm and an emission wavelength of 590 nm.

The H_2O_2 concentration was measured in MEM PAM immediately after plasma exposure and in aged-PAM after 1, 8, and 12 h in order to evaluate degradation of H_2O_2. To evaluate the effect of serum on H_2O_2 concentration, a serum-free PAM made by MEM and 1% antibiotics was used and the H_2O_2 concentration was measured after 8 h aging. Correspondingly, the H_2O_2 concentration was analyzed in EMEM PAM immediately after plasma exposure.

II.4   LEVEL OF CASPASE-3 IN PAM TREATED SCABER CELLS

Caspases are part of a large family of cysteine proteases that mediate apoptosis. Upon activation, endoproteases such as caspase-3 cleave a variety of target proteins in cells that causes morphological and functional changes in cells undergoing apoptosis [85]. Some of the morphological changes attributed to this process are evident in the cell morphology and adhesion characteristics. The mechanism of apoptosis is very complex but all apoptosis pathways end up to a same final execution pathway: the cleavage of caspase-3 which leads to "DNA fragmentation, degradation of cytoskeletal and nuclear proteins, cross-linking of proteins, formation of apoptotic bodies, expression of ligands for phagocytic cell receptors, and ultimately uptake by phagocytic cells" [49]. Hence, monitoring the level of caspase-3 is a good indicator of the apoptotic pathway activity [86, 87].

In order to elucidate the mechanism of cell injury in plasma treated SCaBER cells and ascertain the underlying molecular mechanisms involved, the caspase-3 activity was investigated. The caspase-3 activity was measured by ApoAlert1 Caspase Colorimetric Assay Kit (Clontech Laboratories, Inc.). SCaBER cells were seeded in a 24-well plate and were treated with 1 ml of 2 min PAM. Positive control was treated by 1 µM staurosporine (STA) and negative control did not receive any treatment. The control, STA, and PAM treated cells were collected at 4, 6, and 10 h after treatment, were counted to supply at least 2×10^6 cells/ml, and were centrifuged at 2,000 rpm for 5 min following the instructions provided by the manufacturer. Cells lysate was prepared by adding 50 µl of Cell Lysis Buffer to cells pellet and were incubated in a 4 ºC fridge for 10 min.

Then, it was centrifuged for 10 min at 14000 rpm and the supernatant was collected. 50 μl of the supernatant from treated and control samples were mixed with 50 μl of the reaction solution (2X Reaction Buffer/DTT Mix) and 5 μl of caspase-3 substrate (1 mM DEVD-pNA). Samples were incubated in 37 ºC water bath for 1-3 h for eventual absorbance measurement at 405 nm using a microplate reader (AgileReader, ACTGene, Inc.). The results are expressed as an absorbance (a.u.) of each sample compared to the control sample.

II.5   EFFECT OF PLASMA ON REATTACHMENT OF SCABER CELLS

The morphology of the cells and their ability to reattach to the cell culture plate were evaluated after direct plasma treatment. In this experiment, 1 ml/ well of SCaBER cells suspension was added in a 24-well plate and each well was treated with the plasma pencil for 2 and 5 min immediately after seeding and prior to active cell attachment. The control samples did not receive any plasma treatment. The attachment of cells to the surface of the culture plate was monitored and photos were taken using a bright-field microscope at 0 h (after seeding of cells), 1.5, 3, 4.5, 6, and 24 h after plasma exposure. Between these imaging times, the cell culture plate was stored in an incubator at 37 ºC humidified with 5% CO_2.

II.6   TIME-LAPSE IMAGING OF THE MDCK CELLS

Results of PAM treatment on MDCK cells suggested that LTP affects cell proliferation in normal cells. These preliminary results on MDCK cells were encouraging and add a profound understanding of how PAM treatment impacts cell proliferation and migration. Time-lapse imaging was used to monitor changes in cells during PAM treatment. Here, MDCK cells were seeded at 8×10^4 cells per well in a 24-well plate and the plate was incubated overnight at 37 ºC humidified with 5% CO_2. Then, two portions of 5 min EMEM PAM (1 ml each), as explained in the PAM preparation method (Section II.2.2), were used to treat cells 10% HEPES solution was added to the media in order to buffer the pH during imaging. Since, PAM created with lower exposure time (4 min or below) did not induce a noticeable change in cell viability of MDCK cells and very long exposure time such as 10 min PAM caused severe cell death, 5 min plasma exposure was selected to provide PAM with a moderate intensity (refer to cell viability results of PAM shown in Section IV.1). After the PAM application, a time-lapse microscopy of control and PAM treated samples was started. The 24-well plate was fixed on an automated stage at a temperature of 37 °C. Phase-contrast images were acquired at 10X magnification using an inverted microscope

(DMi8, Leica Microsystems) equipped with a CCD camera (Andor Technology Ltd). Images were captured every 10 min for a period of 48 h (288 images) after PAM addition. ImageJ software (NIH) was used for the processing and analysis of the resulting images.

II.7   IMMUNOFLUORESCENCE

Immunofluorescence is a common method in biological and clinical research to visually and quantitatively detect specific proteins in cultured cells and tissues. In this method, two antibodies are used: primary and secondary antibodies. The primary antibody selectively attach to a specific antigen and the secondary antibody which is conjugated to a fluorescent dye will attach to the primary antibodies. Eventually, fluorescence microscopy leads to excitation and emission in the fluorescence dyes and visualization of labeled cells.

For immunofluorescence experiments, 80,000 cells per well of MDCK cells were grown overnight on a collagen coated (0.2 mg/ml col1) square coverslips which were placed in a 6-well plate. Cells were then covered with 2 portions (1 ml each) of 5 min EMEM PAM in addition to 1 ml of the fresh complete cell culture media and then placed in a humidified incubator with 5% CO_2 for 48 h at 37 ^{o}C. For the control samples, the older media were replaced by 3 ml of fresh complete cell culture media. For conducting immunofluorescence, the media were discarded and coverslips were washed with CB buffer (Cytoskeletal buffer: 10 mM MES, 3 mM $MgCl_2$, 0.14 M KCl, pH 6.8). This was followed by a 15 min incubation in a permeabilization/fixing solution containing 4% paraformaldehyde, 1.5% BSA and 0.5% Triton in CB buffer at room temperature. Cells were then washed three times with PBS, for 5 min each time. Samples were then incubated with an appropriate dilution of each of the primary antibodies or 488-phalloidin for 1 h, followed by three PBS washes and were again incubated for 1 h with the secondary antibodies. Following the first PBS wash after the secondary antibodies incubation, cells were incubated in DAPI (4',6-Diamidino-2-Phenylindole) diluted in PBS for 5 min. Each coverslip was mounted on a glass slide and stored overnight at 4 °C prior to imaging. Fluorescence images of cells were acquired using an epi-fluorescence microscope (DMi8, Leica Microsystems) equipped with a CCD camera (Andor Technology Ltd) and 10X, 20X, and 40X objectives. All chemicals used for immunofluorescence were from Fisher Scientific unless otherwise mentioned. The following primary antibodies and their dilution were: beta-catenin (BD Biosciences, 1:100 dilution) to mark cell-cell adhesions, paxillin (Santa Cruz Biotech, 1:100) to mark cell-surface adhesions and Ki-67

(Dako, 1:150) to mark proliferating cell nuclei. Phalloidin-488 (Molecular Probes, 1:200) was used to mark filamentous actin. The secondary antibodies used were (all from Jackson ImmunoResearch) anti-mouse (1:200) and anti-rabbit (1:200) IgG.

II.8   STATISTICAL ANALYSES

Statistical analyses were performed using Statistical Package for the Social Sciences (SPSS, IBM, USA) software and results were analyzed using independent *t*-test or chi-square test. A p-value below 0.05 was considered to be statistically significant (* $p < 0.05$), ** $p < 0.01$, *** $p < 0.001$). In statistics, the p-value is the probability of observing a given sample results when the null hypothesis is true.

II.9   SUMMARY

In this chapter, the low temperature plasma source (plasma pencil), cell lines, and cell culture media used in this work were introduced. This was followed by a detailed presentation of all the experimental methods and procedures including the various assays used in this research. SCaBER cells with squamous cell carcinoma disease from a urinary bladder were used to evaluate the anti-tumor effects of LTP on epithelial cancerous cells. Cells were initially treated by direct plasma exposure. Then, as an indirect treatment method, plasma activated media were examined. Trypan blue exclusion assay and MTS assay were successfully employed to inspect cells viability after treatment. Caspase-3 activation level in PAM-treated SCaBER cells was assessed to diagnose the cell injury mechanism induced by plasma treatment. To assess damaging effects of LTP treatment on DNA, a molecular beacon of DNA was treated by the plasma pencil and the extent of damage was analyzed. Since, LTP-generated ROS are mainly responsible for the anti-tumor properties of plasma, the concentration of hydrogen peroxide –as one of the most stable and impactful ROS- in PAM was measured by means of a molecular probe (Amplex red kit). The temporal effectiveness of PAM and the stability of hydrogen peroxide generated in PAM were analyzed. A normal/healthy epithelial cell line, MDCK, was used to evaluate the effects of PAM on non-cancerous cells. Time-lapse microscopy in addition to immunofluorescence was employed to gain further understanding of PAM treatment effects on proliferation, morphology, and migration of normal cells.

CHAPTER III

RESULTS AND DISCUSSION OF EXPERIMENTS AND TREATMENT OF CANCER CELLS

III.1 EFFECTS OF PLASMA ON THE VIABILITY OF CANCER CELLS

III.1.1 Direct Treatment of Cancer Cells

SCaBER cells were treated with direct plasma exposure and the results are shown in Figure 9. Trypan blue exclusion assay was used to count the number of live and dead cells at 0 h (immediately after treatment), 12, and 24 h after the treatment. As it shows, the longer the exposure time to plasma, the lower the number of survived cells. For instance, at 12 h post-treatment the viability of cells reduced to around 50% for 2 min plasma treatment time while it reduced to more than 80% for 3 min treatment time. It is also shown that 4 and 6 min plasma exposure led to more than a log reduction in the viability of cells. Moreover, at longer post-plasma treatment times a higher number of dead cells was observed, which is known as the delayed effect. LTP treatments for 2 and 3 min diminished the viability of SCaBER cells to more than 70 and 90 percent after 24 h, respectively.

The measurement of cells viability immediately after LTP exposure is shown in Figure 10. This figure shows that the number of live and dead cells did not change meaningfully in the control and LTP treated samples. This result indicates that LTP treatment at different exposure time did not induce immediate physical damage. In fact, the interaction between SCaBER cells and LTP-generated reactive species requires a sufficient time to show an effect. It is of note to mention that the result of LTP treatment on the viability of cells is highly dependent on the initial cell concentration and this is the reason of the slight difference in the number of cells in Figure 10.

No changes were observed in the viability of SCaBER which were treated with only a flow of helium gas without plasma. This result indicates that helium gas did not have a harmful effect on cells during the LTP treatment.

A

B
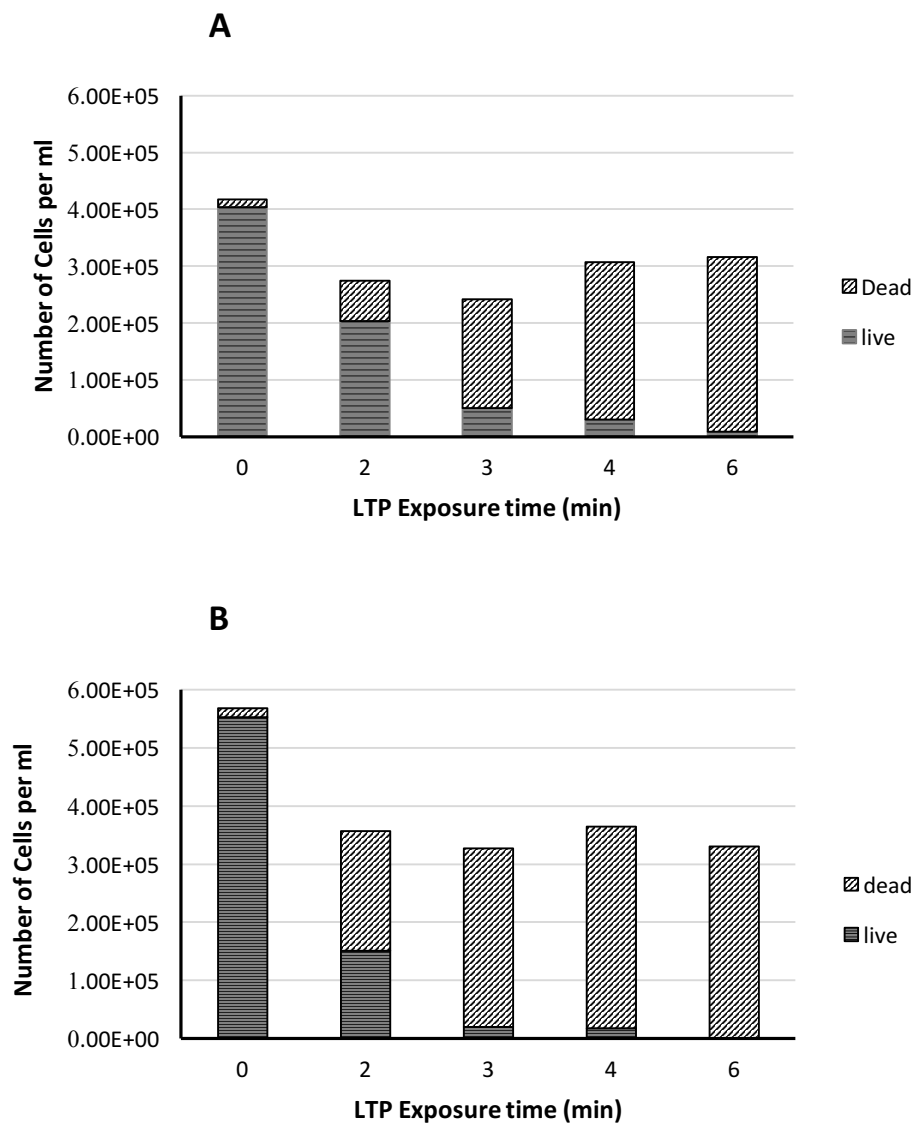
Figure 9. The Viability of SCaBER cells treated with direct plasma exposure shows the number of dead and live cells. The viability was monitored at A) 12 and B) 24 h post-plasma treatment using a trypan blue exclusion assay.
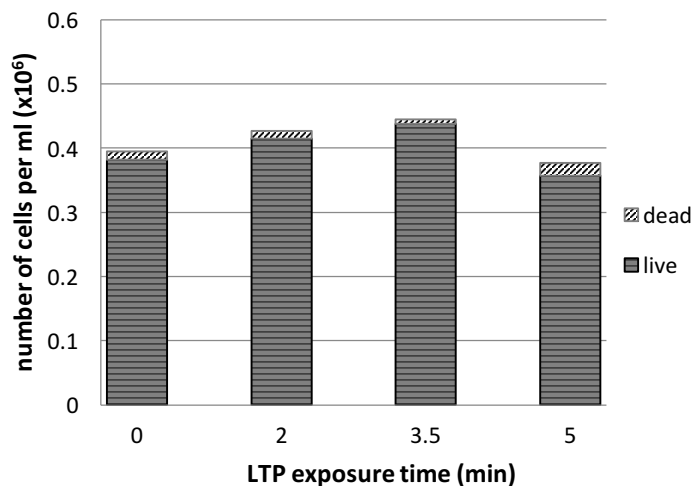
Figure 10. The number of live and dead SCaBER cells assessed immediately after direct plasma treatment.

III.1.2 PAM Treatment of Cancer Cells

As presented in the previous chapter, plasma activated media (PAM) is an indirect way to submit cancer cells to plasma exposure. In this protocol, adhered cells were treated with PAM which was produced by the exposure of cell culture media to the plasma pencil at a designated exposure time. Figure 11 shows the effect PAM treatment on SCaBER cells when used immediately after preparation. Let's call it immediate-PAM to differentiate it from aged-PAM. In this experiment, liquid media was exposed to plasma for 2, 3, and 4 min while 0 min represents the control, untreated media. The MTS assay was used to evaluate the number of metabolically active cells at 12, 24, and 48 h post-PAM application. The percentage of metabolically active cells was calculated by normalizing the number of cells in PAM treated samples to the control at each measurement time. During treatment time, cells were covered by PAM for the entire time. As can be seen in Figure 11, the viability of cells decreases with increasing the PAM exposure time. The metabolic activity of cells treated with 2 min PAM reduced to more than 80% at 12 h post-PAM treatment. 3 and 4 min PAM induced a log reduction in the cell viability. No significant changes were observed in the percentage of cells viability of 3 and 4 min PAM at the delayed measurement times of 24 and 48 h while, this is not the case in 2 min PAM. For 2 min PAM, the percent of viable

cells was around 13, 30, and 55% at 12, 24, and 48 h, respectively. This increase in the percentage of viable cells indicates that the effectiveness of 2 min PAM reduces over the delayed measurement times. It appears that cells gradually recovered from the induced oxidative stress at 24 and 48 h of PAM application.

Results of both PAM treatment and direct treatment reveal the capability of plasma-based treatment in inducing cell death in cancerous SCaBER cells. In addition, the anti-cancer properties of plasma-based treatment is related to the amount of plasma exposure time. Since it is known that RONS play the major role in the anti-cancer properties of plasma-based treatment, it can be expected that increasing the plasma exposure time increases the concentration of LTP-generated ROS and RNS which enhances the anti-cancer properties of plasma-based treatment. Measurement of the concentration of hydrogen peroxide in PAM will be presented and discussed later in this chapter as it will help better understanding of the role of ROS in the LTP cancer treatment.
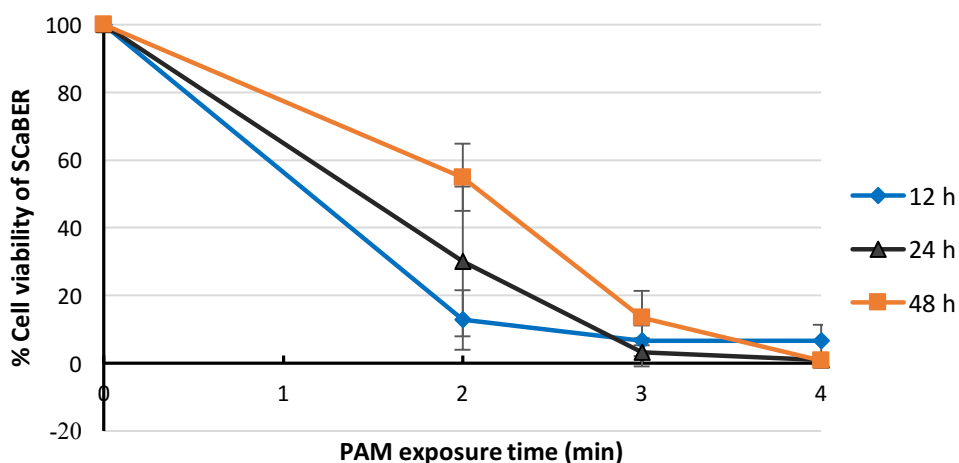
Figure 11. The effect of PAM produced by different exposure time on the viability of SCaBER cells using MTS assay. Metabolic activity of cells was measured at 12, 24, and 48 h post-PAM treatment. Results from 3 independent experiments with two replications are shown as means ± SD (standard deviation) [88].

Effects of aged-PAM on SCaBER cells viability

Stored or aged-PAM was used to investigate how long PAM remains effective against cancer cells after its preparation. It is proposed that the concentration and lifetime of reactive species induced in PAM determine the shelf life of PAM. In this procedure, PAM was stored for 1, 8, and 12 h before the application.

Figure 12 indicates the effects of PAM with different aging times on the viability of SCaBER cells. The percentage of viable cells was measured at 12 h after PAM treatment using MTS assay. This result indicates that PAM efficiency decreases with increasing aging time. However, reduction in the efficiency of PAM is more remarkable at shorter exposure times such as 2 min. Although, at longer exposure time (such as 4 min) PAM remained highly effective against SCaBER cells even after 12 h aging. Aging the 2 min PAM for 1 h caused only ~ 8% reduction in its efficiency while, aging for 8 and 12 h led to around 48% and 83% efficiency reduction, respectively. Aging the 3 min PAM up to 8 h did not change its efficiency whereas, 12 h aging resulted in 17% reduction in the efficiency. On the other hand, no significant reduction was observed in the efficiency of 4 min PAM even after 12 h aging. Based on these data, the shelf life of PAM (stored at room temperature) is dependent on the duration of plasma exposure time. Accordingly, the concentration of LTP-generated RONS in PAM is higher at longer exposure time and therefore PAM requires a longer aging time to lose its anti-cancer efficacy.

To demonstrate changes in viability of cells treated with aged-PAM, MTS assay was utilized at 12, 24, and 48 h post-PAM treatment. **Error! Reference source not found.** 13 A, B, and C show results of the MTS assay for 1, 8, and 12 h aged-PAM, respectively. As can be seen, the percentage of cell viability is approximately the same in all aged-PAM which indicates that there was not a delayed effect in results of aged-PAM at 12, 24, and 48 h post-PAM application. As it was mentioned earlier once PAM was added to each well, cells were exposed to it the entire time of treatment up to the time of cell viability assay, which means either 12, 24, or 48 h.
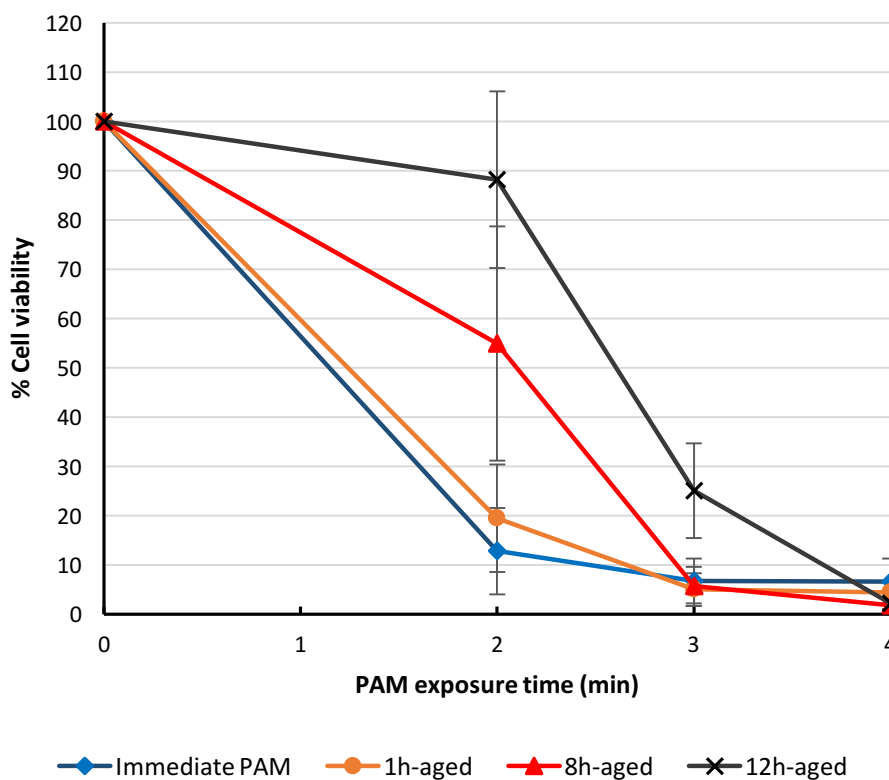
Figure 12. Effectiveness of immediate PAM and aged-PAM to induce cell death in SCaBER cells when stored for 1, 8, and 12 h before utilizing. Metabolic activity of cells was measured at 12 h post-PAM application. Cells were exposed to PAM the entire 12 h of treatment. Results are shown as means ± SD from 3 independent experiments with two samples replications.

A

B
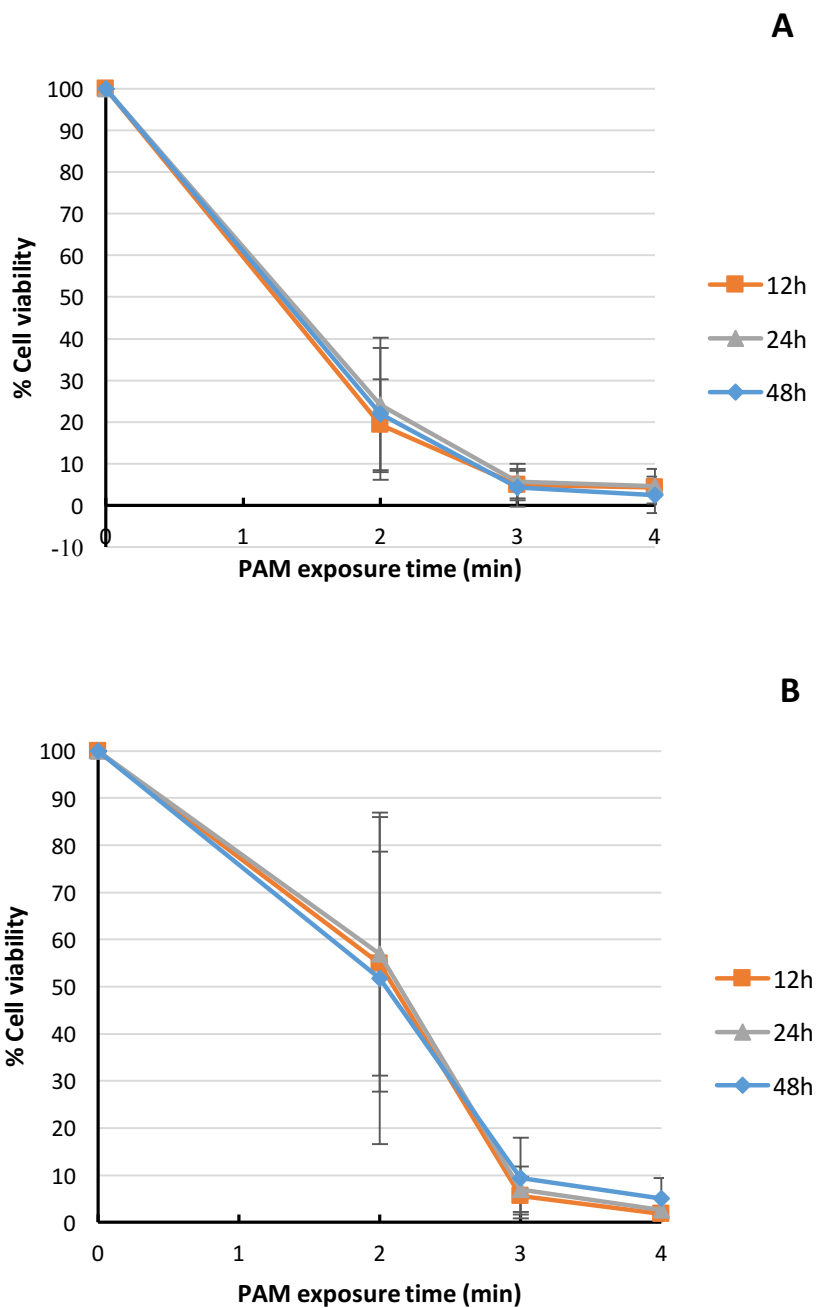
Figure 13. Percentage of metabolically active SCaBER cells treated with aged-PAM at 12, 24, and 48 h post aged-PAM treatment. PAM was aged at room temperature for A) 1 h, B) 8 h, and C) 12 h before application. Results are shown as means ± SD from 3 independent experiments with two samples replications.

Figure 13. (Continued).

C
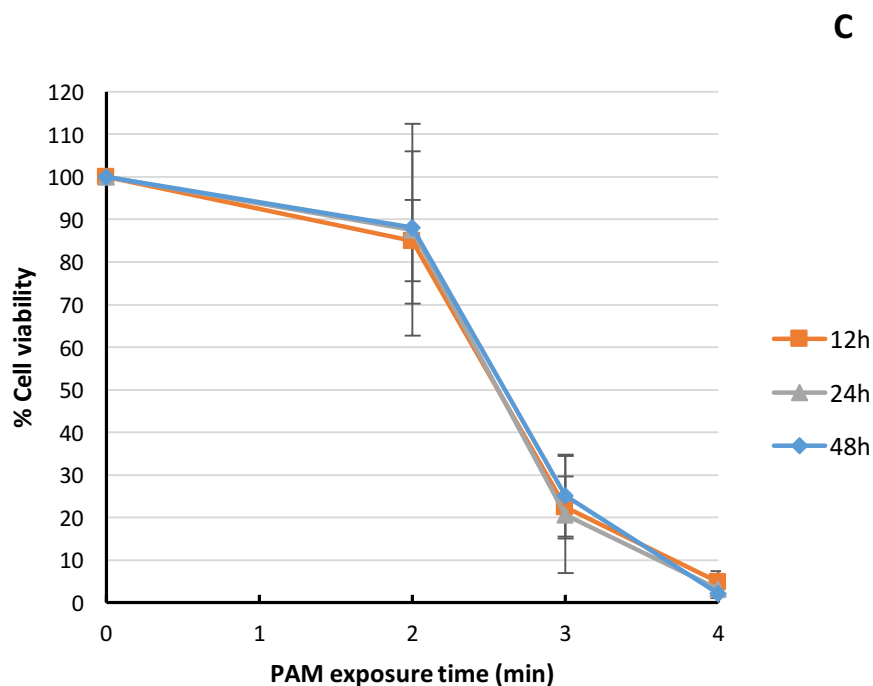
III.1.3 Effects of aliquoted PAM on SCaBER cells viability

It was observed that PAM treatment has a dose-dependent cytotoxic effect which was measured at different plasma exposure times as was shown in Figure 11. It is expected that diluting PAM with non-treated media may reduce the concentration of LTP-generated reactive species and the effectiveness of PAM against cells, similar to the influence of plasma exposure time. To evaluate the validity of this hypothesis, effects of aliquoted PAM on SCaBER cells viability was measured. Results of aliquoted PAM on cell viability of SCaBER cells at 12 and 24 h post-treatment time are shown in Figure 14. SCaBER cells were treated with a 4 min PAM diluted with fresh media with the following ratio: 1:8, 1:4, 1:2, and 1:1; C is the control sample and 1:1 is 4 min PAM (no dilution). Cell viability was measured A) 12 h and B) 24 h after treatment using MTS assay. Data are mean ± SD from three independent experiments. A and B. In this experiment, 4 min PAM was diluted with fresh media and cell viability was measured at 12 and 24 h post-PAM application using MTS assay. As Figure 14. SCaBER cells were treated with a 4 min PAM diluted with fresh

media with the following ratio: 1:8, 1:4, 1:2, and 1:1; C is the control sample and 1:1 is 4 min PAM (no dilution). Cell viability was measured A) 12 h and B) 24 h after treatment using MTS assay. Data are mean ± SD from three independent experiments. A and B indicate, 1:1 dilution which is a pure 4 min PAM was the most effective PAM against cells viability. Consequently, the effectiveness of aliquoted PAM decreased by increasing the dilution ratio (1:2 and 1:4). In the case of 1:8 dilution, a minor growth was observed in the percent of
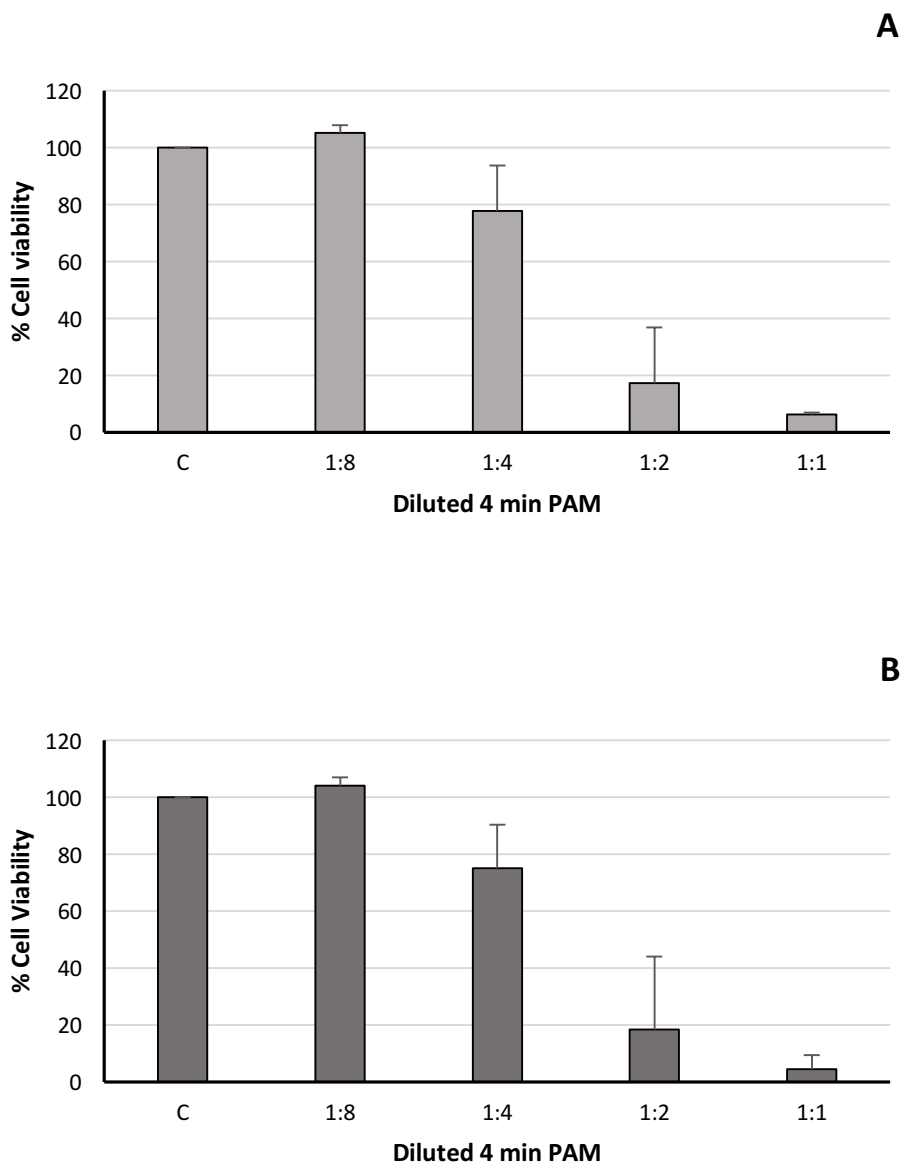
A

B

Figure 14. SCaBER cells were treated with a 4 min PAM diluted with fresh media with the following ratio: 1:8, 1:4, 1:2, and 1:1; C is the control sample and 1:1 is 4 min PAM (no dilution).

Cell viability was measured A) 12 h and B) 24 h after treatment using MTS assay. Data are mean ± SD from three independent experiments.

metabolically active cells (around 5%). Again, no delayed effect was observed in the MTS result of aliquoted PAM at 12 and 24 h after treatment. As a result, it is assumed that decreasing the portion of PAM in an aliquoted solution resulted in a decrease in ROS levels and ultimately a reduction in the effectiveness of treatment against SCaBER cells.

To provide a better understanding of the characteristics of an aliquoted PAM, it is assumed that dilution ratio has a somewhat similar function as the plasma exposure time. For instance, it is expected that 1:2 dilution of 4 min PAM would be equivalent (have similar killing effect) to a 2 min PAM. Based on this assumption, in Figure 14A and B 1:2 dilution of 4 min PAM will be shown as 2 min plasma exposure time. Respectively, 1:4 and 1:8 dilution ratio is equivalent to 1 min and 30 s plasma exposure time. To examine our assumption, results of the aliquoted PAM from Figure 14. SCaBER cells were treated with a 4 min PAM diluted with fresh media with the following ratio: 1:8, 1:4, 1:2, and 1:1; C is the control sample and 1:1 is 4 min PAM (no dilution). Cell viability was measured A) 12 h and B) 24 h after treatment using MTS assay. Data are mean ± SD from three independent experiments. will be shown as a function of the exposure time and will be compared with the result of immediate PAM (from Figure 11). This comparison is shown in Figure 15A and B. Interestingly, one can see that the trend of both graphs is very similar, which indicates that there is a correlation between the dilution ratio and the time of plasma exposure. Consequently, the effectiveness of PAM against SCaBER cells can be modulated by a dilution other than the exposure time.
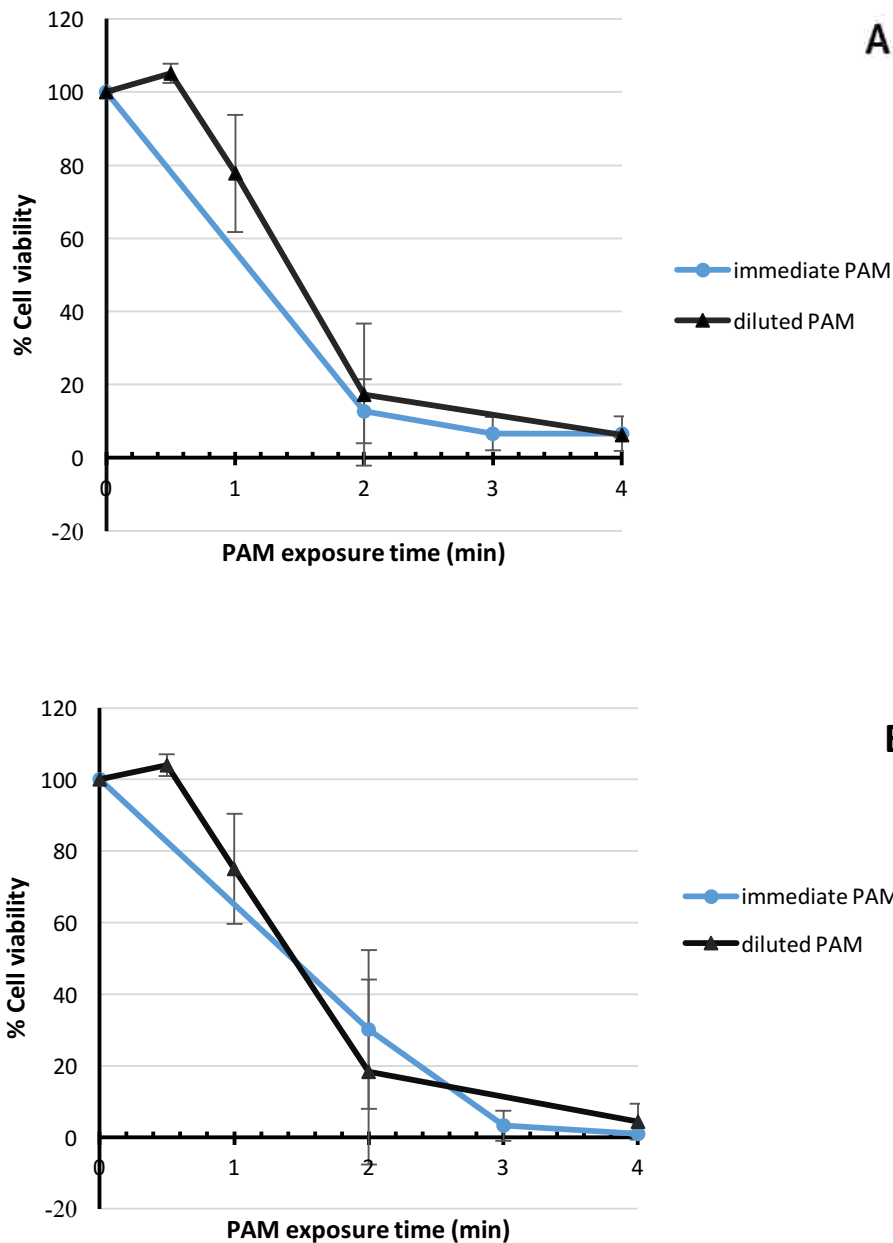
Figure 15. Comparison between the effectiveness of immediate PAM and diluted 4 min PAM on the viability of SCaBER cells assessed at A) 12 h and B) 24 h post-PAM application. The dilution ratio in aliquoted PAM was converted to the plasma exposure time: 30 s (1:8), 1 min (1:4), 2 min (1:2), and 4 min (1:1).

III.1.4 SCaBER Cells Treated with Staurosporine

To measure the potency of PAM against cancer cells, a comparison between the efficacy of PAM and staurosporine, an apoptosis-inducing drug, was conducted. Figure 16 shows the number of live cells treated with 1 ml of 4 min PAM and 1 µM staurosporine in a 24-well plate after 10 and 24 h using trypan blue exclusion assay. It is clear that 4 min PAM is at least as effective as staurosporine in killing the SCaBER cells. In fact, PAM outperforms staurosporine by killing an order of magnitude higher number of cells at 10 h post treatment while both seem to have a similar effect for longer times. The number of live cells indicates that 4 min PAM applied for 10 h over SCaBER cells has an efficiency equivalent to 1 µM staurosporine applied for 24 h.
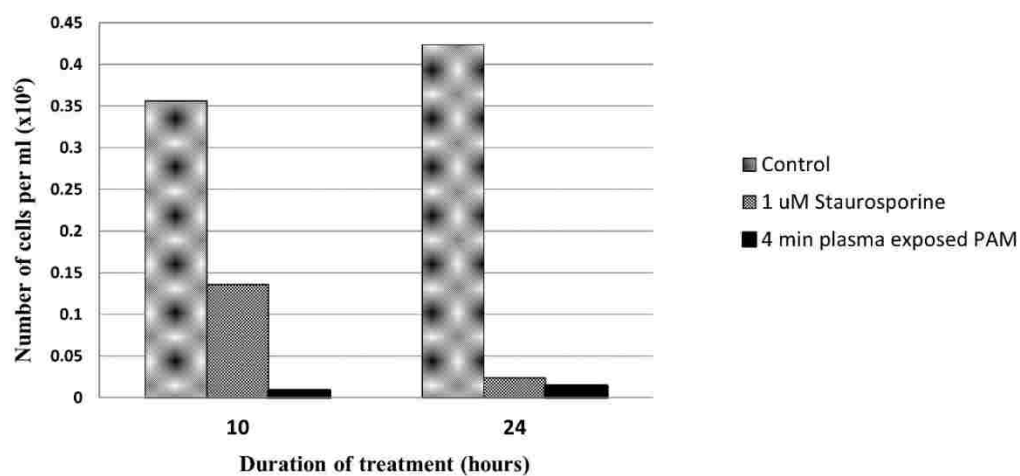
Figure 16. Staurosporine vs. PAM treatment. SCaBER cells were incubated by 1 µM staurosporine and 4 min PAM and cells viability counted at 10 h and 24 h after treatment using the trypan blue exclusion assay [89].

III.2 CONCENTRATION OF HYDROGEN PEROXIDE IN PAM

Hydrogen peroxide is an important ROS by being able to penetrate the cell membrane. It intermediates in many reactions and results in more ROS production such as $OH^•$ although, it is not a radical species [59]. The concentration of H_2O_2 was measured in MEM PAM and in serum-free PAM immediately after PAM preparation and over times after aging (see Figure 17). The Amplex red measurements indicate the presence of hydrogen peroxide in PAM in an exposure time-dependent manner. As can be seen in Figure 17A, the concentration of H_2O_2 increases in PAM by increasing the plasma exposure time. 2 and 4 min PAM contained around 130 and 350 µM of hydrogen peroxide, respectively.

It was found that H_2O_2 degrades in PAM over time. The longer the aging time, the lower the concentration of H_2O_2. For instance, H_2O_2 concentration in 2 min PAM reduces by 18%, 45%, and 80% after 1, 8, and 12 h aging, respectively. Interestingly, it was observed that the effectiveness of PAM against SCaBER cells reduces as a function of aging time. Looking at the results of 2 min PAM efficiency in Figure 12 and at the level of H_2O_2 for different aging times in Figure 17A indicates that both killing efficiency and H_2O_2 concentration follow a similar reduction trend. The correlation between the efficiency of PAM and the H_2O_2 level for different aging times manifests the important role of hydrogen peroxide in the anti-cancer effect of PAM. Similar to the 2 min PAM, aging led to H_2O_2 concentration reduction in 4 and 6 min PAM. In 4 min PAM, H_2O_2 concentration reduces by around 15%, 40%, and 72% after 1, 8, and 12 h aging, respectively. However, in the case of 4 min PAM, the level of ROS concentration was still above a tolerable level for SCaBER cells even after 12 h aging. Although H_2O_2 concentration was reduced by around 70% at 12 h after aging, its toxicity level was still drastically high for SCaBER cells as it caused a log reduction in cells viability.

Figure 17B presents H_2O_2 concentration in a serum-free PAM after 8 h aging. The level of H_2O_2 is approximately 2 times higher in a serum-free PAM than in PAM containing serum (Figure 17A), depending on the plasma exposure time. At a longer exposure time, such as 6 min PAM, differences between the two concentrations is a bit lower which reveals the limited scavenging capacity of the serum. According to the Fenton reaction which was proposed by Haber and Weiss [90]:

$$Fe^{2+} + H_2O_2 \rightarrow Fe^{3+} + OH^• + OH^- \tag{3}$$

$$OH^• + H_2O_2 \rightarrow HO_2^• + H_2O, \tag{4}$$

H_2O_2 reduces into $OH^{\bullet}$ and $HO_2^{\bullet}$ (hydroperoxyl radical) in the presence of Cu^{2+} or Fe^{2+} ions. Serum added in a cell culture media contains metallic compounds like ferrous ions. As it is expected presence of it in PAM scavenged the LTP-generated hydrogen peroxide. This result specifies the importance of chemical formulation of media in modulating the concentrations of ROS and determining the stability of PAM.
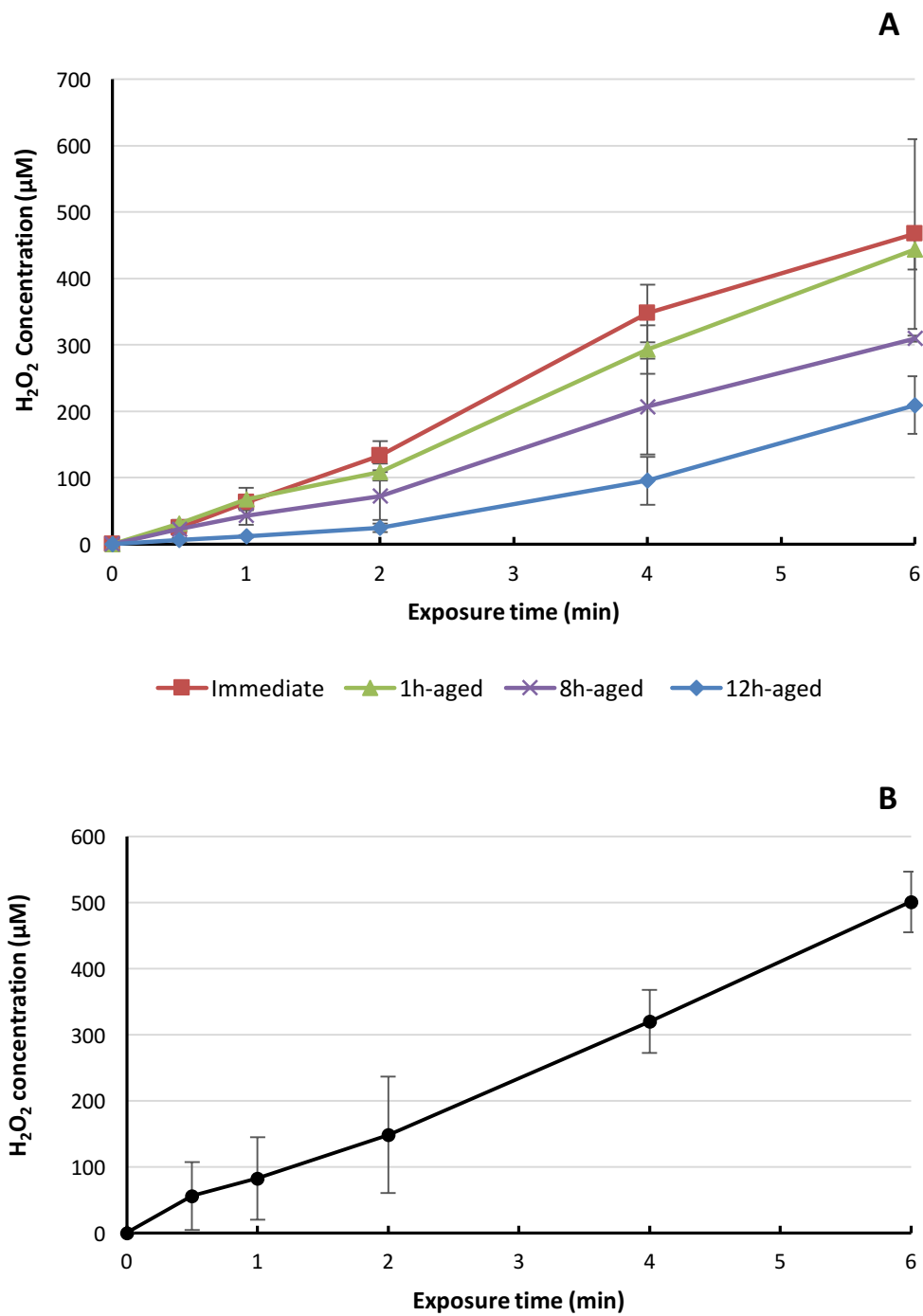
Figure 17. A) Concentration of H_2O_2 versus plasma exposure time measured in MEM immediately after plasma exposure and 1, 8, and 12 h after aging. B) H_2O_2 concentration in a serum-free PAM was measured after 8 h aging. Data represent the mean ± SD of three independent experiments.

EMEM PAM was used to treat MDCK normal cells and the H_2O_2 concentration in it was measured immediately after plasma exposure as shown in Figure 18. This result indicates that the level of H_2O_2 in EMEM PAM (including serum) is proportional to the exposure time, similar to MEM PAM. The goal of this experiment was to examine how the slight difference between the chemical compositions of these two media is important in their subsequential effect on cells viability. Comparing the result of Figure 18 with the one of immediate MEM PAM showed in Figure 17A reveals that the H_2O_2 concentration (μM) is in the same order of magnitude in both types of PAM. This outcome supports our assumption and indicates that the minor differences in EMEM and MEM chemical formula have a negligible impact on the cell viability results.
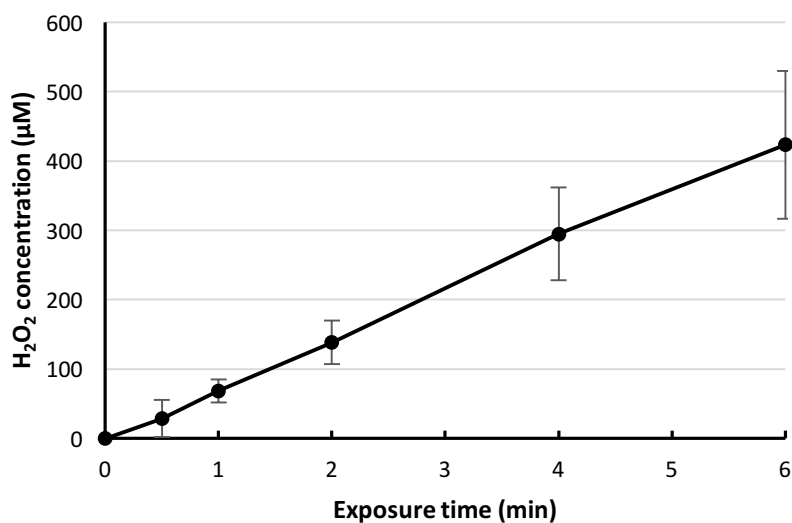
Figure 18. H_2O_2 concentration was measured in EMEM PAM immediately after plasma exposure.

III.3   RESULTS OF CASPASE-3 ACTIVITY IN PAM TREATED SCaBER CELLS

Caspase-3 is a widely used indicator of apoptosis. Caspase-3 is a member of caspases family and is considered to be the most important executioner among other caspases [91]. In order to understand the mechanism of cell injury in plasma treated SCaBER cells, the caspase-3 activity was investigated using ApoAlert1 Caspase Colorimetric Assay Kit (Clontech Laboratories, Inc.). Figure 19A and B shows the level of caspase-3 measured in SCaBER cells treated by 2 min PAM and staurosporine. Caspase-3 is an early apoptosis inducer [92] therefore cells morphology and activity measurements were conducted at short time after PAM treatments. In staurosporine treated samples, morphology of cells began changing drastically after 6 h and most of cells were dead by 10 h. Hence, caspase-3 measurement was conducted at 4 and 6 h after staurosporine treatment. Likewise, the measurement in 2 min PAM treated cells was conducted up to 10 h post-PAM application before widespread cells death. As can be seen in Figure 19B, the magnitude of absorbance in the PAM treated samples does not show a meaningful elevation in the caspase-3 activity compared to the control. The highest level of caspase-3 in PAM treated samples was measured at 6 h, with around 1.5-fold increase. The highest level of caspase-3 activity was detected in staurosporine treated cells at 6 h after treatment with around 4-fold increase in comparison with the control. These outcomes suggest that cell injury pathway induced by PAM treatment could be a caspase-independent apoptosis or a necrotic cell death.
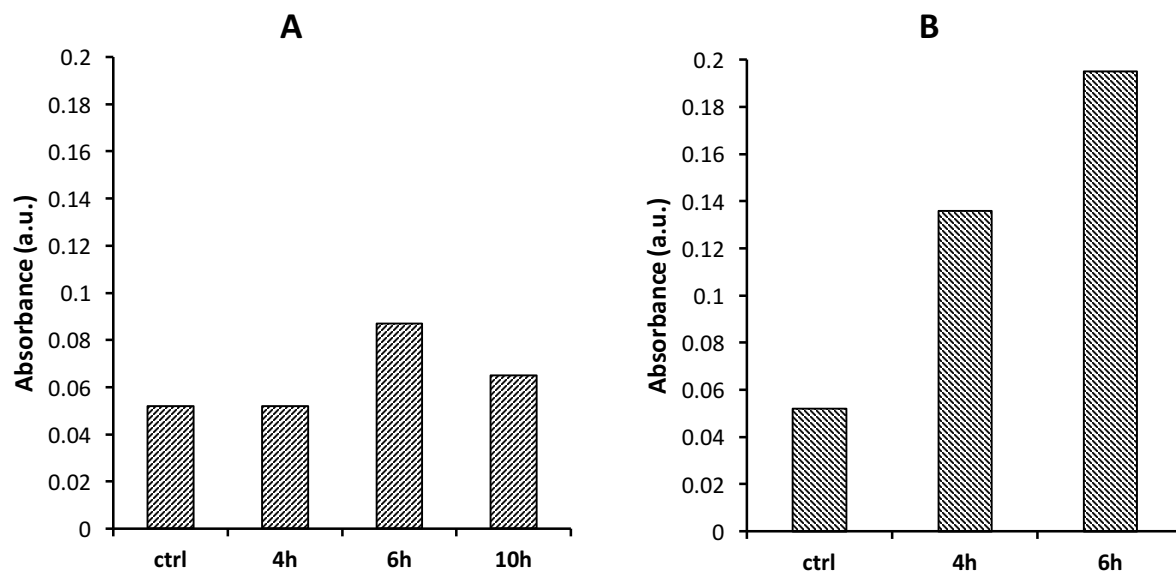
Figure 19. Level of caspase-3 in A) 2 min PAM treated SCaBER cells and B) staurosporine treated cells which was measured at various times after treatment using Apoalert kit. Absorbance (a.u.) was measured at 405 nm in both control and treated samples.

Caspase inhibitors are used to explore the overall roles of proteases in an apoptotic process. Synthetic tetrapeptides DEVD-CHO and DEVD-fmk are examples of caspase-3 inhibitors in which the first one is a reversible inhibitor and the latter is irreversible [93]. In another experiment, caspase-3 inhibitor was used to validate (examine) the result achieved by caspase-3 assay kit. This inhibitor blocks apoptosis through caspase-3 activation. For this purpose, SCaBER cells cultured in a 96-well plate were incubated with DEVD-fmk 100 μM for 30 min prior to any treatment. Then, the inhibitor solution was discarded and cells were either treated with 2 and 4 min PAM or were treated with only fresh media (negative control). As a positive control, SCaBER cells sample did not receive any DEVD-fmk inhibitor incubation and were treated with PAM as before. Cell viability was assessed at 8 and 12 h post-PAM application using MTS assay. Cells morphology was monitored using bright-field microscopy.

After addition of caspase-3 inhibitor, it was observed that the morphology of cells was changed and cell-surface attachment was gradually diminished (see Figure 20A). However, non-PAM treated cells (negative control) recovered their normal morphology after removal of inhibitor solution (see Figure 20B).

Figure 21 are images of PAM treated SCaBER cells after 12 h in two conditions: with and without DEVD-fmk incubation. The bright-field images, as shown in Figure 21A-D, indicate that samples underwent similar morphological changes independent of the inhibitor addition. Besides, MTS assay results supported the morphological observations and indicated that cells viability results were similar in both conditions in 2 and 4 min PAM treated samples Figure 22 shows the result of MTS assay measured at 12 h post-PAM application in samples pre-incubated with DEVD-fmk inhibitor (shaded bars) versus samples not incubated with the inhibitor (blank bars). There is not a meaningful difference between two groups indicating that PAM treatment suppressed cell viability of both groups in a similar trend. According to this result, caspase-3 inhibitor could not prevent cell death induced by PAM treatment. This failure in blocking cell death indicates that PAM treatment induces caspase-independent cell death in SCaBER cells. The mechanism of cell death could be via mitochondrial-mediated, lysosomal membrane permeabilization, or necrotic cell death.
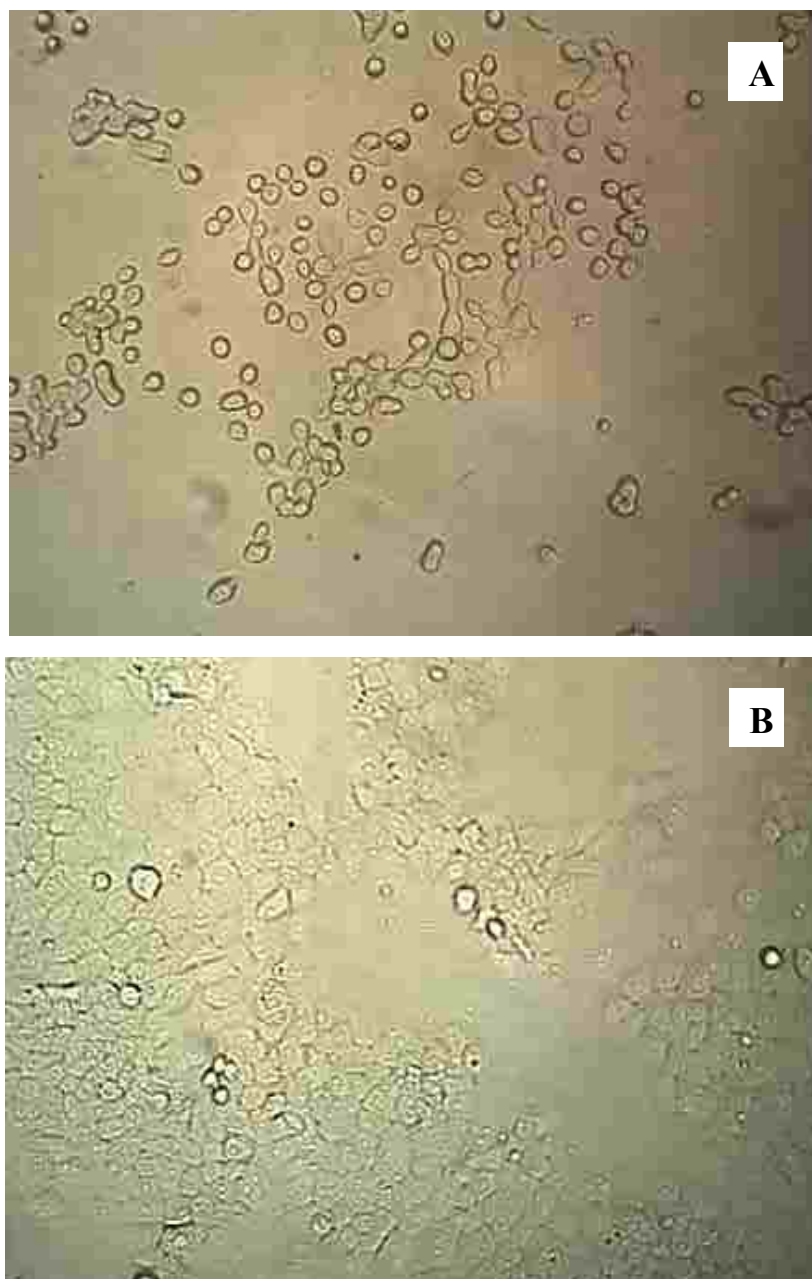
Figure 20. SCaBER cells were incubated with 100 µM DEVD-fmk (caspase-3 inhibitor) for 30 min. Image of cells taken at A) 45 min and B) 12 h after incubation. After addition of DEVD-fmk, cell-surface attachment was gradually diminished (A); however, cells recovered their normal and spread morphology after removal of the inhibitor solution (B).

Caspase-3 inhibitor   **No inhibitor**
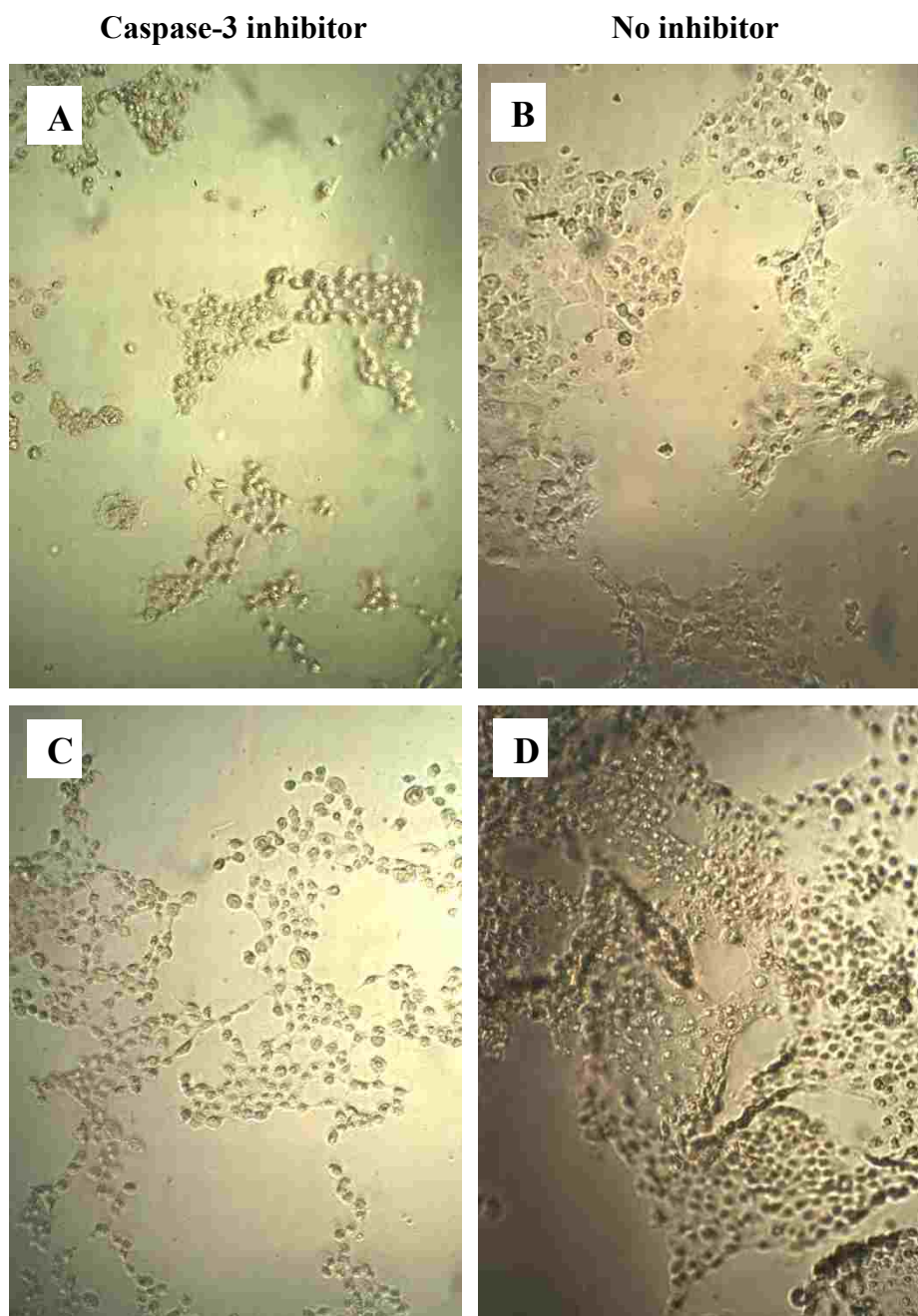
Figure 21. Images of SCaBER cells at 12 h of PAM treatment. A) and B): 2 min PAM treatment with and without prior incubation with 100 µM DEVD-fmk, respectively. C) and D): 4 min PAM treatment with and without prior incubation with 100 µM DEVD-fmk, respectively. Cells morphology and damages in both groups with and without inhibitor incubation are similar which indicate that PAM treatment induces similar effect on SCaBER cells independent of the DEVD-fmk inhibitor addition. The MTS assay result supported these observations.
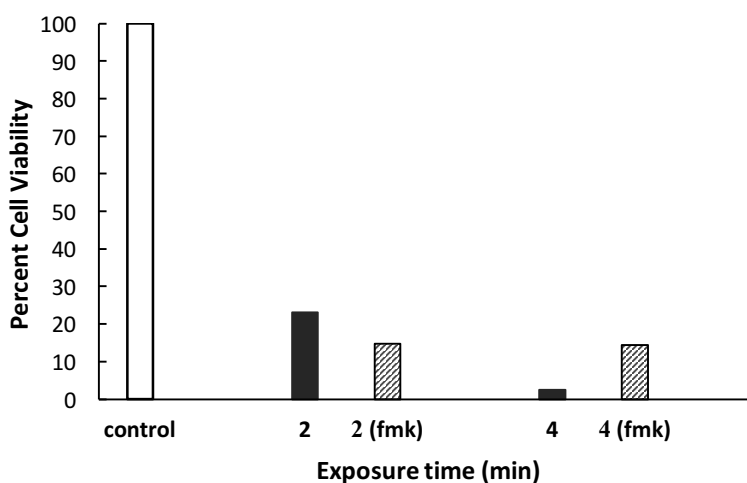
Figure 22. The percentage of the metabolically active cells at 12 h after PAM application using MTS assay. Shaded bars are cells pre-incubated with DEVD-fmk inhibitor and black bars are samples not incubated with the inhibitor. Since there is not a meaningful difference between cell viability of these two groups and caspase-3 inhibitor did not prevent cell death induced by PAM treatment, it is concluded that the mechanism of cell death was caspase independent.

III.4   EFFECTS OF PLASMA ON REATTACHMENT OF SCABER CELLS

The time evolution of SCaBER cells attachment was monitored after direct plasma treatment and are shown in Figure 23. The cells were treated with the plasma pencil after seeding and before cells started to attach to the surface of the plate. Round-shaped cells remain in suspension and are not actively attaching to the bottom of the cell culture plate. However, after reattachment the morphology of cells turn into a spread shape. As can be seen in Figure 23, all the cells were in suspension at zero hour (right after plasma treatment). At later times, cells started attaching to the surface of the plate. As shown in Figure 23A, at 1.5 h after seeding cells in the control sample started to attach to the surface (around 50% of the cells were attached) and cell morphology exhibits a spread shape. However, for the 2 min treated sample the attachment of cells initiated after 3 h (see Figure 23B). For the case of 5 min treated sample, most cells remained in rounded

morphology up to 4.5 h after seeding (Figure 23C) which indicates the attachment process experiences a longer delay. These observations suggested that plasma exposure induces an alteration in cell membrane characteristic resulting in a delay in the attachment of the SCaBER cells to the surface of the plate depending on the plasma exposure time. Results of this experiment were published in [94].

Immunofluorescence experiments – following the method discussed earlier in Section II.7 – was used to determine if any adverse effects on the actin of SCaBER cells was detectable. Actin is made of a group of proteins which polymerizes to form actin filaments in the cytoskeleton of eukaryotic cells. SCaBER cells were treated by 2 min PAM and immunofluorescence was conducted 4 h after PAM application. Images from immunofluorescence assay of control and PAM treated samples are shown in Figure 24. The overall filamentous actin organization in the control and PAM treated samples did not differ significantly.

Other investigations reported that plasma treatment affects cell attachment, similar to our observations. It was shown that a miniature plasma jet detached cells from the surface of a cell culture plate [32]. Detached cells remained metabolically active as they were able to adhere to a surface and grow successfully after transplanting to a new plate. Similar results were reported for non-small cells lung cancer (NSCLC) [29]. According to this research, cell detachment occurred at the area of the direct impact of the plasma needle even after a short exposure time but detached cells that remained alive could reattach to the surface. Also, the presence of a thin layer of culture media inhibited the cell detachment. They concluded that cell detachment by the plasma needle was the result of a physical process on the cells [30].
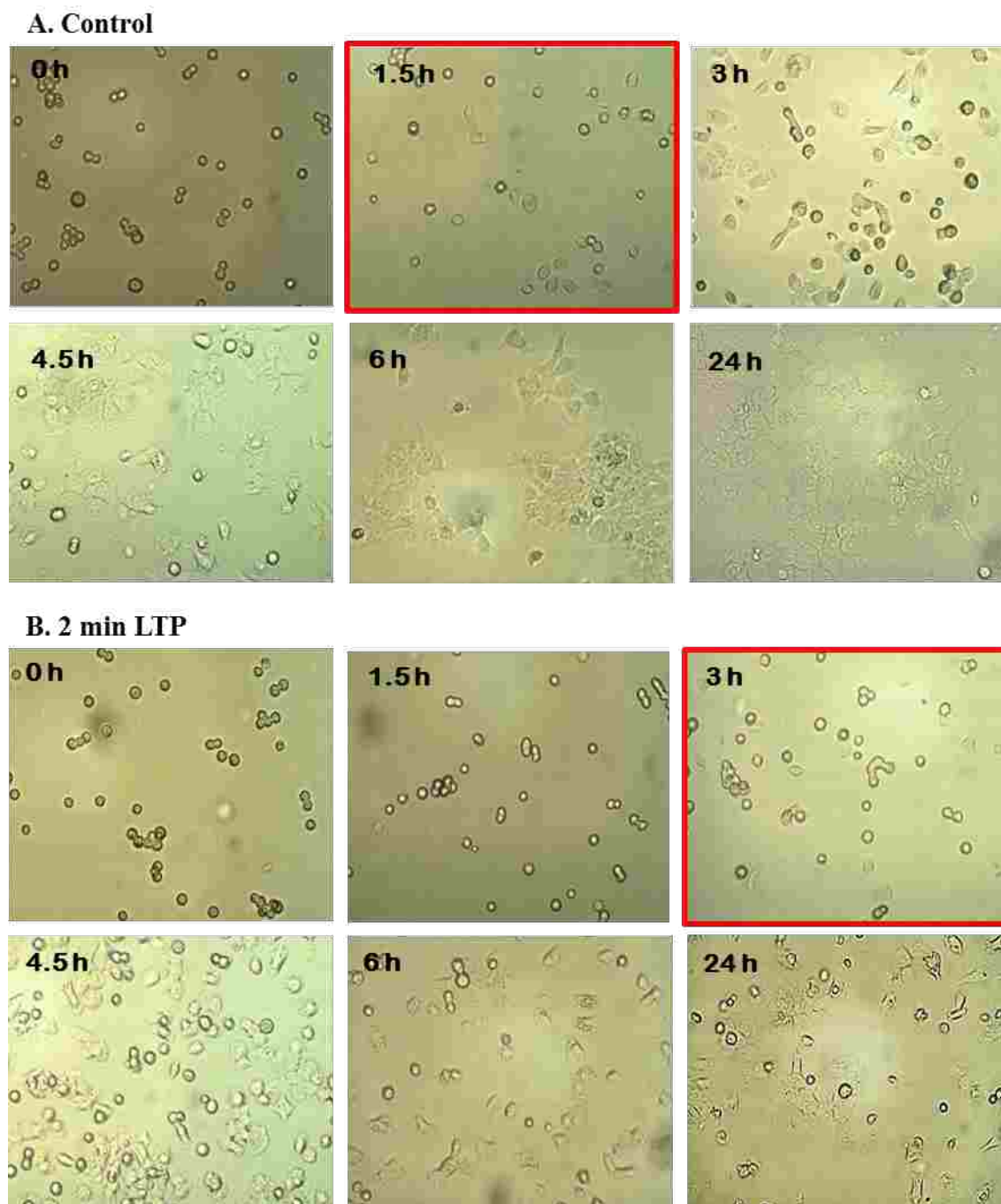
Figure 23. Images of SCaBER cells attaching to the surface of a culture plate at different times after seeding. Photos were taken at specific times as noted on each image. Panel A) is the control SCaBER cells, panel B) is a 2 min LTP treatment, and panel C) is a 5 min LTP treatment [94].

Figure 23. (Continued).

C. 5 min LTP
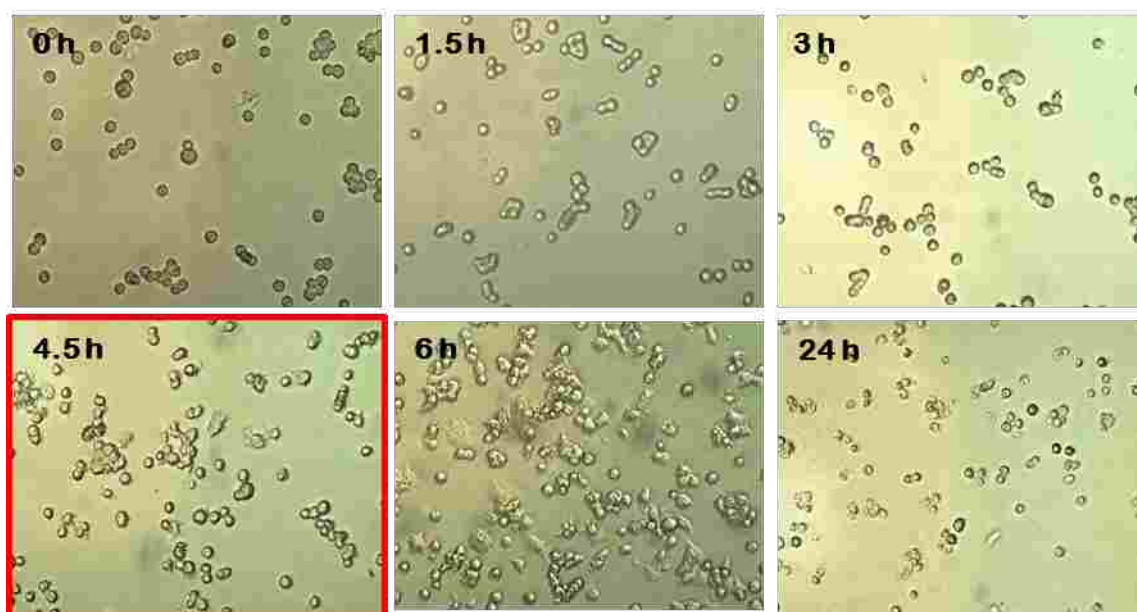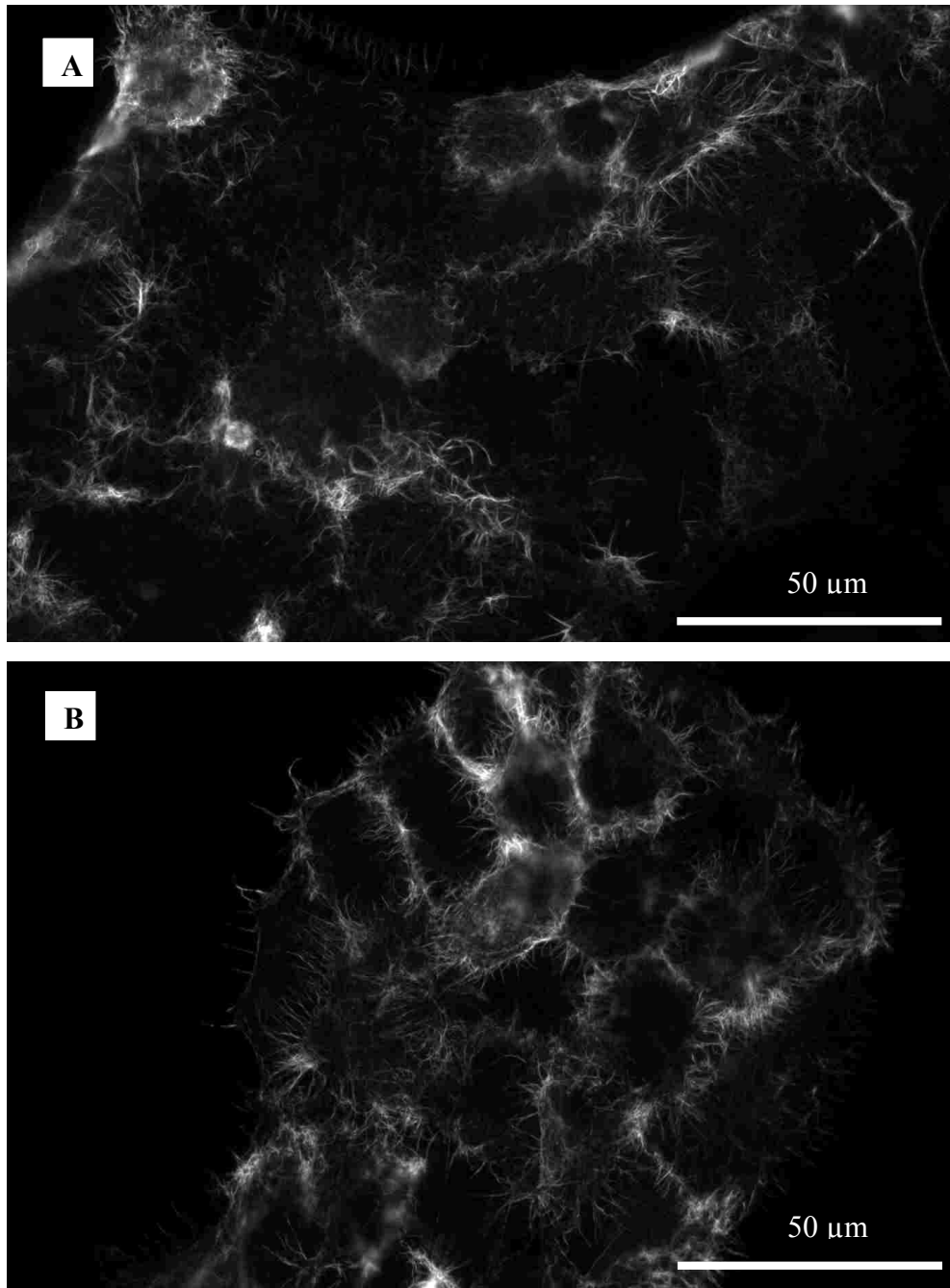
Figure 24. Images of fluorescence immunostaining of actin filaments in SCaBER cells A) control and B) PAM treated sample. SCaBER cells were treated by 2 min PAM and immunofluorescence was conducted 4 h after PAM treatment. This result shows that PAM treatment did not cause any damages or adverse effects on the actin filaments of SCaBER cells as the immunostaining images of control and PAM are similar. Scale bar of 50 μm at 40X magnification.

III.5   SUMMARY

In this chapter, effects of LTP treatment on epithelial cells were investigated and results of experiments were represented and discussed. The first part showed the effects of direct and PAM treatment on the viability of SCaBER cells. It was observed that the viability of cells decreases by increasing the plasma exposure time. It was also reported that diluted PAM has an equivalent effect on cells viability as the plasma exposure time. Results of aged-PAM on SCaBER cells were shown. It was found that the efficiency of PAM against SCaBER cells decreases over time. This reduction in the efficiency of PAM was more remarkable at shorter plasma exposure time since, longer plasma-exposed PAM remained highly effective.

Measuring the concentration of H_2O_2 in PAM confirms the important role of ROS in the anti-cancer properties of PAM. The concentration of H_2O_2 was moderately high in PAM when measured right after plasma exposure. However, its concentration gradually dropped over time. It was shown that there is a similar trend between the reduction of PAM efficiency and the decrease in H_2O_2 concentration. This correlation supports the hypothesis that LTP treatment instigates oxidative stress in cells and the dose of LTP-generated ROS determines the fatal effects of the treatment. Furthermore, it was shown that LTP treatment results in DNA damage by manifesting rapture in a treated molecular beacon. Mechanism of cell injury was evaluated in PAM treated SCaBER cells by analyzing caspase-3 activity. The outcome of this experiment suggested that the cell death is through caspase-independent pathways.

CHAPTER IV

RESULTS OF PAM TREATMENT ON NORMAL CELLS

IV.1   PAM TREATMENT OF NORMAL CELLS

One of the important aspects of a cancer treatment method is to have minimum killing or side effects on normal cells in the tissue surrounding a tumor. Therefore, it is important to understand how plasma treatment affects normal healthy cells. Effects of PAM treatment was assessed on normal epithelial cells from a canine kidney tissue (MDCK) and the results are shown in Figure 25. Figure 25**Error! Reference source not found.**A shows the percentage of the metabolically active cells analyzed at 12, 24, and 48 h post-PAM applications. Cells were exposed to PAM the entire time of treatment prior to MTS assay which was 12, 24, and 48 h. These results indicated no significant changes in the viability of MDCK cells up to 3 min PAM. Using 4 min and 6 min PAM induced around 10% and 20% reduction in metabolic activity of normal cells after 12 h, respectively. However, PAM created with a longer exposure time (10 min PAM) resulted in one log reduction in the metabolic activity of cells. As seen in Figure 25**Error! Reference source not found.**A, there was no delayed effect of PAM (12, 24, and 48 h of PAM treatment resulted in equivalent kill ratio).

For a better interpretation of MDCK response to PAM treatment, the raw data of cell viability (cells/ml) are shown in Figure 25**Error! Reference source not found.**B. The number of viable cells was quantified with MTS and trypan blue exclusion assays. The black column (initial cell concentration) represents the number of cells at the time of PAM application. As can be seen in **Error! Reference source not found.**B, within the 48 h of monitoring, the number of live cells grew in the control as well as in samples treated by PAM that was created with a lower exposure time. In the case of 10 min PAM, the number of metabolically active cells was lower than the initial cell concentration which clearly reveals widespread cell death. In PAM samples up to 3 min, the trend of cell proliferation is similar to the control; however, cells growth in 4 and 6 min PAM was decreased slightly. This reduction in cells growth (lower number of live cells) can be due to an inhibition of cell proliferation. Results of further experiments supported this observation which will be discussed under the time-lapse microscopy and immunofluorescence results. Therefore, it was concluded that the dose of plasma exposure is highly consequential in determining the harmful

effect of PAM on normal cells. PAM with a moderate intensity (i.e. moderate exposure time) can affect cells proliferation while, a highly
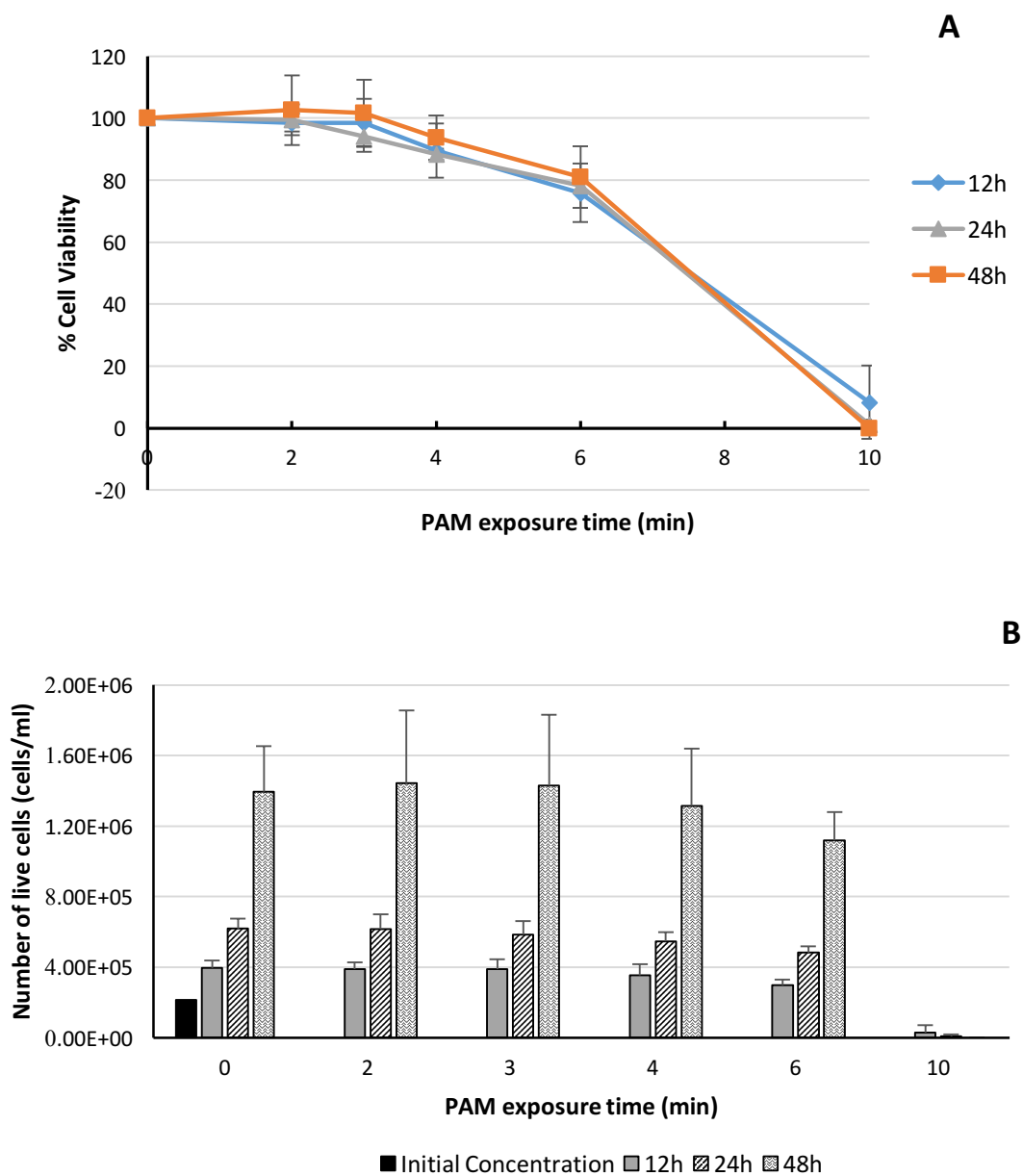
Figure 25. Effect of PAM produced by different exposure times on the viability of non-cancerous MDCK cells using MTS assay and trypan blue exclusion assay at 12, 24, and 48 h post-PAM treatment: A) Percent of cell viability normalized to the control and B) number of metabolically active cells (cells/ml). Initial concentration represents the number of cells at the time of PAM treatment. Results from 3 independent experiments with two replications are shown as means ± SD.

plasma activated medium (i.e. longer exposure time such as 10 min PAM) can induce significant cell death in normal cells.

Figure 26 shows the response of SCaBER and MDCK cells to PAM treatment at 12 h post-PAM application. As it clearly shows, SCaBER cells were considerably more susceptible to PAM treatment than MDCK cells. For instance, a 4 min PAM induced more than 90% reduction in the viability of SCaBER cells in contrast to MDCK cells which underwent only 10% reduction. This clearly reveals that, unlike the case of SCaBER, PAM treatment does not have severe damaging effects on normal MDCK cells at exposure time below 4 min.
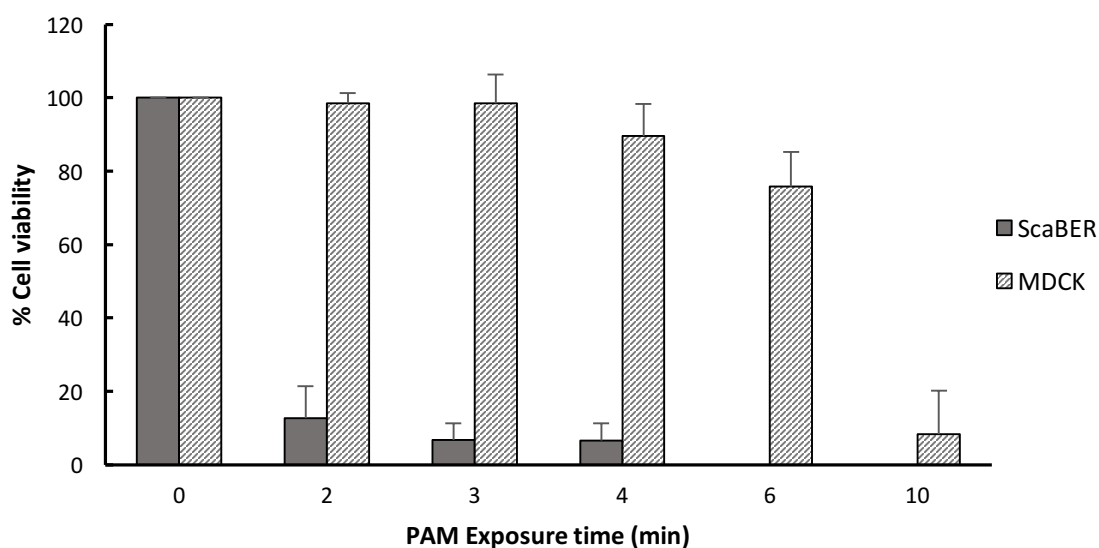
Figure 26. Cell viability of SCaBER and MDCK cells treated by PAM with different exposure times measured 12 h post PAM application.

As it is mentioned earlier, it is important that a therapeutic method has no or a minimum impact on normal cells and surrounding tissues of a treated tumor hence, an ideal method will selectively target cancer cells without harming normal cells. This reflects the selective effect of a treatment method. Other research groups investigated the response of cancer and normal cells to LTP-treatment and reported similar results in that, cancer cells were more susceptible to the LTP treatment than normal cells, depending on the cell type [33, 37, 50, 95, 96].

Iseki *et al.* used two independent ovarian cancer and normal fibroblast cells to evaluate the selective effect of plasma on cells viability and proliferation. They reported that direct plasma treatment was effective to kill cancer cells while normal fibroblast cells were mostly undamaged [97]. In another study, Kim *et al.* [98] showed that cancer cells were more influenced by the direct plasma treatment than normal cells although both cell types were under an NO-mediated oxidation. They measured NO concentration in normal and cancer cells and reported that the level of NO was lower in the normal cells (foreskin fibroblast and bronchial epithelial) than the cancerous type (lung adenocarcinoma cells). In addition, they reported that the concentration of NO_2^- was higher in cancer cells compared to the normal cells. NO_2^- and NO_3^- are the by-products of NO and are used as convenient markers of NO [99]. As mentioned earlier, NO has cytotoxic effects such as reactions with proteins and nucleic acids plus induction of NO-mediated apoptosis [98]. In another work, Guerrero-Preston and colleagues [96] showed that direct LTP treatment selectively killed the HNSCC (head and neck squamous cell carcinoma) cells with a non-apoptotic mechanism while minimally affected normal oral cavity epithelial cells.

The answer to the question of why cancer cells are more susceptible to LTP treatment than normal cells lays to the characteristic differences of these cells that originated from their metabolism. A low concentration of ROS are beneficial for cells and have an important role in regulating cell signaling pathways and affects cellular processes such as metabolism, proliferation, differentiation, and survival processes like apoptosis, antioxidant response, and DNA damage response [42, 57, 74]. NADPH (nicotinamide adenine dinucleotide phosphate) and NOX (NADPH oxidase) are involved in the production of a low level of ROS via an oxidation-reduction (also known as redox) process [100]. A moderate level of ROS activates stress-responsive genes such as HIF1A (Hypoxia-inducible factor 1-alpha) which, in turns, leads to the expression of proteins that modulate pro-survival signals in cells [101]. Ultimately, a high dose of ROS creates irreversible havoc in cells by causing damages to macromolecules and DNA, resulting in

apoptosis. Under these conditions, antioxidant molecules act as a cell defense system to defeat ROS damage by reducing excessive level of ROS such as reduced GsH (glutathione) and TrX (trithorax) [101].

Metabolic activity of cancer cells is different from normal cells. In fact, tumor cells set up mutations in their metabolic activities in order to support their abnormal growth and survival. Following are three basic requirements for dividing cancer cells which need to be modified: generating ATP faster to sustain the energy level in a tumor cell, enhancing biosynthesis of macromolecules, and increasing the maintenance of intracellular redox to keep it at an appropriate level [101]. Therefore, these alterations result in a high ROS production and a high antioxidant level in cancerous cells.

Figure 27 is a schematic that indicates how the ROS level relates to cells viability. As it was explained earlier, lower level (yellow) of ROS is beneficial in cell proliferation and survival. However, excessively high level (purple) of ROS causes detrimental oxidations that can result in cell death. The antioxidant system protects cells from such oxidative damages by reducing ROS from a high accumulated level. In a cancer cell, abnormal metabolism and protein translation generate irregular high levels of ROS. The mutations and adaptations in a cancer cell allow cells to avoid the detrimental effects of high ROS levels by regulating antioxidants and ROS in such a way that the cell survives in a moderate level of oxidative stress (blue).
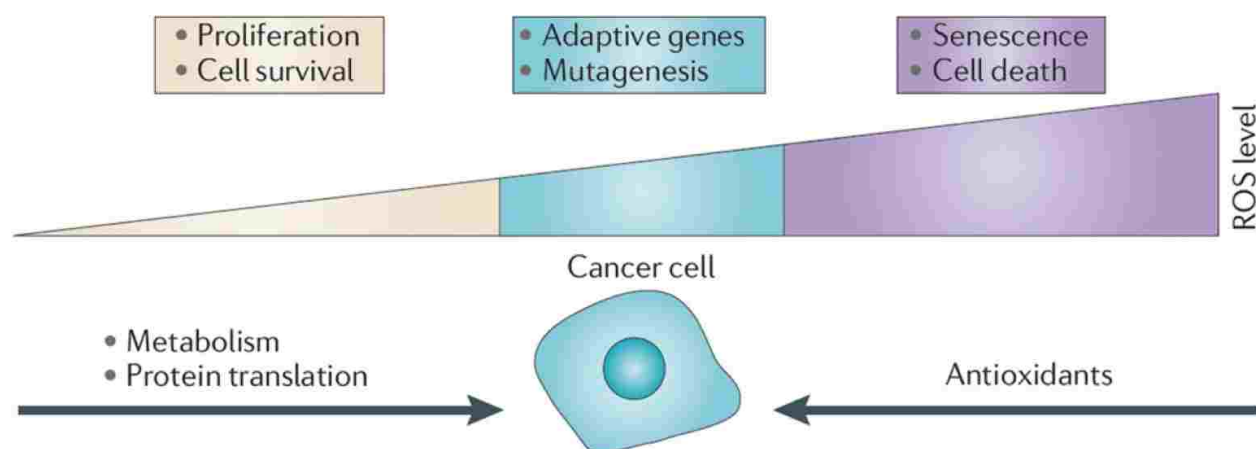
Figure 27. Reprinted by permission from Nature Publishing Group: Cairns *et al* [101]. Low levels of ROS in helping cell survival and proliferation while, high ROS levels cause detrimental damages. Cancer cells encounter an abnormally high oxidative stress and adapt to survive this condition by expressing more antioxidants to maintain a moderate level of ROS.

Because of the abnormal high level of ROS in cancer cells, they are more susceptible to a redox increment than normal cells. [1]. Therefore, one can regulate a dose of oxidative stress which causes an irreversible damage to cancer cells while normal cells survive under such a dose. Since the ROS levels in cancer cells are abnormally high, an induction of redox stress may push the level of ROS above an acceptable threshold and results in cell death. However, normal cells with their lower basal ROS level and higher antioxidant capacities can better survive the oxidative stress [1]. Consequently, the difference between intracellular ROS level in cancer and normal cells is one way to explain the selective effect of plasma. Figure 28 illustrates the basic idea behind the selective effect of redox stress.
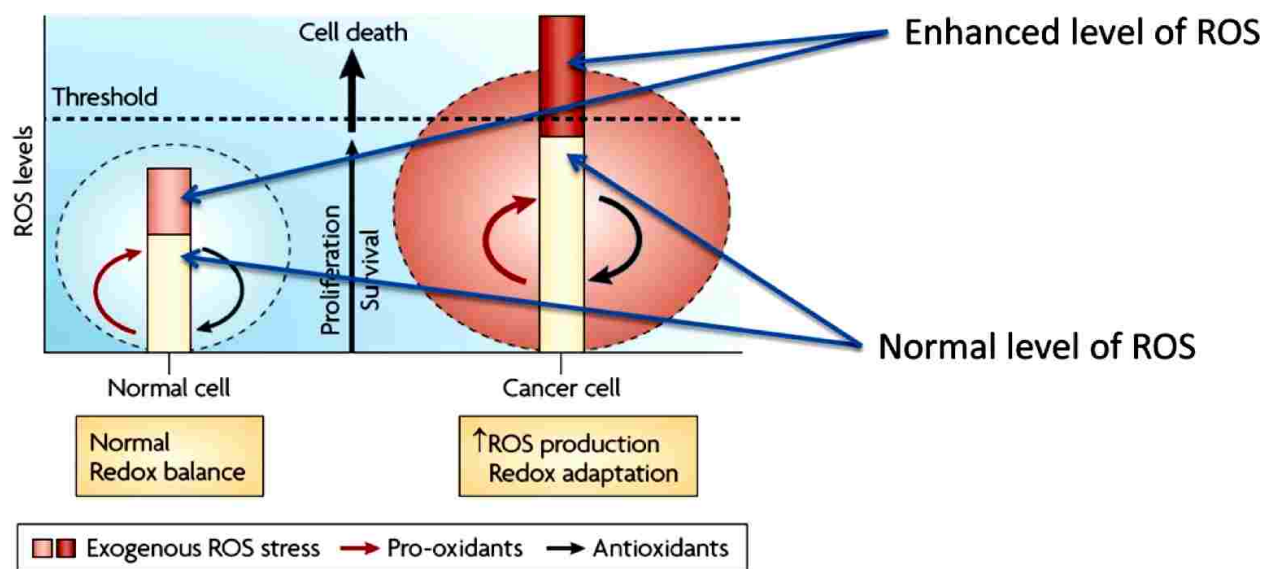
Figure 28. Reprinted by permission from Nature Publishing Group: Trachootham *et al.* [102]. Illustration of the base level of ROS in normal and cancer cells. An enhanced ROS stress pushes

the intracellular ROS which in the case of cancer cells may exceed the survival threshold and results in detrimental cell damages or cell death.

IV.2   TIME-LAPSE IMAGING OF MDCK CELLS

In order to ascertain the effect of moderate PAM treatment on MDCK cell morphology, proliferation, and migration in PAM and control samples, time-lapse phase imaging of the cells was carried out. As the result of MTS assay of MDCK cells in Figure 25B indicates, PAM treatment with moderate intensity affects cells proliferation rather than inducing widespread cell death. In this experiment, phase images of cells were taken every 10 min and continued up to 48 h after PAM addition. Figure 29A and B show images of control and PAM treated samples acquired at various time points. These images are selected from movies that are provided as online supplementary material. Figure 29A and Supplementary Movie 1 of a control sample demonstrate a rapid proliferation in cells over 48 h. In contrast, cells in the PAM treated sample did not show a similar increase in population number which is visually clear in Figure 29B and in the Supplementary Movie 2 of the PAM sample. Nevertheless, no major physical cell damage or shrinkage were observed in the time-lapse movies. These data support the results from the impact of moderate PAM on MDCK cells obtained by MTS assay.

The reduction in the number of live MDCK cells at the 48 hour time point in the PAM treated sample (compared to the control case) could be the net result of a combination of an increase in the rate of cell death and an inhibition of cell proliferation. To delineate the relative contributions of these factors, the number of dividing cells in the time-lapse sequence was manually counted using the ImageJ software and was normalized to the total number of cells at 0 h. Figure 30 shows an example of a dividing cell in a time-lapse sequence. During mitosis, the cell temporary rounds up, divides into two and the daughter cells re-spread onto the surface [103]. Such cell division events can be clearly seen in our phase time-lapse sequences, as shown in Figure 30: the cell morphology changes from being spread to round (associated with higher brightness in the periphery) indicating a loss of peripheral focal adhesions. After cell division, daughter cells spread back to recoup their interphase morphology (Figure 30).
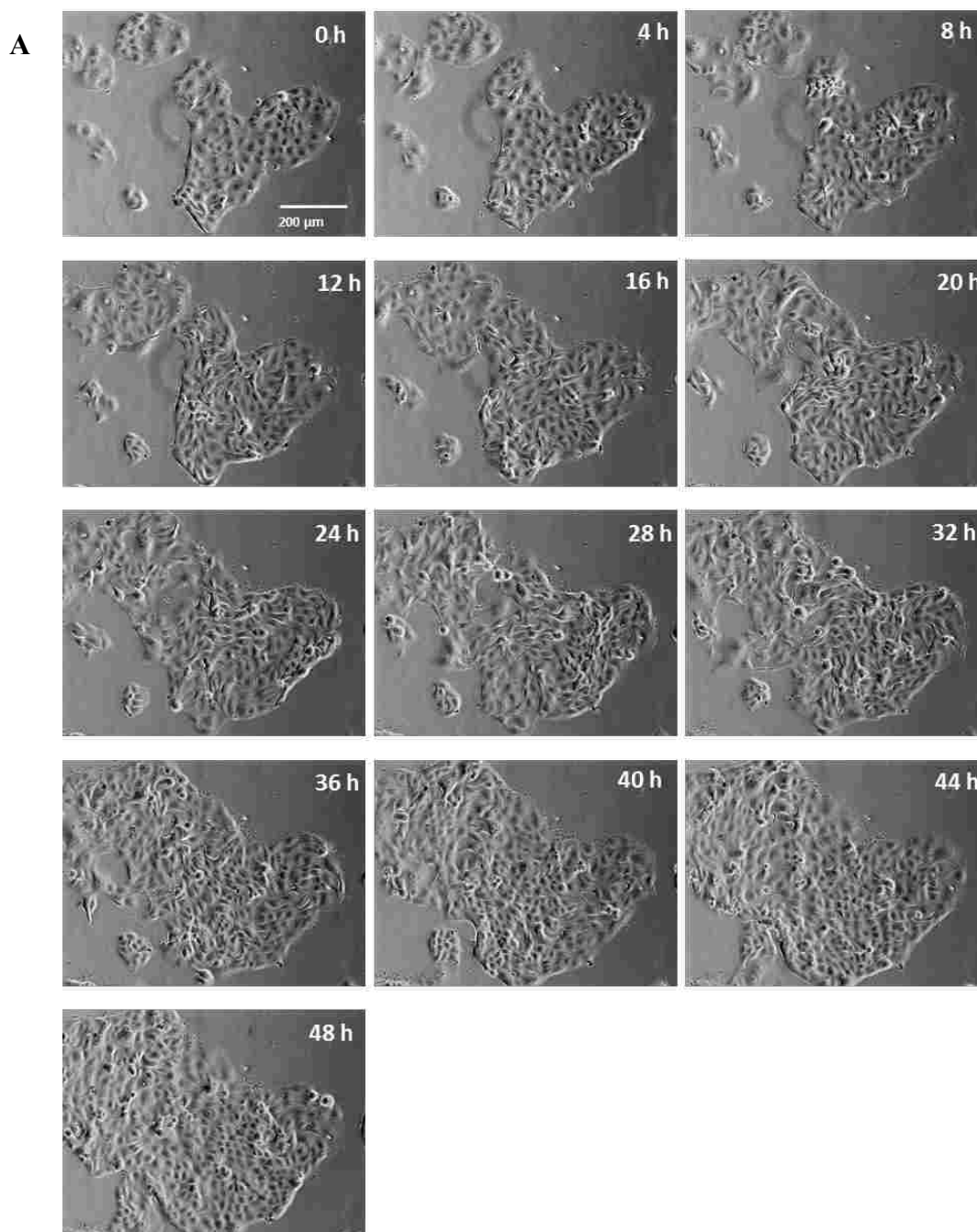
Figure 29. Phase contrast images of A) control and B) PAM treated MDCK cells obtained by time-lapse microscopy at different hours for a duration of 48 h. Cells in the control sample multiplied during the 48 h of time-lapse imaging and cell islands were expanded while, the number of cells in the PAM treated sample did not increase in population likewise. Nevertheless, no major physical cell damage or shrinkage are observable in theses time-lapse images. These data suggest that a moderate PAM affect proliferation of MDCK cells. Scale bar: 200 μm.

Figure 29. (Continued).

B
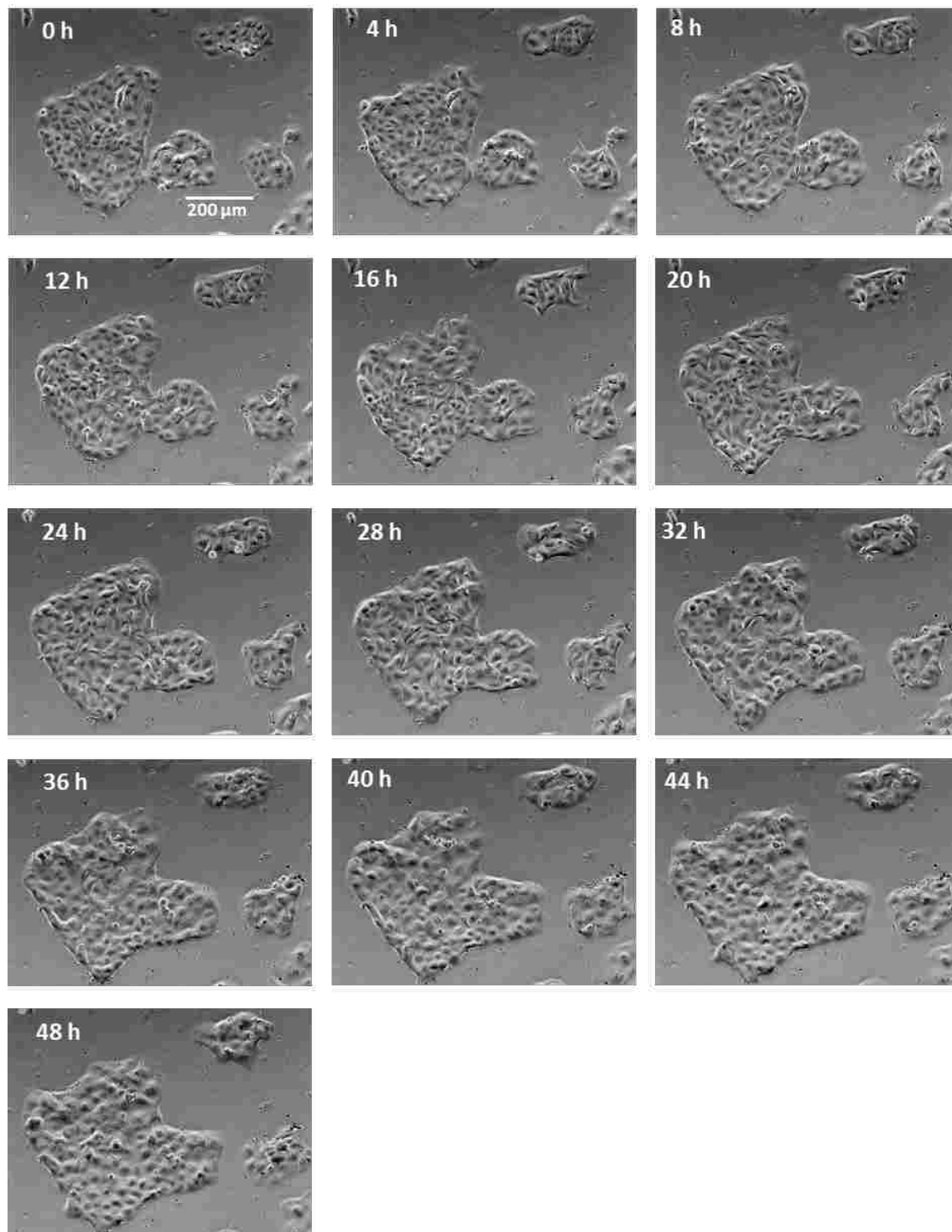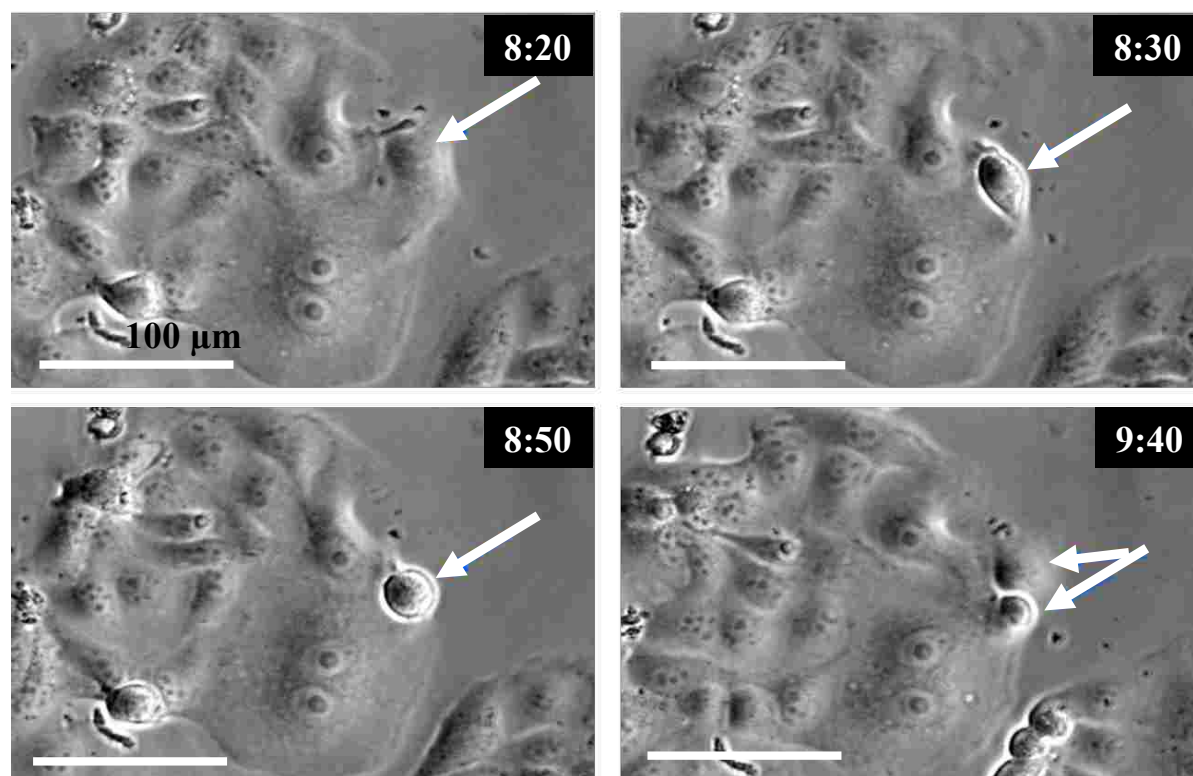
Figure 30. Phase-contrast images obtained from time-lapse imaging (of control sample) show reshaping of a dividing cell (arrow) which adopts a round morphology from a spread shape and the daughter cells then re-spread after cell division. White arrows show a cell going through cell division process and is divided into two daughter cells. Time is indicated in hour:min. Scale bar of 100 μm.

Figure 31 shows the number of division events normalized by the initial number of cells in the control and PAM samples. The numbers of dividing cells were counted in each movie acquired from 48 h of time-lapse imaging. According to these data, the number of dividing events (cell division) decreased by around 75% in PAM treated sample. This result indicates that cell proliferation was significantly reduced in PAM treated cells ($p < 0.001$) and suggests that mitigation in the cell growth was associated with cell proliferation inhibition rather than widespread cell death.
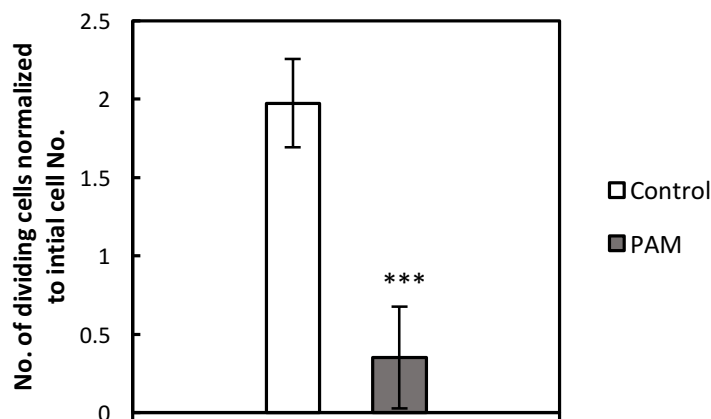
Figure 31. Number of division events normalized by initial number of cells in control and PAM as quantified from time-lapse images during 48 h of PAM treatment. Data represent averages from 6 movies from two independent experiments as means ± SD. An independent *t*-test indicates that cell proliferation was significantly lower in PAM treated samples (mean = 1.97, SD= 0.28) than control (mean = 0.40, SD= 0.32), t(10) = 8.987, *** P<0.001.

IV.3   INHIBITION OF PROLIFERATION OF MDCK CELLS

In order to confirm the inhibition of cell proliferation induced by PAM, the nuclear localization of Ki-67, a marker of cell proliferation, was ascertained using immunofluorescence. Ki-67 is a protein that is present in all active phases of a cell cycle including G_1 (growth and metabolism phase), S (DNA replication phase), G_2 (growth of structural elements and preparation for mitosis), and M (mitosis or cell division). However, Ki-67 is absent in the G_0 (resting cells) phase [104]. That is why the expression of human Ki-67 protein is associated with cell proliferation activity. Therefore, it is an excellent marker for determining the "growth fraction" of both normal and tumor cells and antibodies against Ki-67 protein are used to mark and diagnose proliferative cells [105]. Figure 32A shows immunofluorescence images from control and PAM treated MDCK cells in which Ki-67 has been stained. Ki-67 staining is markedly brighter in cells that are actively involved in proliferation. The number of Ki-67 stained cells were counted in at least 8 immunofluorescence images obtained with 10x magnification from PAM and control samples. Figure 32B shows the percent of Ki-67 stained cells, on average, in immunofluorescence images. As shown, the number

of Ki-67 stained cells is lower in PAM treated cells than in the control which indicates inhibition of proliferation. A chi-square test indicated a significant association between treatment and number of marked cells, $x^2(1) = 20.53, p < 0.05$. In fact, the percentage of stained cells in the control sample was 1.7 times higher than that for the PAM treated cells with a 95% confidence interval of (1.34, 2.11). This result supports the lower rate of cell proliferation in PAM samples as observed using time-lapse imaging and the lower rate of cell division as shown in Figure 31.

A

B
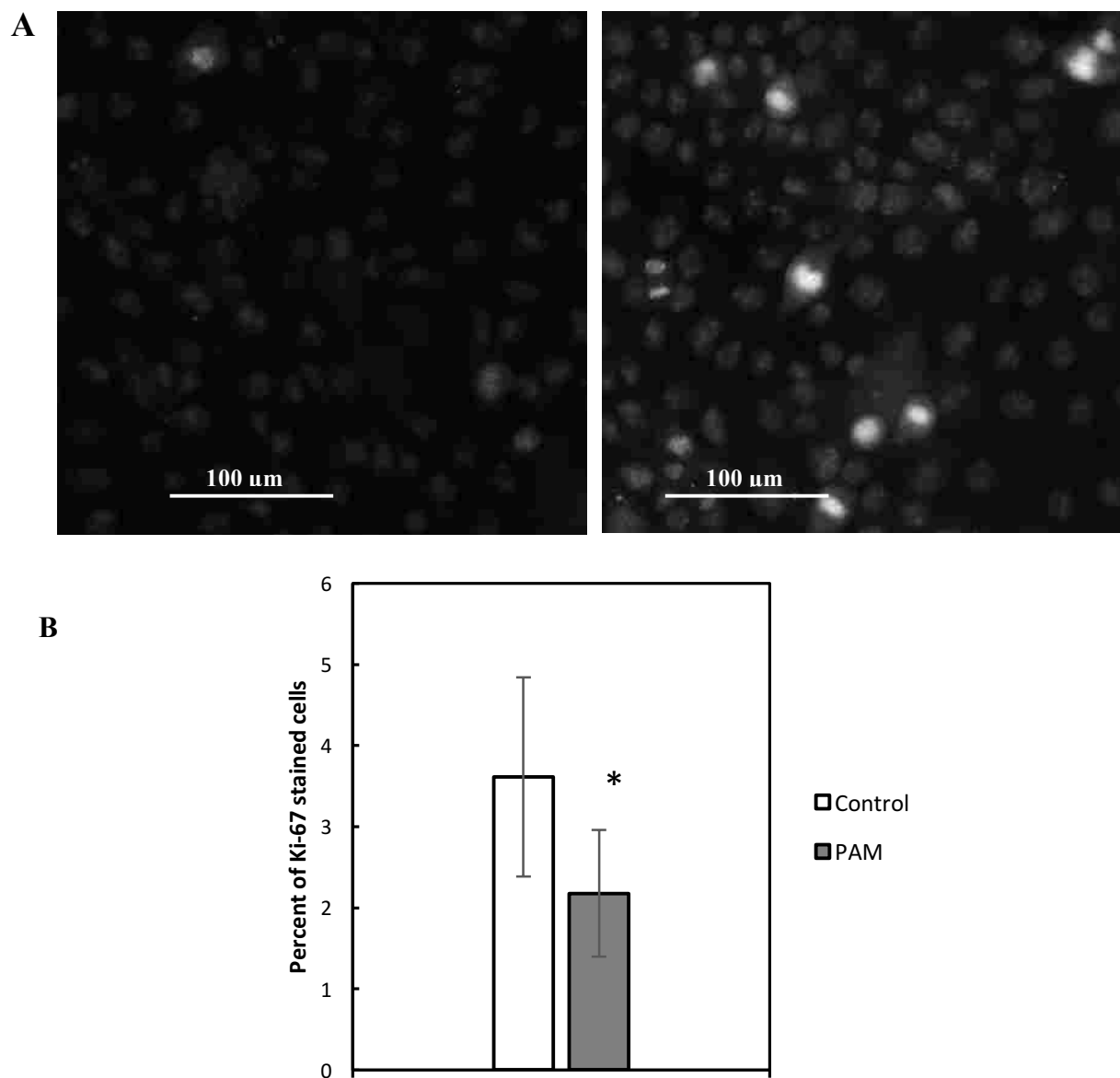
Figure 32. A) Immunofluorescence images of a control (right) and a PAM treated (left) sample. Nuclei are stained with DAPI to visualize cells. Cells with higher brightness are stained with Ki-67. B) The average percentage of Ki-67 stained cells in immunofluorescence images in PAM and control sample. PAM treatment inhibits ki-67 and arrests cell proliferation in MDCK cells. Data represent averages from at least 8 images from of two independent experiments as means ± SD. * $P<0.05$ (chi-square test).

IV.4 EFFECT OF PAM TREATMENT ON CELL MIGRATION

Time-lapse movies of MDCK cells upon PAM treatment also suggested that PAM treatment may have affected random migration of cells within MDCK islands. To test this quantitatively, single cells within the MDCK islands were tracked in the control and PAM time-lapse sequences using MtrackJ (ImageJ software) and the average speed of single cells was measured. Supplementary Movies (Movie 3 and 4) of tracked cells are prepared and available. **Error! Reference source not found.**A shows the average speed of single cells in PAM and control samples. This result indicates that the speed of PAM treated cells is lower than that of the control, which indicates PAM treatment decreases average cell migration speed. Results of an independent t-test indicates that speed of single cells in PAM treated sample (mean = 16.78 µm/h, SD= 3.27 µm/h) is statistically significantly lower than the control (mean = 23.23 µm/h, SD= 3.43 µm/h), t(37) = 5.994, p < 0.001. **Error! Reference source not found.**B and C show the trace of a cell migration in a control and PAM treated sample, respectively. These visually indicate that a single cell in the control sample trailed a wider area and the cell migration is more pronounced compared to the traced cell in PAM sample.

Cell-cell and cell-matrix adhesion are essentials in the architecture of epithelial cells. Molecular complexes control both types of adhesion and interact with the extracellular environment and regulate cell cytoskeleton organization [106]. Cell-cell and cell-matrix adhesion play an important role in cell migration and tissue integrity and a disruption in the function of these two can affect cell migration. Immunofluorescence experiments were then performed to determine if any adverse effects on the actin and adhesion apparatus of MDCK cells underlies the decreased migration speed. Comparing immunostaining images in both PAM and control samples in

A-D reveals that both beta-catenin and paxillin (markers of cell-cell and cell-substrate adhesion, respectively) were expressed and distributed similarly. Likewise, the overall filamentous actin organization in the control and PAM treated samples did not differ significantly as can be seen in immunofluorescence images from marked filamentous actin in

E-F. According to the immunofluorescent result, PAM treatment does not damage or interrupt cell-cell and cell-substrate adhesions neither actin structures in MDCK cells. Since these morphological properties were not affected adversely by PAM treatment they may not be associated with the decreased cell migration.
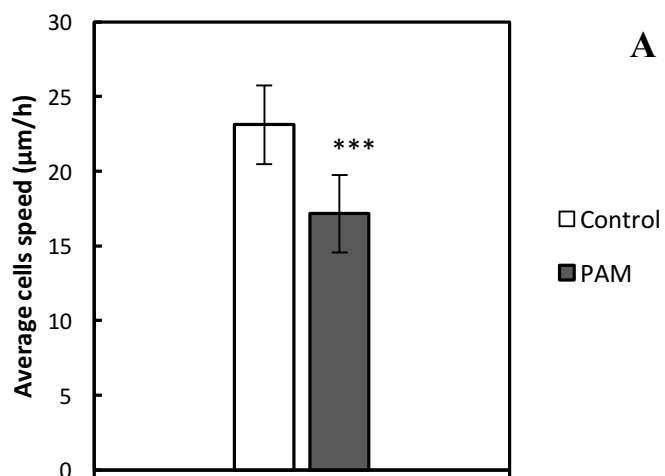
Figure 33. A) The average speed of single cells tracked in the time-lapse movies of PAM and control MDCK samples. Data represent an average in μm/h from 8 tracked cells of two independent experiments: means ± SD. *** $p<0.001$ (independent t-test). Trace of a cell migration during time-lapse imaging is labeled by red color in B) control sample and C) PAM treated sample.

Figure 33. (Continued).
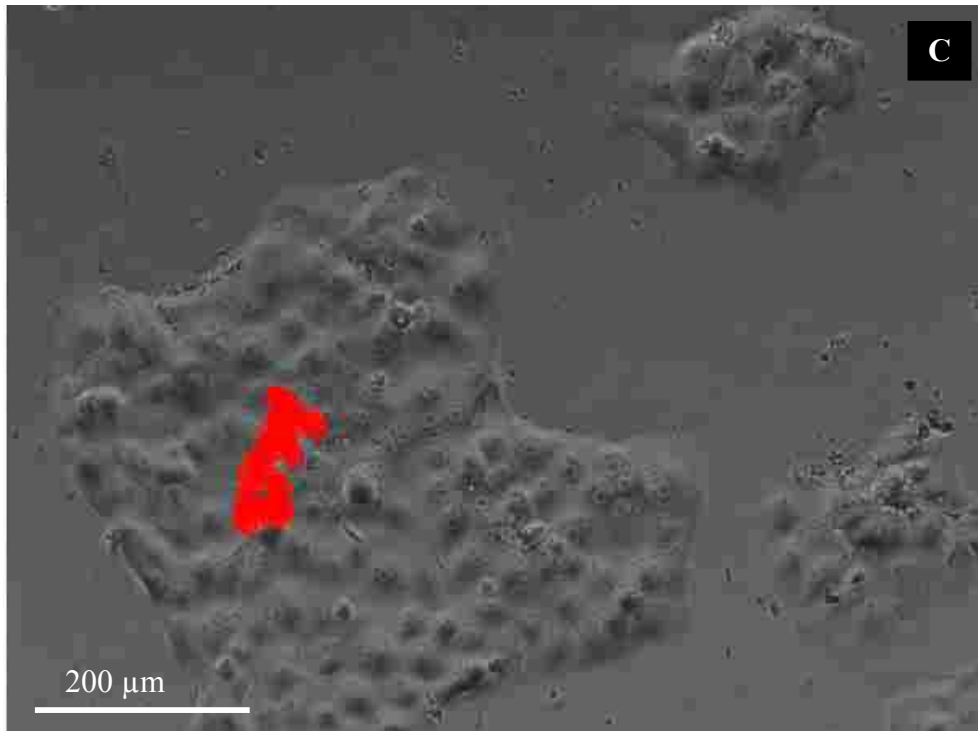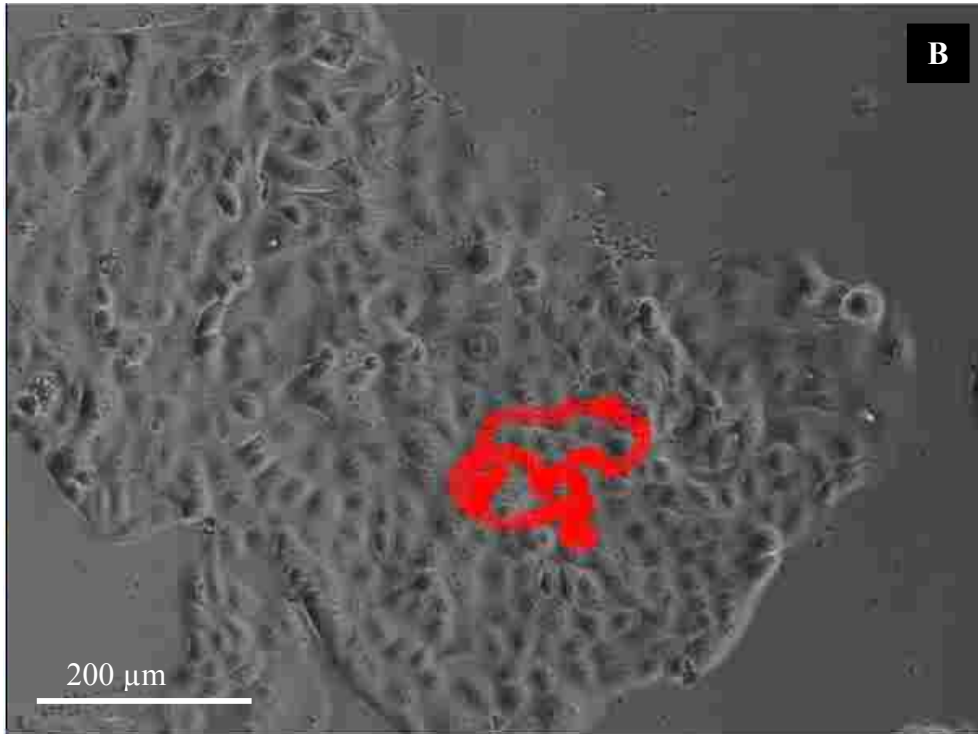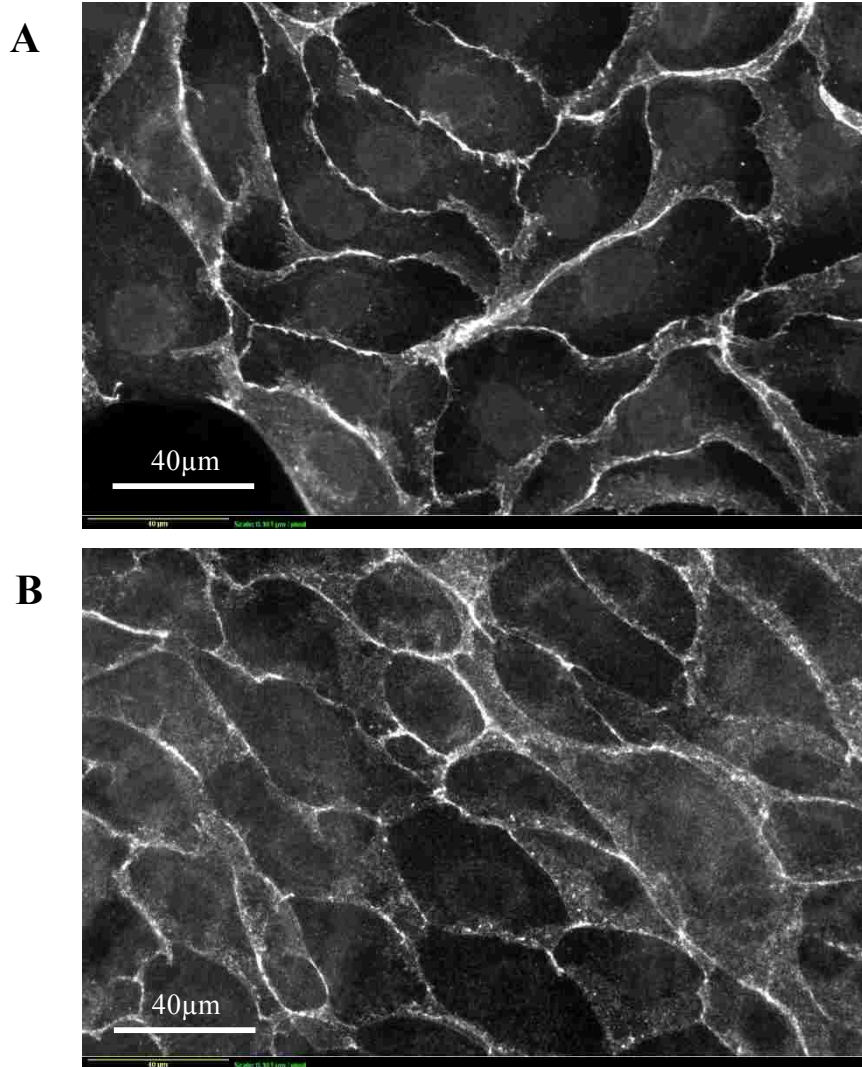
Figure 34. Morphological characterization of MDCK cells: A) and B): immunofluorescence staining with anti-Beta-catenin to mark cell-cell adhesion of control and PAM treated samples, respectively. The expressions of bright lines in cell-cell borders are similar in both control and PAM treated samples indicating that moderate PAM treatment does not interrupt cell-cell adhesion in MDCK cells. C) and D): Immunofluorescence staining with anti-paxillin to mark cell-surface adhesion in control and PAM treated samples, respectively. PAM treatment does not reduce cell-surface adhesion since anti-paxillin markers are expressed and distributed similarly in both control and PAM treated samples. E) and F): Phalloidin-488 was used to mark filamentous actin in control and PAM treated samples, respectively. PAM treatment does not interrupt actin filaments as the marked actin filaments in PAM treated sample are distributed and localized similar to control sample and there is no evidence of under-expression or disruption.

Figure 34. (Continued).

C
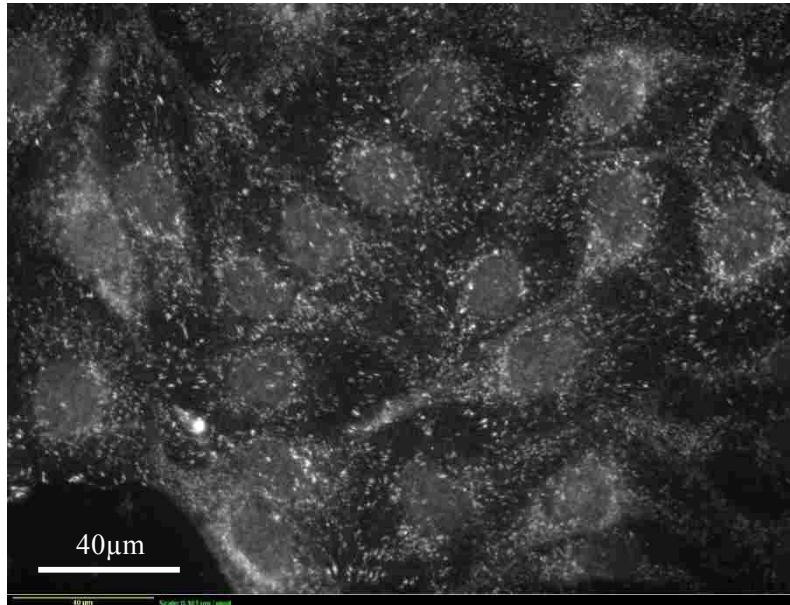
D
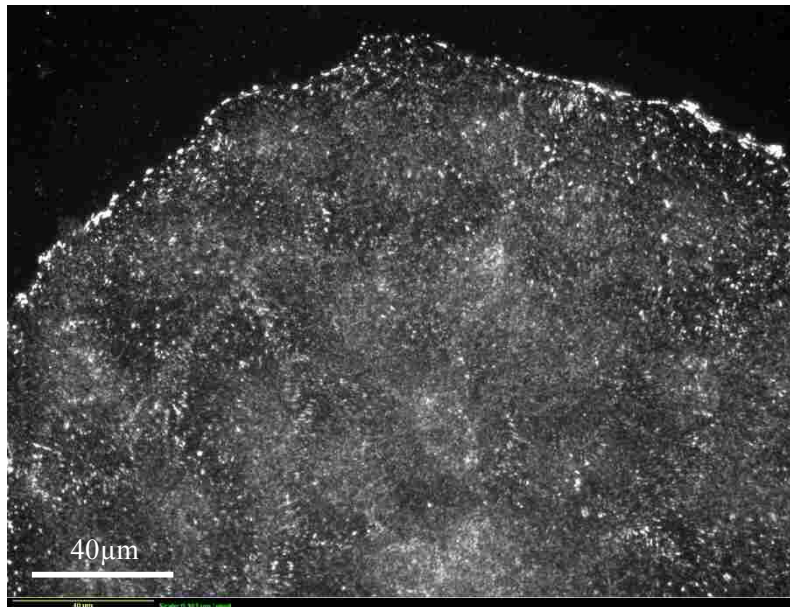
Figure 34. (Continued).

E

40μm

F

40μm
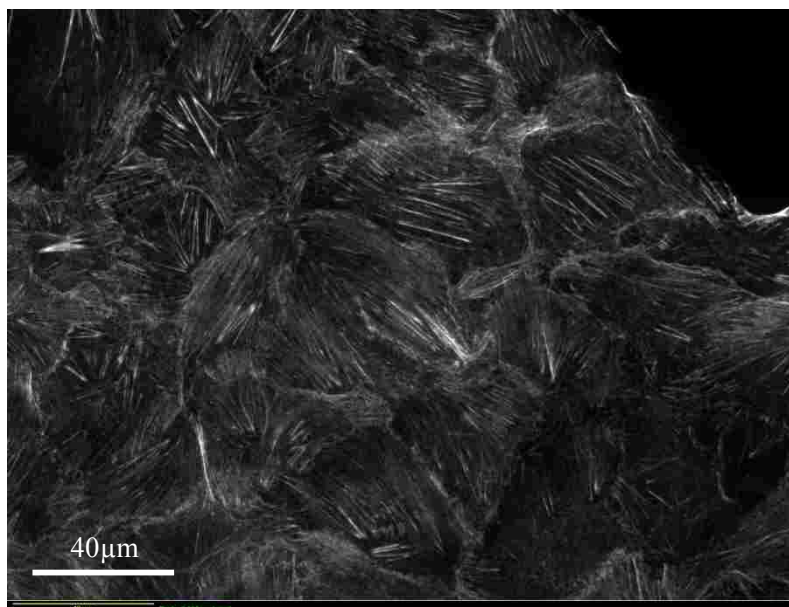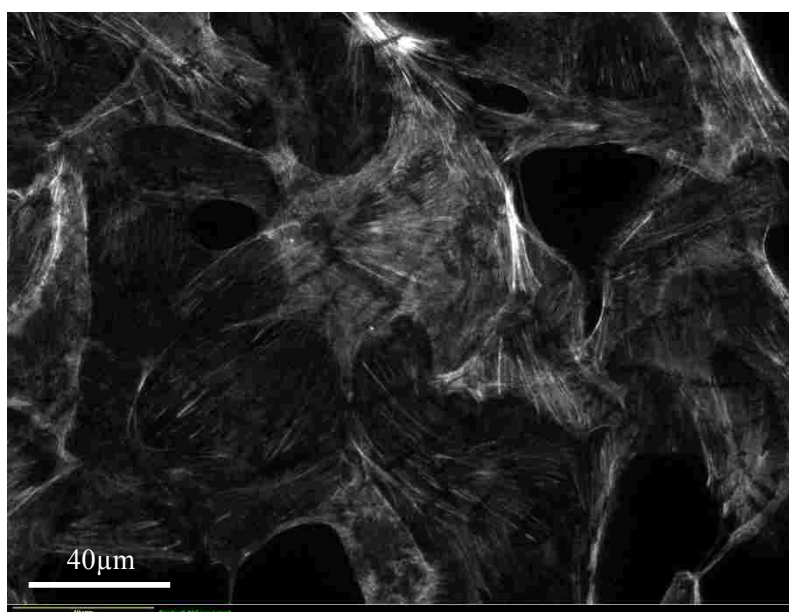
IV.5   SUMMARY

In this chapter, effects of PAM treatment on epithelial non-cancerous MDCK cells were investigated and results of experiments were represented and discussed. PAM treatment affected cell viability of normal cells in a dose-dependent manner. The result of the MTS assay indicated that MDCK cells are relatively vigorous against PAM treatment. A similar dose of PAM (4 min) which induced a widespread cell death in SCaBER cells led to only a minor reduction in MDCK cells viability. In fact, a 10 minute plasma exposure time is required to observe a similar killing phenomenon in normal cells. It was shown that lower dose of plasma exposure (3 min and lower) did not affect viability of cell significantly while, moderate dose of PAM (4 and 6 min) led to a reduction in cell viability. Two-day time-lapse microscopy was run to monitor effects of moderate PAM treatment on MDCK cells. The results showed that cells did not multiply like control cells when they were treated with moderate intensity PAM. The number of cell division events counted in time-lapse movies showed a lower number in PAM treated samples. Moreover, immunostaining of MDCK cells showed a lower number of Ki-67 marked cells in PAM treated cells compared to control cells. All these results were in agreement and indicated that PAM treatment can impact cell growth in MDCK samples by inhibiting proliferation in cells. In addition, it was observed that PAM decreased average cell migration speed. Despite cell proliferation and migration inhibitions in MDCK cells after the PAM treatment, no significant changes were observed in their morphological characteristics including cell adhesions and actin filaments organization.

CHAPTER V

CONCLUSION

V.1   SUMMARY AND OUTLOOKS

In this dissertation, effects of low temperature plasma (LTP) treatment on cancerous epithelial SCaBER cells and normal epithelial Canine Kidney (MDCK) cells were investigated. Epithelial cells are adherent ones that cover flat surfaces and fill most of the cavities of many organs of the body. Epithelial cells are different in size and shape but all are tightly packed together with almost no intercellular spaces. In this research, epithelial cells were grown *in vitro* overnight to provide sufficient time for active adherence of cells to the bottom of the plate. In treatment procedures, cells were exposed to the plasma pencil at different plasma exposure time.

The direct treatment of SCaBER cells suppressed viability of cells in a dose-dependent manner by manifesting less live cells and higher dead cells at post-treatment times. Moreover, it was proved that helium gas flow alone does not affect cells viability. In this method, cells adhered to the button of cell culture plate were covered with cell culture media during plasma exposure. The higher the exposure time of plasma, the lower the number of cells that survived. A widespread cell death was observed at 3 min and higher plasma exposure time. The viability assessment immediately after direct LTP treatment showed that cells were alive which indicates there was no sudden physical damage to the treated cells. Basically, the interaction between plasma reactive species and cells requires a sufficient time to show an effect.

Although, the most feasible ways to transport the reactive species from a gas phase plasma to a target sample is via direct exposure it was shown that using plasma activated media (PAM) can also be effective in killing cancer cells. Treating a liquid by LTP results in the activation of the treated liquid by generating or dissolving reactive species in it. Indeed, PAM allows for storage of long-lived reactive species for a specific time and for later application. This procedure provides an indirect treatment of a sample. The complete cell culture media used in growing SCaBER or MDCK cells were used to make PAM. In this research, a standard protocol was used consistently to make PAM in which, 1 ml of the cell culture media in a 24-well plate were exposed to the plasma pencil for a designated time. In this application, PAM was used either immediately after preparation or after a storage time. This is referred to as aged-PAM in this dissertation.

Results indicated that immediate PAM application inhibits cell viability in SCaBER cells in an exposure time-dependent manner when PAM covered cells for a sufficient time of 24 or 48 h. Similar to the direct treatment, increasing the plasma exposure time resulted in lower viable cells at post-PAM application times. Both methods revealed the capability of plasma-based treatment in inducing cell death in cancerous SCaBER cells.

On the other hand, the anti-cancer properties of PAM reduced over time and its efficiency in killing SCaBER cells was decreased by aging. In fact, reactive species in a liquid environment have a specific lifetime and degradation rate and they can vary depending on parameters like pH, temperature, and chemical compositions of the treated media. The result of using aged-PAM in treating SCaBER cells indicated that the killing effect of PAM was reduced over time. In particular, 2 min PAM efficiency decreases by around 10, 50, and 80 percent when it was aged for 1, 8, and 12 h, respectively. However, it was observed that the trend of the reduction in the efficiency of aged-PAM was not quite similar for 2, 3, and 4 min PAM. In PAM created by longer plasma exposure times, such as 4 min, aging did not impact its efficacy and cytotoxicity as it was as effective as immediate application whereas, 2 min PAM gradually lost its anti-cancer properties. This indicates that degradations of RONS in 4 min PAM within the 12 h of aging could not decline their concentration to a tolerable level for SCaBER cells and 4 min PAM was still very toxic to cells. As a result, the anti-cancer properties of PAM treatment seems to be dependent on the duration of plasma exposure or aging time which are linked to the concentration and stability of reactive species in PAM.

Reactive species including oxygen, nitrogen, and free radical species are known to have important impacts in biological systems. A positive impact would be intracellular signaling in the regulation of metabolic pathways and a negative impact would for example be the detrimental roles in the operation of the immune system. Several investigations have reported that RONS are crucially involved in the anti-cancer properties of plasma-based treatment. Particularly, hydrogen peroxide is known to be very effective ROS by being able to penetrate the cell membrane. It is one of the most long-lived species and can be an intermediary in many reactions that produce more ROS. Therefore, its concentration and stability measurements in PAM and aged-PAM illuminated its role in the achieved results. Using Amplex-red as a molecular probe revealed that application of the plasma pencil leads to the creation of a relatively high amount of hydrogen peroxide in PAM. The concentration of hydrogen peroxide increased with plasma exposure time. As a result, it is the

concentration of LTP-generated ROS and RNS in PAM which causes the exposure-time dependent effect of plasma and determines its anti-cancer properties.

As expected, aging of PAM resulted in degradation and reduction of hydrogen peroxide concentration. Interestingly, the trend of reduction in hydrogen peroxide concentration was similar to aged-PAM efficiency in killing SCaBER cells. Cell culture media are very complex to study. Therefore, determining the reactions and the concentrations of RONS induced by plasma exposure is not a trivial matter. Stability of reactive species is highly dependent on the chemical composition of media and presence of scavengers. For instance, hydrogen peroxide is reduced into hydroxyl radical and hydroperoxyl radical in the presence of ferrous ions. The serum added in a cell culture media contains metallic compounds including ferrous ions. Deletion of serum from PAM resulted in higher level of hydrogen peroxide. It was shown that the lack of serum in media leads to an increase of the level of hydrogen peroxide by 50% for 8 h aged-PAM. This result proves the scavenging role of serum in PAM and more than that, specifies the importance of the chemical composition of media in modulating the concentrations of ROS and determining the stability of PAM.

Gas plasma is a cocktail of free radical, ions, electrons and reactive species which interacts with media during the plasma exposure time. First, species that are created in the gas-phase in plasma at some distance far away from the media can travel and diffuse into the media, which results in the activation of the exposed media. Second, at the point where plasma contacts the surface of the media, species in the gas phase can be dissolved into the liquid and lead to the activation of media. Finally, UV radiation from the plasma can cause photolysis of the media mainly resulting in the creation of radical species. All these mechanisms may lead to the formation of ROS and RNS in media and creation of PAM [107]. Once gas species including electrons, ions, and radicals either diffuse into or are formed in the media. A series of reactions within the media may occur and in turn, leads to the creation of more reactive species. Some of the reactions like solvation of electrons are short-lived while some other products in a liquid have relatively longer lifetimes.

The transport rates of various species from the gas phase into liquid are determined by Henry's Law. According to Henry's Law, at a constant temperature, the number of gas species that dissolves in a liquid is proportional to the partial pressure of that gas in the vapor phase. Table 2**Error! Reference source not found.** shows Henry's Law Constants for water as the solvent. A larger Henry's constant (it is dimensionless) means there is a higher possibility that the gas species

dissolve in a liquid. For instance, H_2O_2 (Henry's law constant: 1.92×10^6) in water will dissolve faster than OH (6.92×10^2) and OH faster than O_3 (3×10^{-1}).

Table 2. Henry's Dimensionless Law Constant [108].

Species	Henry's law constant
OH	6.92×10^2
H_2O_2	1.92×10^6
O_3	3×10^{-1}
NO	4.4×10^{-2}
NO_2	2.8×10^{-1}
NO_3	4.15×10^1
N_2O_3	6×10^2
N_2O_4	3.69×10^1
N_2O_5	4.85×10^1
HNO_2	1.15×10^3
HNO_3	4.8×10^6
HOONO	4.8×10^{6}[a]

[a] Approximated by analogy to HNO_3.

Therefore, formation of a species such as hydrogen peroxide from hydroxyl radical recombination

$$2\,^\bullet OH \rightarrow H_2O_2 \tag{5}$$

can occur in three different regions: hydrogen peroxide is created in the gas bulk and is transported to liquid

$$2\,^\bullet OH_{(g)} + M \rightarrow H_2O_{2(g)} + M \tag{6}$$

or it is created in liquid

$$2\,^\bullet OH_{(aq)} \rightarrow H_2O_{2(aq)} \tag{7}$$

or it is created at the interface of gas − liquid and the interfacial reaction leads to incorporation of the hydrogen peroxide into liquid.

$$2\,^\bullet OH_{(in)} \rightarrow H_2O_{2(in)}. \tag{8}$$

Therefore, one of the questions to be answered is the mechanism of penetration/generation of hydrogen peroxide in PAM.

In addition to its effect on a cancer cell line, the effect of PAM on normal epithelial cells was analyzed. Despite the lethal impact of PAM on SCaBER cells, no significant reduction in the viability of normal MDCK cells was observed. The metabolic activity of MDCK cells was not meaningfully impacted by 3 min or less PAM. On the other hand, 4 min PAM which resulted in a log reduction (90%) in viability of SCaBER cells only reduced viability of MDCK cells by 10%. These results clearly indicate that normal MDCK cells are much more robust against PAM treatment and seem to be able to tolerate a higher level of oxidative stress. To induce a widespread cell death in normal cells a longer plasma exposure time was required (10 min). The difference in the response of cancer and normal cells to PAM treatment refers to their intracellular resources of antioxidants and their dissimilar metabolic activities. It is known that cancer cells, due to their high metabolic activities, contain a higher level intercellular ROS and a lower amount of antioxidants. Therefore, cancer cells can be more vulnerable to an externally enhanced oxidative stress. An overload of oxidative stress induces severe cellular damage leading to redox state alteration, defense and repair systems destruction. Consequently, MDCK cells are able to overcome the oxidative stress induced by PAM treatment while SCaBER cells undergo an irreversible damage. If cells become unable to restore the oxidative balance, a number of pathological processes are evoked which are known as apoptotic models including lipid peroxidation, the loss of intracellular calcium homeostasis, and change in metabolic pathways. On the other hand, an extreme concentration of external oxidative stress causes necrosis rather than apoptosis [109]. As discussed in the introduction chapter, some researchers reported that they observed a higher dose of plasma exposure led to necrotic cell death in different cell types while apoptosis occurred at a lower dose of plasma exposure. Executioner caspase-3 measurement in SCaBER cells treated by 2 min PAM did not show an increase in the level of cleaved caspase-3. In addition, the use of caspase-3 inhibitor (DEVD-fmk) did not block cell death. These results indicated that the mechanism of cell death in SCaBER induced by PAM treatment was caspase-independent. Therefore, the cell injury can be through necrosis pathway or a caspase-independent apoptosis pathway.

Besides the research on epithelial cells, a molecular beacon was used to evaluate harmful effects of plasma exposure on DNA. The logic of this experiment is that if plasma exposure causes any rapture in the stem of the treated DNAoligo, an immediate separation of the fluorophore–quencher

pairs leads to spontaneous fluorescent illumination. Hence, the measured fluorescence intensity correlates to the amount of damaged DNA units. This result indicated that LTP treatment induces breaks in DNA structure in an exposure time-dependent manner: a higher dose of plasma treatment leads to damage in more MB units.

To achieve a better understanding of the PAM interaction with normal cells time-lapse imaging and immunofluorescent assays were used to evaluate cell morphology and proliferation. MDCK cells cultured in a 24-well plate were treated with a moderate level of PAM (5 min) and a sequence of images taken every 10 min was recorded using time-lapse microscopy. Results demonstrated that cells in the control sample multiplied during the 48 h of imaging and cell islands were expanded while the number of cells in the PAM treated sample did not increase in population likewise. Monitoring of PAM treated and control MDCK cells suggests that it is likely that PAM application inhibits proliferation in normal cells rather than killing or harming cell morphology. To clarify what phenomenon (proliferation inhibition or cell death) was dominant in the diminished cell population, the numbers of dividing cells were manually counted in each movie. The result showed the number of dividing events (cell division) decreased by around 75% in PAM treated samples. This indicates that cell proliferation was significantly reduced in PAM treated cells and confirmed the visual observation of time-lapse imaging. Consequently, mitigation in the cell growth was associated with cell proliferation inhibition rather than widespread cell death.

Active phases of a cell cycle are G_1 (growth and metabolism phase), S (DNA replication phase), G_2 (growth of structural elements and preparation for mitosis), and M (mitosis or cell division) and G_0 is the resting phase. Ki-67 is a protein that is present in all active phase but it is absent in the G_0 phase. Marking of this protein is a method to identify cell proliferation activity in PAM treated cells compared to control. The result of immunostaining showed that the number of marked cells with Ki-67 is higher in control than PAM sample. In fact, the percentage of stained cells in the control sample was 1.7 times higher than that for the PAM treated cells and it supports the lower rate of cell proliferation in PAM samples as observed using time-lapse imaging and the lower rate of cell division.

In addition, it was observed that PAM decreased average cell migration speed. Single cells within the MDCK islands were tracked in the control and PAM time-lapse sequences and the average speed of single cells was measured. This result indicated that the speed of PAM treated cells is about 25% lower than that of the control.

A reduction in cell-cell and cell-substrate adhesion can affect cell migration and tissue integrity. For this reason, immunofluorescence assays were performed to determine if PAM treatment induces any adverse effects on the cell-cell adhesion, cell-substrate adhesion, and actin filament structures of MDCK cells. Despite cell proliferation and migration inhibitions in MDCK cells, no significant changes were observed in their morphological characteristics after the PAM treatment. Beta-catenin is a protein from the complex family of cadherin which regulates and coordinates cell–cell adhesion. Paxillin is a protein that is expressed in focal adhesions of non-striated cells and its role is to regulate cell-substrate adhesion. Actin is a group of proteins which are polymerized to form actin filaments in the cytoskeleton of eukaryotic cells. An immunostaining assay was used to mark and visualize these proteins to evaluate whether their expressions are reduced or disrupted after PAM treatment. Immunostaining images in both PAM and control samples revealed that both beta-catenin and paxillin were expressed and distributed similarly which means PAM treatment did not impact the cell adhesion apparatus. Likewise, the overall filamentous actin organization in the control and PAM treated samples did not differ significantly. Therefore, PAM treatment does not damage or impact morphological properties of MDCK cells and these may not be associated with the decreased cell migration.

V.2 RECOMMENDATION FOR FUTURE WORK

The results indicated that PAM is capable of inducing cell death in urinary bladder carcinoma cells while the same dose of PAM does not significantly impact viability and morphology of normal canine kidney epithelial cells. These preliminary achievements are very important and encouraging to continue the research on the anti-cancer effects of PAM. Other cell lines or primary cell types can be studied to advance this research. Each cell type has different resources and characteristics. Therefore, they will respond differently to PAM treatment and the exact same results may not necessarily be observed. Hence, extensive research on various types of cancer cell lines will help to gain a better understanding how practically PAM treatment can be effective in cancer therapy. The concentration and stability of H_2O_2 was measured in PAM. The results indicated the important role hydrogen peroxide plays in killing SCaBER cells by showing that there is a correlation between H_2O_2 concentration and PAM effectiveness. Identifying and measuring concentrations of other reactive oxygen and nitrogen species which have important biological impacts is the next step. There are several designated assays to measure the level of reactive species in the liquid

phase, quantitatively. It is suggested to identify and measure the concentration of other important reactive species such as ozone, superoxide onion, peroxynitrite, and nitric oxide in PAM. This research will help determine what species and reactions are essential for PAM effectiveness. Moreover, knowing the relation between ROS level and cytotoxic effects of PAM can be used to modify PAM in order to reach a desired result.

An increment in the level of caspase-3 activity was not observed in SCaBER cells treated by 2 min PAM and it was concluded that cell death was caspase-independent. Work can be conducted to identify the mechanism of SCaBER cell injury to understand if it is through a necrosis pathway or through a caspase-independent apoptosis such as mitochondrial-mediated or lysosomal membrane permeabilization.

Finally, it is suggested that the level of intracellular ROS should be studied. An analysis of the temporal evolution in extracellular ROS (hydrogen peroxide) in PAM was performed but changes in the level of intracellular ROS was still unknown. There are reagents that can be used to detect and quantify concentrations of RONS in permeabilized or live cells by fluorescein instruments such as microscopes and fluorescent microplate readers. Evaluating level of intracellular ROS and locations where they are expressed more is a complex process but very important in order to gain a deeper understanding of the interaction of cells with oxidative stress in PAM.

REFERENCES

[1]   D. B. Graves, "The emerging role of reactive oxygen and nitrogen species in redox biology and some implications for plasma applications to medicine and biology," *Journal of Physics D-Applied Physics.* **2012**, 45**,** 263001.

[2]   X. Yan, Z. Xiong, F. Zou, S. Zhao, X. Lu, G. Yang, G. He, K. Ostrikov, "Plasma-induced death of HepG2 cancer cells: Intracellular effects of reactive species," *Plasma Processes and Polymers.* **2012**, 9**,** 59.

[3]   X. Lu, G. V. Naidis, M. Laroussi, S. Reuter, D. B. Graves, K. Ostrikov, "Reactive species in non-equilibrium atmospheric-pressure plasmas: Generation, transport, and biological effects," *Physics Reports.* **2016**, 630**,** 1.

[4]   M. Laroussi, "Low-temperature plasmas for medicine?," *IEEE Transactions on Plasma Science.* **2009**, 37**,** 714.

[5]   T. Von Woedtke, S. Reuter, K. Masur, K. D. Weltmann, "Plasmas for medicine," *Physics Reports.* **2013**, 530**,** 291.

[6]   M. Keidar, A. Shashurin, O. Volotskova, M. Ann Stepp, P. Srinivasan, A. Sandler, B. Trink, "Cold atmospheric plasma in cancer therapya)," *Physics of Plasmas.* **2013**, 20**,** 057101.

[7]   M. Laroussi, "Sterilization of contaminated matter with an atmospheric pressure plasma," *IEEE Transactions on Plasma Science.* **1996**, 24**,** 1188.

[8]   G. Isbary, T. Shimizu, Y. F. Li, W. Stolz, H. M. Thomas, G. E. Morfill, J. L. Zimmermann, "Cold atmospheric plasma devices for medical issues," *Expert Review of Medical Devices.* **2013**, 10**,** 367.

[9]   G. Fridman, M. Peddinghaus, M. Balasubramanian, H. Ayan, A. Fridman, A. Gutsol, A. Brooks, "Blood coagulation and living tissue sterilization by floating-electrode dielectric barrier discharge in air," *Plasma Chemistry and Plasma Processing.* **2006**, 26**,** 425.

[10]   D. Dobrynin, G. Friedman, A. Fridman, A. Starikovskiy, "Inactivation of bacteria using DC corona discharge: Role of ions and humidity," *New journal of physics.* **2011**, 13**,** 103033.

[11]   S. Kalghatgi, G. Fridman, M. Cooper, G. Nagaraj, M. Peddinghaus, M. Balasubramanian, V. N. Vasilets, A. F. Gutsol, A. Fridman, G. Friedman, "Mechanism of blood coagulation by non-thermal atmospheric pressure dielectric barrier discharge," *IEEE Transactions on Plasma Science.* **2007**, 35, 1559.

[12]   M. Laroussi, T. Akan, "Arc-free atmospheric pressure cold plasma jets: A review," *Plasma Processes and Polymers.* **2007**, 4**,** 777.

[13]   X. Lu, M. Laroussi, V. Puech, "On atmospheric-pressure non-equilibrium plasma jets and plasma bullets," *Plasma Sources Science and Technology.* **2012**, 21**,** 034005.

[14]   T. Nosenko, T. Shimizu, G. E. Morfill, "Designing plasmas for chronic wound disinfection," *New Journal of Physics.* **2009**, 11**,** 115013.

[15]   G. Isbary, J. Heinlin, T. Shimizu, J. L. Zimmermann, G. Morfill, H. U. Schmidt, R. Monetti, B. Steffes, W. Bunk, Y. Li, T. Klaempfl, S. Karrer, M. Landthaler, W. Stolz, "Successful and safe use of 2 min cold atmospheric argon plasma in chronic wounds: results of a randomized controlled trial," *The British Journal of Dermatology.* **2012**, 167**,** 404.

[16]   S. A. Ermolaeva, A. F. Varfolomeev, M. Y. Chernukha, D. S. Yurov, M. M. Vasiliev, A. A. Kaminskaya, M. M. Moisenovich, J. M. Romanova, A. N. Murashev, Selezneva, II, T. Shimizu, E. V. Sysolyatina, I. A. Shaginyan, O. F. Petrov, E. I. Mayevsky, V. E. Fortov, G. E. Morfill, B. S. Naroditsky, A. L. Gintsburg, "Bactericidal effects of non-thermal argon plasma in vitro, in biofilms and in the animal model of infected wounds," *Journal of Medical Microbiology.* **2011**, 60**,** 75.

[17]   M. Laroussi, C. Tendero, X. Lu, S. Alla, W. L. Hynes, "Inactivation of bacteria by the plasma pencil," *Plasma Processes and Polymers.* **2006**, 3**,** 470.

[18] M. Laroussi, "Low-temperature plasma jet for biomedical applications: A review," *IEEE Transactions on Plasma Science.* **2015**, 43**,** 703.

[19] A. D. Morris, G. B. McCombs, T. Akan, W. Hynes, M. Laroussi, S. L. Tolle, "Cold plasma technology: Bactericidal effects on Geobacillus stearothermophilus and Bacillus cereus microorganisms," *Journal of Dental Hygiene.* **2009**, 83**,** 55.

[20] N. Barekzi, M. Laroussi, "Effects of low temperature plasmas on cancer cells," *Plasma Processes and Polymers.* **2013**, 10**,** 1039.

[21] E. Karakas, A. Munyanyi, L. Greene, M. Laroussi, "Destruction of α-synuclein based amyloid fibrils by a low temperature plasma jet," *Applied Physics Letters.* **2010**, 97**,** 143702.

[22] G. Daeschlein, S. Scholz, R. Ahmed, T. von Woedtke, H. Haase, M. Niggemeier, E. Kindel, R. Brandenburg, K. D. Weltmann, M. Juenger, "Skin decontamination by low-temperature atmospheric pressure plasma jet and dielectric barrier discharge plasma," *The Journal of Hospital Infection.* **2012**, 81**,** 177.

[23] T. Maisch, T. Shimizu, A. Mitra, J. Heinlin, S. Karrer, Y. F. Li, G. Morfill, J. L. Zimmermann, "Contact-free cold atmospheric plasma treatment of Deinococcus radiodurans," *Journal of Industrial Microbiology & Biotechnology.* **2012**, 39**,** 1367.

[24] N. Navabsafa, H. Ghomi, M. Nikkhah, S. Mohades, H. Dabiri, S. Ghasemi, "Effect of BCD plasma on a bacteria cell membrane," *Plasma Science and Technology.* **2013**, 15**,** 685.

[25] Y. F. Li, T. Shimizu, J. L. Zimmermann, G. E. Morfill, "Cold atmospheric plasma for surface disinfection," *Plasma Processes and Polymers.* **2012**, 9**,** 585.

[26] E. A. Ratovitski, X. Cheng, D. Yan, J. H. Sherman, J. Canady, B. Trink, M. Keidar, "Anti-cancer therapies of 21st century: Novel approach to treat human cancers using cold atmospheric plasma," *Plasma Processes and Polymers.* **2014**, 11**,** 1128.

[27] I. E. Kieft, J. L. V. Broers, V. Caubet-Hilloutou, D. W. Slaaf, F. C. S. Ramaekers, E. Stoffels, "Electric discharge plasmas influence attachment of cultured CHO K1 cells," *Bioelectromagnetics.* **2004**, 25**,** 362.

[28] I. E. Kieft, D. Darios, A. J. M. Roks, E. Stoffels, "Plasma treatment of mammalian vascular cells: A quantitative description," *IEEE Transactions on Plasma Science.* **2005**, 33**,** 771.

[29] E. Stoffels, I. E. Kieft, R. E. J. Sladek, L. J. M. v. d. Bedem, E. P. v. d. Laan, M. Steinbuch, "Plasma needle for in vivo medical treatment: Recent developments and perspectives," *Plasma Sources Science and Technology.* **2006**, 15**,** S169.

[30] E. Stoffels, A. J. M. Roks, L. E. Deelmm, "Delayed effects of cold atmospheric plasma on vascular cells," *Plasma Processes and Polymers.* **2008**, 5**,** 599.

[31] A. Shashurin, M. Keidar, S. Bronnikov, R. A. Jurjus, M. A. Stepp, "Living tissue under treatment of cold plasma atmospheric jet," *Applied Physics Letters.* **2008**, 93**,** 181501.

[32] S. Yonson, S. Coulombe, V. Léveillé, R. L. Leask, "Cell treatment and surface functionalization using a miniature atmospheric pressure glow discharge plasma torch," *Journal of Physics D: Applied Physics.* **2006**, 39**,** 3508.

[33] M. Ishaq, S. Kumar, H. Varinli, Z. J. Han, A. E. Rider, M. D. M. Evans, A. B. Murphy, K. Ostrikov, "Atmospheric gas plasma–induced ROS production activates TNF-ASK1 pathway for the induction of melanoma cancer cell apoptosis," *Molecular Biology of the Cell.* **2014**, 25**,** 1523.

[34] G. Fridman, A. Shereshevsky, M. M. Jost, A. D. Brooks, A. Fridman, A. Gutsol, V. Vasilets, G. Friedman, "Floating electrode dielectric barrier discharge plasma in air promoting apoptotic behavior in melanoma skin cancer cell lines," *Plasma Chemistry and Plasma Processing.* **2007**, 27**,** 163.

[35] S. Kalghatgi, C. M. Kelly, E. Cerchar, B. Torabi, O. Alekseev, A. Fridman, G. Friedman, J. Azizkhan-Clifford, "Effects of non-thermal plasma on mammalian cells," *Plos One.* **2011**, 6**,** e16270.

[36] S. J. Kim, T. H. Chung, S. H. Bae, S. H. Leem, "Induction of apoptosis in human breast cancer cells by a pulsed atmospheric pressure plasma jet," *Applied Physics Letters.* **2010**, 97**,** 023702

[37] M. Wang, B. Holmes, X. Cheng, W. Zhu, M. Keidar, L. G. Zhang, "Cold atmospheric plasma for selectively ablating metastatic breast cancer cells," *Plos One.* **2013**, 8**,** e73741.

[38] S. Mirpour, H. Ghomi, S. Piroozmand, M. Nikkhah, S. H. Tavassoli, S. Z. Azad, "The selective characterization of nonthermal atmospheric pressure plasma jet on treatment of human breast cancer and normal cells," *IEEE Transactions on Plasma Science.* **2014**, 42**,** 315.

[39] C.-H. Kim, J. H. Bahn, S.-H. Lee, G.-Y. Kim, S.-I. Jun, K. Lee, S. J. Baek, "Induction of cell growth arrest by atmospheric non-thermal plasma in colorectal cancer cells," *Journal of Biotechnology.* **2010**, 150**,** 530.

[40] C.-H. Kim, S. Kwon, J. H. Bahn, K. Lee, S. I. Jun, P. D. Rack, S. J. Baek, "Effects of atmospheric nonthermal plasma on invasion of colorectal cancer cells," *Applied Physics Letters.* **2010**, 96**,** 243701.

[41] N. Georgescu, A. R. Lupu, "Tumoral and normal cells treatment with high-voltage pulsed cold atmospheric plasma jets," *IEEE Transactions on Plasma Science.* **2010**, 38**,** 1949.

[42] X. Zhang, M. Li, R. Zhou, K. Feng, S. Yang, "Ablation of liver cancer cells in vitro by a plasma needle," *Applied Physics Letters.* **2008**, 93**,** 021502.

[43] N. Barekzi, M. Laroussi, "Dose-dependent killing of leukemia cells by low-temperature plasma," *Journal of Physics D: Applied Physics.* **2012**, 45**,** 422002.

[44] M. Vandamme, E. Robert, S. Lerondel, V. Sarron, D. Ries, S. Dozias, J. Sobilo, D. Gosset, C. Kieda, B. Legrain, J. M. Pouvesle, A. L. Pape, "ROS implication in a new antitumor strategy based on non-thermal plasma," *International Journal of Cancer.* **2012**, 130**,** 2185.

[45] N. K. Kaushik, H. Uhm, E. Ha Choi, "Micronucleus formation induced by dielectric barrier discharge plasma exposure in brain cancer cells," *Applied Physics Letters.* **2012**, 100**,** 084102.

[46] N. Barekzi, M. Laroussi, G. Konesky, S. Roman, "Effects of low temperature plasma on prostate cancer cells using the Bovie Medical J-Plasma® device," *Plasma Processes and Polymers.* **2016***,* 13, 1189.

[47] J. Schlegel, J. Köritzer, V. Boxhammer, "Plasma in cancer treatment," *Clinical Plasma Medicine.* **2013**, 1**,** 2.

[48] M. Thiyagarajan, L. Waldbeser, A. Whitmill, "THP-1 leukemia cancer treatment using a portable plasma device," *Studies in Health Technology and Informatics.* **2012**, 173**,** 515.

[49] S. Elmore, "Apoptosis: A review of programmed cell death," *Toxicologic Pathology.* **2007**, 35**,** 495.

[50] M. Keidar, R. Walk, A. Shashurin, P. Srinivasan, A. Sandler, S. Dasgupta, R. Ravi, R. Guerrero-Preston, B. Trink, "Cold plasma selectivity and the possibility of a paradigm shift in cancer therapy," *British Journal of Cancer.* **2011**, 105**,** 1295.

[51] M. Vandamme, E. Robert, S. Dozias, J. Sobilo, S. Lerondel, A. Le Pape, J. M. Pouvesle, "Response of human Glioma U87 xenografted on mice to non thermal plasma treatment," *Plasma Medicine.* **2011**, 1**,** 27.

[52] M. Vandamme, E. Robert, S. Pesnel, E. Barbosa, S. Dozias, J. Sobilo, S. Lerondel, A. Le Pape, J. M. Pouvesle, "Antitumor effect of plasma treatment on U87 Glioma xenografts: Preliminary results," *Plasma Processes and Polymers.* **2010**, 7**,** 264.

[53] L. Brullé, M. Vandamme, D. Riès, E. Martel, E. Robert, S. Lerondel, V. Trichet, S. Richard, J. M. Pouvesle, A. Le Pape, "Effects of a non thermal plasma treatment alone or in combination with gemcitabine in a MIA PaCa2-luc orthotopic pancreatic carcinoma model," *PLoS ONE.* **2012**, 7**,** e52653.

[54] L. Partecke, K. Evert, J. Haugk, F. Doering, L. Normann, S. Diedrich, F. U. Weiss, M. Evert, N. Huebner, C. Guenther, C. Heidecke, A. Kramer, R. Bussiahn, K.-D. Weltmann, O. Pati, C. Bender, W. von Bernstorff, "Tissue tolerable Plasma (TTP) induces apoptosis in pancreatic cancer cells in vitro and in vivo," *BMC Cancer.* **2012**, 12**,** 473.

[55] R. M. Walk, J. A. Snyder, P. Srinivasan, J. Kirsch, S. O. Diaz, F. C. Blanco, A. Shashurin, M. Keidar, A. D. Sandler, "Cold atmospheric plasma for the ablative treatment of neuroblastoma," *Journal of Pediatric Surgery.* **2013**, 48**,** 67.

[56] S. F. AbdulSalam, F. S. Thowfeik, E. J. Merino, "Excessive reactive oxygen species and exotic DNA lesions as an exploitable liability," *Biochemistry.* **2016**, 55**,** 5341.

[57] B. D'Autreaux, M. B. Toledano, "ROS as signalling molecules: mechanisms that generate specificity in ROS homeostasis," *Nature Reviews Molecular Cell Biology.* **2007**, 8**,** 813.

[58] B. E. Lehnert, R. Iyer, "Exposure to low-level chemicals and ionizing radiation: reactive oxygen species and cellular pathways," *Human & Experimental Toxicology.* **2002**, 21**,** 65.

[59] J. Nordberg, E. S. Arner, "Reactive oxygen species, antioxidants, and the mammalian thioredoxin system," *Free Radicical Biology and Medice.* **2001**, 31**,** 1287.

[60] D. Hanahan, R. A. Weinberg, "The hallmarks of cancer," *Cell.* **2000**, 100**,** 57.

[61] A. Sudhakar, "History of cancer, ancient and modern treatment methods," *Journal of Cancer Science & Therapy.* **2009**, 1**,** 1.

[62] J. M. Brown, A. J. Giaccia, "The unique physiology of solid tumors: Opportunities (and problems) for cancer therapy," *Cancer Research.* **1998**, 58**,** 1408.

[63] M. Kuroki, N. Shirasu, "Novel treatment strategies for cancer and their tumor-targeting approaches using antibodies against tumor-associated antigens," *Anticancer Research.* **2014**, 34**,** 4481.

[64] E. R. Spelten, J. H. A. M. Verbeek, A. L. J. Uitterhoeve, A. C. Ansink, J. van der Lelie, T. M. de Reijke, M. Kammeijer, J. C. J. M. de Haes, M. A. G. Sprangers, "Cancer, fatigue and the return of patients to work—A prospective cohort study," *European Journal of Cancer.* **2003**, 39**,** 1562.

[65] J. Jarrige, M. Laroussi, E. Karakas, "Formation and dynamics of plasma bullets in a non-thermal plasma jet: influence of the high-voltage parameters on the plume characteristics," *Plasma Sources Science and Technology.* **2010**, 19, 065005.

[66] E. Karakas, *Characterizations of atmospheric pressure low temperature plasma jets and their applications*, Old Dominion University, **2011**.

[67] X. Lu, M. Laroussi, "Dynamics of an atmospheric pressure plasma plume generated by submicrosecond voltage pulses," *Journal of Applied Physics.* **2006**, 100**,** 063302.

[68] N. Mericam-Bourdet, M. Laroussi, A. Begum, E. Karakas, "Experimental investigations of plasma bullets," *Journal of Physics D: Applied Physics.* **2009**, 42**,** 055207.

[69] E. Karakas, M. Laroussi, "Experimental studies on the plasma bullet propagation and its inhibition," *Journal of Applied Physics.* **2010**, 108**,** 063305.

[70] E. Karakas, M. A. Akman, M. Laroussi, "The evolution of atmospheric-pressure low-temperature plasma jets: jet current measurements," *Plasma Sources Science and Technology.* **2012**, 21**,** 034016.

[71] A. T. C. Collection, *ATCC animal cell culture guide: Tips and techniques for continuous cell lines*, American Type Culture Collection, **2012**.

[72] N. Kaushik, N. Uddin, G. B. Sim, Y. J. Hong, K. Y. Baik, C. H. Kim, S. J. Lee, N. K. Kaushik, E. H. Choi, "Responses of solid tumor cells in DMEM to reactive oxygen species generated by non-thermal plasma and chemically induced ROS systems," *Scientific Report.* **2015**, 5**,** 8587.

[73] F. A. Villamena, *Chemistry of reactive species*, John Wiley & Sons, Inc., Hoboken, NJ, USA **2013**.

[74] P. D. Ray, B. W. Huang, Y. Tsuji, "Reactive oxygen species (ROS) homeostasis and redox regulation in cellular signaling," *Cellular Signalling.* **2012**, 24**,** 981.

[75] C. Auclair, E. Cramer, J. Hakim, P. Boivin, "Studies on the mechanism of NADPH oxidation by the granule fraction isolated from human resting polymorphonuclear blood cells," *Biochimie.* **1976**, 58**,** 1359.

[76] M. Schieber, N. S. Chandel, "ROS function in redox signaling and oxidative stress," *Current Biology: CB.* **2014**, 24**,** R453.

[77] L. Pauling, "The discovery of the superoxide radical," *Trends in Biochemical Sciences.* **1979**, 4**,** N270.

[78] S. F. AbdulSalam, F. S. Thowfeik, E. J. Merino, "Excessive reactive oxygen species and exotic DNA lesions as an exploitable liability," *Biochemistry.* **2016***,* 10.1021/acs.biochem.6b00703

[79] P. Held, "An introduction to reactive oxygen species: Measurement of ROS in cells," *Application Guide*, B. I. Inc., ed., BioTek Instruments Inc., 2012.

[80] T. P. Devasagayam, J. P. Kamat, "Biological significance of singlet oxygen," *Indian Journal of Experimental Biology.* **2002**, 40**,** 680.

[81] D. B. Graves, "Low temperature plasma biomedicine: A tutorial review," *Physics of Plasmas.* **2014**, 21**,** 080901.

[82] L. Adams, M. C. Franco, A. G. Estevez, "Reactive nitrogen species in cellular signaling," *Experimental Biology and Medicine.* **2015**, 240**,** 711.

[83] E. H. Sarsour, M. G. Kumar, L. Chaudhuri, A. L. Kalen, P. C. Goswami, "Redox control of the cell cycle in health and disease," *Antioxidants & Redox Signaling.* **2009**, 11**,** 2985.

[84] C. M. Munoz, L. A. van Meeteren, J. A. Post, A. J. Verkleij, C. T. Verrips, J. Boonstra, "Hydrogen peroxide inhibits cell cycle progression by inhibition of the spreading of mitotic CHO cells," *Free Radical Biology and Medicine.* **2002**, 33**,** 1061.

[85]   D. R. McIlwain, T. Berger, T. W. Mak, "Caspase functions in cell death and disease," *Cold Spring Harbor Perspectives in Biology.* **2013**, 5**,** a008656.

[86]   S. Kumar, *Apoptosis: Biology and mechanisms*, Springer Science & Business Media, **2013**.

[87]   G. Mor, A. Alvero, *Apoptosis and cancer: Methods and protocols*, Humana Press, **2007**.

[88]   S. Mohades, N. Barekzi, H. Razavi, V. Maruthamuthu, M. Laroussi, "Temporal evaluation of the anti-tumor efficiency of plasma-activated media," *Plasma Processes and Polymers.* **2016**, 13**,** 1206.

[89]   S. Mohades, M. Laroussi, J. Sears, N. Barekzi, H. Razavi, "Evaluation of the effects of a plasma activated medium on cancer cells," *Physics of Plasmas.* **2015**, 22**,** 122001.

[90]   J. P. Kehrer, "The Haber–Weiss reaction and mechanisms of toxicity," *Toxicology.* **2000**, 149**,** 43.

[91]   R. C. Smart, E. Hodgson, *Molecular and biochemical toxicology*, Wiley, **2013**.

[92]   T. Sundquist, R. Moravec, A. Niles, M. O'Brien, T. Riss, " Timing your apoptosis assays " *Cell Notes*, 16, Promega Corporation, **2006**, pp. 18.

[93]   P. Ekert, J. Silke, D. Vaux, "Caspase inhibitors," *Cell Death and Differentiation.* **1999**, 6**,** 1081.

[94]   S. Mohades, N. Barekzi, M. Laroussi, "Efficacy of low temperature plasma against SCaBER cancer cells," *Plasma Processes and Polymers.* **2014**, 11**,** 1150.

[95]   Y. Ma, C. S. Ha, S. W. Hwang, H. J. Lee, G. C. Kim, K. W. Lee, K. Song, "Non-thermal atmospheric pressure plasma preferentially induces apoptosis in p53-mutated cancer cells by activating ROS stress-response pathways," *Plos One.* **2014**, 9**,** e91947.

[96]   R. Guerrero-Preston, T. Ogawa, M. Uemura, G. Shumulinsky, B. L. Valle, F. Pirini, R. Ravi, D. Sidransky, M. Keidar, B. Trink, "Cold atmospheric plasma treatment selectively targets head and neck squamous cell carcinoma cells," *International Journal of Molecular Medicine.* **2014**, 34**,** 941.

[97] S. Iseki, K. Nakamura, M. Hayashi, H. Tanaka, H. Kondo, H. Kajiyama, H. Kano, F. Kikkawa, M. Hori, "Selective killing of ovarian cancer cells through induction of apoptosis by nonequilibrium atmospheric pressure plasma," *Applied Physics Letters.* **2012**, 100**,** 113702.

[98] S. J. Kim, T. H. Chung, "Cold atmospheric plasma jet-generated RONS and their selective effects on normal and carcinoma cells," *Scientific Reports.* **2016**, 6**,** 20332.

[99] C. Zhang, L. M. Walker, P. R. Mayeux, "Role of nitric oxide in lipopolysaccharide-induced oxidant stress in the rat kidney," *Biochem Pharmacol.* **2000**, 59**,** 203.

[100] T. Finkel, "Redox-dependent signal transduction," *FEBS Letters.* **2000**, 476**,** 52.

[101] R. A. Cairns, I. S. Harris, T. W. Mak, "Regulation of cancer cell metabolism," *Nature Reviews Cancer.* **2011**, 11**,** 85.

[102] D. Trachootham, J. Alexandre, P. Huang, "Targeting cancer cells by ROS-mediated mechanisms: a radical therapeutic approach?," *Nature Reviews Drug Discovery.* **2009**, 8**,** 579.

[103] L. P. Cramer, T. J. Mitchison, "Investigation of the mechanism of retraction of the cell margin and rearward flow of nodules during mitotic cell rounding," *Molecular Biology of the Cell.* **1997**, 8**,** 109.

[104] J. Gerdes, H. Lemke, H. Baisch, H. H. Wacker, U. Schwab, H. Stein, "Cell cycle analysis of a cell proliferation-associated human nuclear antigen defined by the monoclonal antibody Ki-67," *Journal of Immunology (Baltimore, MD. 1950).* **1984**, 133**,** 1710.

[105] T. Scholzen, J. Gerdes, "The Ki-67 protein: From the known and the unknown," *Journal of Cellular Physiology.* **2000**, 182**,** 311.

[106] M. Burute, M. Thery, "Spatial segregation between cell-cell and cell-matrix adhesions," *Current Opinion in Cell Biology.* **2012**, 24**,** 628.

[107] P. J. Bruggeman, M. J. Kushner, B. R. Locke, J. G. E. Gardeniers, W. G. Graham, D. B. Graves, R. C. H. M. Hofman-Caris, D. Maric, J. P. Reid, E. Ceriani, D. F. Rivas, J. E. Foster, S. C. Garrick, Y. Gorbanev, S. Hamaguchi, F. Iza, H. Jablonowski, E. Klimova, J. Kolb, F. Krcma, P. Lukes, Z. Machala, I. Marinov, D. Mariotti, S. M. Thagard, D. Minakata, E. C. Neyts, J. Pawlat, Z. L. Petrovic, R. Pflieger, S. Reuter, D. C. Schram, S. Schröter, M. Shiraiwa, B. Tarabová, P. A. Tsai, J. R. R. Verlet, T. v. Woedtke, K. R. Wilson, K. Yasui, G. Zvereva, "Plasma–liquid interactions: A review and roadmap," *Plasma Sources Science and Technology.* **2016**, 25**,** 053002.

[108] R. Sander, "Compilation of Henry's Law Constants (version 4.0) for water as solvent," *Atmospheric Chemistry and Physics.* **2015**, 15**,** 4399.

[109] V. Nikoletopoulou, M. Markaki, K. Palikaras, N. Tavernarakis, "Crosstalk between apoptosis, necrosis and autophagy," *Biochimica et Biophysica Acta (BBA) - Molecular Cell Research.* **2013**, 1833**,** 3448.

APPENDIX A

EFFECT OF PLASMA ON DNAOLIGO

LTP-generated RONS can either directly penetrate into cells through their membranes or react with cell membrane and the by-products of the membrane peroxidation reaction diffuse into the cells. Either of these mechanisms leads to the reaction of RONS with intracellular macromolecules, interruption in cell signaling pathways, and finally cell organelles damage such as compromising the integrity of the DNA structure [1-3]. DNA damages are in the form of single-strand breaks (SSBs) and double-strand breaks (DSBs) [2, 4, 5]. To investigate the DNA damage induced by the plasma pencil, a molecular beacon (MB) was used. Molecular beacons are single strand DNA oligonucleotide which adopts a stem-and-loop shape. The 5′ end of the stem is connected to a fluorophore moiety and the 3′ end is connected to a quenching moiety. The stem of MB keeps the two moieties close together; however, a rapture in the stem results in an immediate separation of the fluorophore–quencher pairs and leads to spontaneous fluorescent illumination [6]. The intensity of illumination is correspondent to the extent of DNA cleavage. Figure shows a schematic of a molecular beacon and the mechanism of fluorescent illumination.
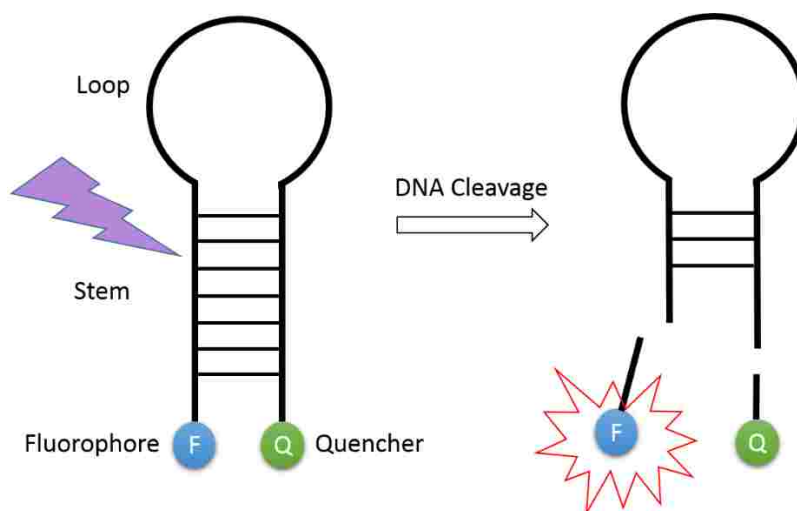

Figure 35. The schematic diagram of the molecular beacon: the blue ball represents a fluorophore (FAM) and the green ball represents a quencher (BHQ-1). Any cleavage in the stem results in the separation of the pair and emission of fluorescent signals [6].

The MB DNA probe was purchased from Eurofins Genomics Company (Virginia, USA) in HPLC (High Performance Liquid Chromatography) purification with the following structure:

[6-FAM]-5′<u>GCACTGAAGC</u>GCCGCACGCCATGTCGAC<u>GCGCTTCAGTGC</u>–3′-[BHQ1].

FAM and BHQ-1 are the fluorescent dye and the quencher, respectively. The underlined letters indicate the stem sequences. In this experiment, a 100 nM MB solution was prepared in 0.1 M sodium phosphate buffer (NaH$_2$PO$_4$), pH 7.4 (Molecular Toxicology, Inc.). The MB solution was heated up to ~87 °C for 3 min in a heat block. Then, MB solution was stored in the dark to provide a gradual temperature reduction in 3 h. This cooling process results in correct stem-loop formation. Next, 400 µl of MB solution was added in an eppendorf tube and was exposed to the plasma pencil for 15 s, 30 s, 1, 2, 3, 4, and 5 min. The distance from the tip of the nozzle to the surface of the liquid was 26 ± 1 mm. Plasma operating conditions were the same as mentioned in Section II.1.1. A control sample was treated with the helium gas without plasma ignition for 5 min. 100 µl of the control and LTP-treated samples were transferred to each well of a black opaque 96-well plate and the fluorescence intensity was measured using a fluorescence microplate reader (BMG Labtech FLUOstar) with the excitation and emission wavelengths of 495 and 520 nm, respectively.

Figure indicates fluorescence intensity collected from control and MB solutions treated directly by plasma pencil. As this figure shows, the fluorescence intensity increases by increasing the LTP exposure time. This result indicates that LTP treatment induces breaks in DNA structure and a higher dose of plasma treatment leads to damage in more MB units. However, this method does not provide further information about the type of damage as single-strand or double-strand breaks. Nor does it determine the number of breaks in a single MB unit. In fact, one break in the DNA stem of the MB is enough to emit fluorescence and more than one break in one MB unit cannot enhance the intensity of emission.

Kurita *et al.* [1] reported that atmospheric pressure plasma jet induced DNA damage in molecular beacon and the fluorescent emission intensity was proportional to the plasma exposure time and the power of plasma source. Among the different types of DNA damage, double-strand breaks (DSBs) are the most dangerous. Since both strands of the DNA double helix are simultaneously broken in this case, the repair process is more difficult. Also, there is a higher possibility of inappropriate rejoining which causes genome instability. Without proper DNA repair, such damages can result in permanent cell cycle arrest or apoptotic cell death [7]. Double-strand breaks can be repaired via pathways including homologous recombination (HR) and non-homologous end

joining (NHEJ) [8]. Research on inducing double-strand DNA breaks due to LTP treatment showed that air plasma is more efficient in causing DSBs that N_2 plasma and atomic oxygen plays the major role among other RONS [5].

Both nucleobases and deoxyribose sugar of DNA are susceptible to be attacked by ROS/RNS. In fact, $O_2^{\bullet-}$ and H_2O_2 are not able to directly induce DNA strand breaks or modify nucleobase under physiological conditions. It has been reported that H_2O_2 treatment of eukaryotic cells resulted in DNA strand breakage, but the damage was negated in the presence of $^{\bullet}OH$ scavengers. Therefore, it is likely that $^{\bullet}OH$ is involved in DNA strand breakage and $O_2^{\bullet-}$ and H_2O_2 *in vivo* will convert into $^{\bullet}OH$ radicals via the Fenton reaction [4].
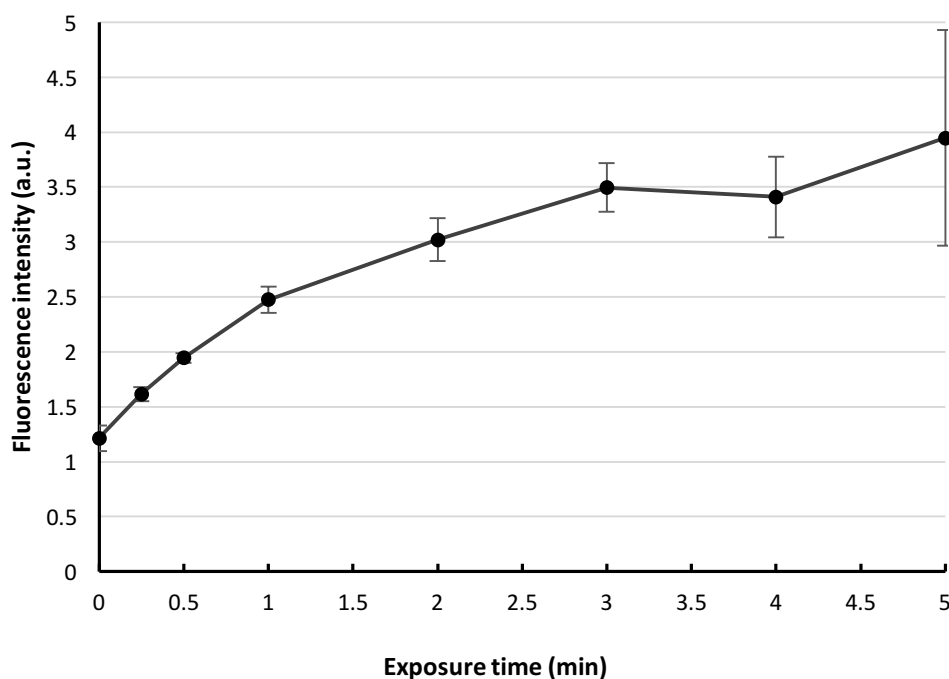
Figure 36. Breaks in molecular beacon was analyzed by measuring the fluorescence intensity as a function of exposure time. Data represent the mean ± SD of two independent experiments.

REFERENCES

[1]   H. Kurita, S. Miyachika, H. Yasuda, K. Takashima, A. Mizuno, "Use of molecular beacons for the rapid analysis of DNA damage induced by exposure to an atmospheric pressure plasma jet," *Applied Physics Letters.* **2015**, 107**,** 263702.

[2]   K. Kim, J. D. Choi, Y. C. Hong, G. Kim, E. J. Noh, J. S. Lee, S. S. Yang, "Atmospheric-pressure plasma-jet from micronozzle array and its biological effects on living cells for cancer therapy," *Applied Physics Letters.* **2011**, 98**,** 073701.

[3]   G. J. Kim, W. Kim, K. T. Kim, J. K. Lee, "DNA damage and mitochondria dysfunction in cell apoptosis induced by nonthermal air plasma," *Applied Physics Letters.* **2010**, 96**,** 021502.

[4]   K. Arjunan, V. Sharma, S. Ptasinska, "Effects of atmospheric pressure plasmas on isolated and cellular DNA—A review," *International Journal of Molecular Sciences.* **2015**, 16**,** 2971.

[5]   Y. Lee, K. Kim, K. T. Kang, J. S. Lee, S. S. Yang, W. H. Chung, "Atmospheric-pressure plasma jet induces DNA double-strand breaks that require a Rad51-mediated homologous recombination for repair in Saccharomyces cerevisiae," *Archives of Biochemistry and Biophysics.* **2014**, 560**,** 1.

[6]   J. B. Biggins, J. R. Prudent, D. J. Marshall, J. S. Thorson, "A continuous assay for DNA cleavage using molecular break lights," *Methods in Molecular Biology (Clifton, N.J.).* **2006**, 335**,** 83.

[7]   D. Branzei, M. Foiani, "Regulation of DNA repair throughout the cell cycle," *Nature Reviews Molecular Cell Biology.* **2008**, 9**,** 297.

[8]   E. Sonoda, H. Hochegger, A. Saberi, Y. Taniguchi, S. Takeda, "Differential usage of non-homologous end-joining and homologous recombination in double strand break repair," *DNA Repair.* **2006**, 5**,** 1021.

APPENDIX B

PERMISSIONS FROM THE COPYRIGHT HOLDER

**NATURE PUBLISHING GROUP LICENSE
TERMS AND CONDITIONS**

Mar 29, 2017

This Agreement between Soheila Mohades ("You") and Nature Publishing Group ("Nature Publishing Group") consists of your license details and the terms and conditions provided by Nature Publishing Group and Copyright Clearance Center.

License Number	3917120129151
License date	Jul 27, 2016
Licensed Content Publisher	Nature Publishing Group
Licensed Content Publication	Nature Reviews Drug Discovery
Licensed Content Title	Targeting cancer cells by ROS-mediated mechanisms: a radical therapeutic approach?
Licensed Content Author	Dunyaporn Trachootham, Jerome Alexandre and Peng Huang
Licensed Content Date	May 29, 2009
Licensed Content Volume	8
Licensed Content Issue	7
Type of Use	reuse in a dissertation / thesis
Requestor type	academic/educational
Format	print and electronic
Portion	figures/tables/illustrations
Number of figures/tables/illustrations	1
High-res required	no
Figures	This sketch illustrates the basic idea behind the use of redox chemotherapeutics. ROS levels in both normal and cancer cells are controlled by a balance between pro- and antioxidants, but both rates are higher in cancer cells, leading to higher baseline ROS concentration in cancer cells.
Author of this NPG article	no
Your reference number	
Title of your thesis / dissertation	Low temperature plasma for the treatment of epithelial cancer cells
Expected completion date	Dec 2016
Estimated size (number of pages)	100
Requestor Location	Soheila Mohades 231 KAUFMAN HALL, NORFOLK, VA 23529

NORFOLK, VA 23529
United States
Attn: Soheila Mohades

**NATURE PUBLISHING GROUP LICENSE
TERMS AND CONDITIONS**

Mar 29, 2017

This Agreement between Soheila Mohades ("You") and Nature Publishing Group ("Nature Publishing Group") consists of your license details and the terms and conditions provided by Nature Publishing Group and Copyright Clearance Center.

License Number	3912070361334
License date	Jul 18, 2016
Licensed Content Publisher	Nature Publishing Group
Licensed Content Publication	Nature Reviews Cancer
Licensed Content Title	Regulation of cancer cell metabolism
Licensed Content Author	Rob A. Cairns, Isaac S. Harris and Tak W. Mak
Licensed Content Date	Feb 1, 2011
Licensed Content Volume	11
Licensed Content Issue	2
Type of Use	reuse in a dissertation / thesis
Requestor type	academic/educational
Format	print and electronic
Portion	figures/tables/illustrations
Number of figures/tables/illustrations	1
High-res required	no
Figures	Figure 6 | relationship between the levels of rOS and cancer
Author of this NPG article	no
Your reference number	
Title of your thesis / dissertation	Low temperature plasma for the treatment of epithelial cancer cells
Expected completion date	Dec 2016
Estimated size (number of pages)	100
Requestor Location	Soheila Mohades 231 KAUFMAN HALL, NORFOLK, VA 23529 NORFOLK, VA 23529 United States Attn: Soheila Mohades
Billing Type	Invoice
Billing Address	Soheila Mohades 231 KAUFMAN HALL, NORFOLK, VA 23529

NORFOLK, VA 23529
United States
Attn: Soheila Mohades

Total   0.00 USD

Terms and Conditions

Terms and Conditions for Permissions

Nature Publishing Group hereby grants you a non-exclusive license to reproduce this material for this purpose, and for no other use,subject to the conditions below:

1. NPG warrants that it has, to the best of its knowledge, the rights to license reuse of this material. However, you should ensure that the material you are requesting is original to Nature Publishing Group and does not carry the copyright of another entity (as credited in the published version). If the credit line on any part of the material you have requested indicates that it was reprinted or adapted by NPG with permission from another source, then you should also seek permission from that source to reuse the material.

2. Permission granted free of charge for material in print is also usually granted for any electronic version of that work, provided that the material is incidental to the work as a whole and that the electronic version is essentially equivalent to, or substitutes for, the print version.Where print permission has been granted for a fee, separate permission must be obtained for any additional, electronic re-use (unless, as in the case of a full paper, this has already been accounted for during your initial request in the calculation of a print run).NB: In all cases, web-based use of full-text articles must be authorized separately through the 'Use on a Web Site' option when requesting permission.

3. Permission granted for a first edition does not apply to second and subsequent editions and for editions in other languages (except for signatories to the STM Permissions Guidelines, or where the first edition permission was granted for free).

4. Nature Publishing Group's permission must be acknowledged next to the figure, table or abstract in print. In electronic form, this acknowledgement must be visible at the same time as the figure/table/abstract, and must be hyperlinked to the journal's homepage.

5. The credit line should read:
   Reprinted by permission from Macmillan Publishers Ltd: [JOURNAL NAME] (reference citation), copyright (year of publication)
   For AOP papers, the credit line should read:
   Reprinted by permission from Macmillan Publishers Ltd: [JOURNAL NAME], advance online publication, day month year (doi: 10.1038/sj.[JOURNAL ACRONYM].XXXXX)

   Note: For republication from the *British Journal of Cancer,* the following credit lines apply.
   Reprinted by permission from Macmillan Publishers Ltd on behalf of Cancer Research UK: [JOURNAL NAME] (reference citation), copyright (year of publication)For AOP papers, the credit line should read:
   Reprinted by permission from Macmillan Publishers Ltd on behalf of Cancer Research UK: [JOURNAL NAME], advance online publication, day month year (doi: 10.1038/sj.[JOURNAL ACRONYM].XXXXX)

6. Adaptations of single figures do not require NPG approval. However, the adaptation should be credited as follows:

   Adapted by permission from Macmillan Publishers Ltd: [JOURNAL NAME] (reference citation), copyright (year of publication)

   Note: For adaptation from the *British Journal of Cancer,* the following credit line applies.
   Adapted by permission from Macmillan Publishers Ltd on behalf of Cancer Research UK:

[JOURNAL NAME] (reference citation), copyright (year of publication)

7. Translations of 401 words up to a whole article require NPG approval. Please visit http://www.macmillanmedicalcommunications.com for more information.Translations of up to a 400 words do not require NPG approval. The translation should be credited as follows:

    Translated by permission from Macmillan Publishers Ltd: [JOURNAL NAME] (reference citation), copyright (year of publication).

    Note: For translation from the _British Journal of Cancer,_ the following credit line applies.
    Translated by permission from Macmillan Publishers Ltd on behalf of Cancer Research UK: [JOURNAL NAME] (reference citation), copyright (year of publication)

We are certain that all parties will benefit from this agreement and wish you the best in the use of this material. Thank you.
Special Terms:
v1.1

Questions? customercare@copyright.com or +1-855-239-3415 (toll free in the US) or +1-978-646-2777.

JOHN WILEY AND SONS LICENSE
TERMS AND CONDITIONS

Oct 21, 2016

This Agreement between Soheila Mohades ("You") and John Wiley and Sons ("John Wiley and Sons") consists of your license details and the terms and conditions provided by John Wiley and Sons and Copyright Clearance Center.

License Number	3973770405837
License date	Oct 21, 2016
Licensed Content Publisher	John Wiley and Sons
Licensed Content Publication	Plasma Processes and Polymers
Licensed Content Title	Modeling of a Microwave Plasma Driven Biomass Pyrolitic Conversion for Energy Production
Licensed Content Author	Dmitry L. Tsyganov,Neli Bundaleska,Elena Tatarova
Licensed Content Date	Oct 17, 2016
Licensed Content Pages	1
Type of use	Dissertation/Thesis
Requestor type	University/Academic
Format	Print and electronic
Portion	Figure/table
Number of figures/tables	1
Original Wiley figure/table number(s)	Figure 1b
Will you be translating?	No
Title of your thesis / dissertation	Low temperature plasma for the treatment of epithelial cancer cells
Expected completion date	Dec 2016
Expected size (number of pages)	100
Requestor Location	Soheila Mohades 231 KAUFMAN HALL, NORFOLK, VA 23529 NORFOLK, VA 23529 United States Attn: Soheila Mohades
Publisher Tax ID	EU826007151
Billing Type	Invoice
Billing Address	Soheila Mohades 231 KAUFMAN HALL, NORFOLK, VA 23529 NORFOLK, VA 23529 United States Attn: Soheila Mohades
Total	0.00 USD

TERMS AND CONDITIONS

This copyrighted material is owned by or exclusively licensed to John Wiley & Sons, Inc. or one of its group companies (each a"Wiley Company") or handled on behalf of a society with which a Wiley Company has exclusive publishing rights in relation to a particular work (collectively "WILEY"). By clicking "accept" in connection with completing this licensing transaction, you agree that the following terms and conditions apply to this transaction (along with the billing and payment terms and conditions established by the Copyright Clearance Center Inc., ("CCC's Billing and Payment terms and conditions"), at the time that you opened your RightsLink account (these are available at any time at http://myaccount.copyright.com).

Terms and Conditions

- The materials you have requested permission to reproduce or reuse (the "Wiley Materials") are protected by copyright.

- You are hereby granted a personal, non-exclusive, non-sub licensable (on a stand-alone basis), non-transferable, worldwide, limited license to reproduce the Wiley Materials for the purpose specified in the licensing process. This license, and any CONTENT (PDF or image file) purchased as part of your order, is for a one-time use only and limited to any maximum distribution number specified in the license. The first instance of republication or reuse granted by this license must be completed within two years of the date of the grant of this license (although copies prepared before the end date may be distributed thereafter). The Wiley Materials shall not be used in any other manner or for any other purpose, beyond what is granted in the license. Permission is granted subject to an appropriate acknowledgement given to the author, title of the material/book/journal and the publisher. You shall also duplicate the copyright notice that appears in the Wiley publication in your use of the Wiley Material. Permission is also granted on the understanding that nowhere in the text is a previously published source acknowledged for all or part of this Wiley Material. Any third party content is expressly excluded from this permission.

- With respect to the Wiley Materials, all rights are reserved. Except as expressly granted by the terms of the license, no part of the Wiley Materials may be copied, modified, adapted (except for minor reformatting required by the new Publication), translated, reproduced, transferred or distributed, in any form or by any means, and no derivative works may be made based on the Wiley Materials without the prior permission of the respective copyright owner.**For STM Signatory Publishers clearing permission under the terms of the STM Permissions Guidelines only, the terms of the license are extended to include subsequent editions and for editions in other languages, provided such editions are for the work as a whole in situ and does not involve the separate exploitation of the permitted figures or extracts,** You may not alter, remove or suppress in any manner any copyright, trademark or other notices displayed by the Wiley Materials. You may not license, rent, sell, loan, lease, pledge, offer as security, transfer or assign the Wiley Materials on a stand-alone basis, or any of the rights granted to you hereunder to any other person.

- The Wiley Materials and all of the intellectual property rights therein shall at all times remain the exclusive property of John Wiley & Sons Inc, the Wiley Companies, or their respective licensors, and your interest therein is only that of having possession of and the right to reproduce the Wiley Materials pursuant to Section 2 herein during the continuance of this Agreement. You agree that you own no right, title or interest in or to the Wiley Materials or any of the intellectual property rights therein. You shall have

no rights hereunder other than the license as provided for above in Section 2. No right, license or interest to any trademark, trade name, service mark or other branding ("Marks") of WILEY or its licensors is granted hereunder, and you agree that you shall not assert any such right, license or interest with respect thereto

- NEITHER WILEY NOR ITS LICENSORS MAKES ANY WARRANTY OR REPRESENTATION OF ANY KIND TO YOU OR ANY THIRD PARTY, EXPRESS, IMPLIED OR STATUTORY, WITH RESPECT TO THE MATERIALS OR THE ACCURACY OF ANY INFORMATION CONTAINED IN THE MATERIALS, INCLUDING, WITHOUT LIMITATION, ANY IMPLIED WARRANTY OF MERCHANTABILITY, ACCURACY, SATISFACTORY QUALITY, FITNESS FOR A PARTICULAR PURPOSE, USABILITY, INTEGRATION OR NON-INFRINGEMENT AND ALL SUCH WARRANTIES ARE HEREBY EXCLUDED BY WILEY AND ITS LICENSORS AND WAIVED BY YOU.

- WILEY shall have the right to terminate this Agreement immediately upon breach of this Agreement by you.

- You shall indemnify, defend and hold harmless WILEY, its Licensors and their respective directors, officers, agents and employees, from and against any actual or threatened claims, demands, causes of action or proceedings arising from any breach of this Agreement by you.

- IN NO EVENT SHALL WILEY OR ITS LICENSORS BE LIABLE TO YOU OR ANY OTHER PARTY OR ANY OTHER PERSON OR ENTITY FOR ANY SPECIAL, CONSEQUENTIAL, INCIDENTAL, INDIRECT, EXEMPLARY OR PUNITIVE DAMAGES, HOWEVER CAUSED, ARISING OUT OF OR IN CONNECTION WITH THE DOWNLOADING, PROVISIONING, VIEWING OR USE OF THE MATERIALS REGARDLESS OF THE FORM OF ACTION, WHETHER FOR BREACH OF CONTRACT, BREACH OF WARRANTY, TORT, NEGLIGENCE, INFRINGEMENT OR OTHERWISE (INCLUDING, WITHOUT LIMITATION, DAMAGES BASED ON LOSS OF PROFITS, DATA, FILES, USE, BUSINESS OPPORTUNITY OR CLAIMS OF THIRD PARTIES), AND WHETHER OR NOT THE PARTY HAS BEEN ADVISED OF THE POSSIBILITY OF SUCH DAMAGES. THIS LIMITATION SHALL APPLY NOTWITHSTANDING ANY FAILURE OF ESSENTIAL PURPOSE OF ANY LIMITED REMEDY PROVIDED HEREIN.

- Should any provision of this Agreement be held by a court of competent jurisdiction to be illegal, invalid, or unenforceable, that provision shall be deemed amended to achieve as nearly as possible the same economic effect as the original provision, and the legality, validity and enforceability of the remaining provisions of this Agreement shall not be affected or impaired thereby.

- The failure of either party to enforce any term or condition of this Agreement shall not constitute a waiver of either party's right to enforce each and every term and condition of this Agreement. No breach under this agreement shall be deemed waived or excused by either party unless such waiver or consent is in writing signed by the party granting such waiver or consent. The waiver by or consent of a party to a breach of any provision of this Agreement shall not operate or be construed as a waiver of or consent to any other or subsequent breach by such other party.

- This Agreement may not be assigned (including by operation of law or otherwise) by you without WILEY's prior written consent.

- Any fee required for this permission shall be non-refundable after thirty (30) days from receipt by the CCC.

- These terms and conditions together with CCC's Billing and Payment terms and conditions (which are incorporated herein) form the entire agreement between you and WILEY concerning this licensing transaction and (in the absence of fraud) supersedes all prior agreements and representations of the parties, oral or written. This Agreement may not be amended except in writing signed by both parties. This Agreement shall be binding upon and inure to the benefit of the parties' successors, legal representatives, and authorized assigns.

- In the event of any conflict between your obligations established by these terms and conditions and those established by CCC's Billing and Payment terms and conditions, these terms and conditions shall prevail.

- WILEY expressly reserves all rights not specifically granted in the combination of (i) the license details provided by you and accepted in the course of this licensing transaction, (ii) these terms and conditions and (iii) CCC's Billing and Payment terms and conditions.

- This Agreement will be void if the Type of Use, Format, Circulation, or Requestor Type was misrepresented during the licensing process.

- This Agreement shall be governed by and construed in accordance with the laws of the State of New York, USA, without regards to such state's conflict of law rules. Any legal action, suit or proceeding arising out of or relating to these Terms and Conditions or the breach thereof shall be instituted in a court of competent jurisdiction in New York County in the State of New York in the United States of America and each party hereby consents and submits to the personal jurisdiction of such court, waives any objection to venue in such court and consents to service of process by registered or certified mail, return receipt requested, at the last known address of such party.

WILEY OPEN ACCESS TERMS AND CONDITIONS
Wiley Publishes Open Access Articles in fully Open Access Journals and in Subscription journals offering Online Open. Although most of the fully Open Access journals publish open access articles under the terms of the Creative Commons Attribution (CC BY) License only, the subscription journals and a few of the Open Access Journals offer a choice of Creative Commons Licenses. The license type is clearly identified on the article.
The Creative Commons Attribution License
The Creative Commons Attribution License (CC-BY) allows users to copy, distribute and transmit an article, adapt the article and make commercial use of the article. The CC-BY license permits commercial and non-
Creative Commons Attribution Non-Commercial License
The Creative Commons Attribution Non-Commercial (CC-BY-NC)License permits use, distribution and reproduction in any medium, provided the original work is properly cited and is not used for commercial purposes.(see below)

Creative Commons Attribution-Non-Commercial-NoDerivs License
The Creative Commons Attribution Non-Commercial-NoDerivs License (CC-BY-NC-ND) permits use, distribution and reproduction in any medium, provided the original work is

properly cited, is not used for commercial purposes and no modifications or adaptations are made. (see below)

Use by commercial "for-profit" organizations
Use of Wiley Open Access articles for commercial, promotional, or marketing purposes requires further explicit permission from Wiley and will be subject to a fee.
Further details can be found on Wiley Online Library
http://olabout.wiley.com/WileyCDA/Section/id-410895.html

Other Terms and Conditions:

v1.10 Last updated September 2015

Questions? customercare@copyright.com or +1-855-239-3415 (toll free in the US) or +1-978-646-2777.

Copyright Clearance Center

Note: Copyright.com supplies permissions but not the copyrighted content itself.

1	2	**3**
PAYMENT	REVIEW	**CONFIRMATION**

Step 3: Order Confirmation

Thank you for your order! A confirmation for your order will be sent to your account email address. If you have questions about your order, you can call us 24 hrs/day, M-F at +1.855.239.3415 Toll Free, or write to us at info@copyright.com. This is not an invoice.

Confirmation Number: 11639093
Order Date: 04/19/2017

If you paid by credit card, your order will be finalized and your card will be charged within 24 hours. If you choose to be invoiced, you can change or cancel your order until the invoice is generated.

Payment Information

Soheila Mohades
smoha013@odu.edu
+1 (757) 683-6707
Payment Method: n/a

Order Details

Journal of Physics D : Applied Physics

Order detail ID:	70389276	
Order License Id:	4092520717247	
ISSN:	0022-3727	
Publication Type:	Journal	
Volume:		
Issue:		
Start page:		
Publisher:	IOP Publishing	

Permission Status: ✅ Granted

Permission type: Republish or display content
Type of use: Thesis/Dissertation

Requestor type	Author of requested content
Format	Print, Electronic
Portion	image/photo
Number of images/photos requested	4
Title or numeric reference of the portion(s)	Figure 4-7
Title of the article or chapter the portion is from	N/A
Editor of portion(s)	N/A
Author of portion(s)	N/A

Volume of serial or monograph	N/A
Issue, if republishing an article from a serial	N/A
Page range of portion	5-7
Publication date of portion	April 2017
Rights for	Main product and any product related to main product
Duration of use	Life of current edition
Creation of copies for the disabled	no
With minor editing privileges	no
For distribution to	Worldwide
In the following language(s)	Original language of publication
With incidental promotional use	no
Lifetime unit quantity of new product	Up to 499
Made available in the following markets	education
The requesting person/organization	Soheila Mohades
Order reference number	
Author/Editor	Soheila Mohades
The standard identifier of New Work	N/A
Title of New Work	LOW TEMPERATURE PLASMA FOR THE TREATMENT OF EPITHELIAL CANCER CELLS
Publisher of New Work	Old Dominion University

| Expected publication date | May 2017 |
| Estimated size (pages) | 105 |

Note: This item will be invoiced or charged separately through CCC's **RightsLink** service. More info $ 0.00

This is not an invoice.

Total order items: 1   **Order Total: 0.00 USD**

VITA

Soheila Mohades was born in Karaj, Iran. She received her B.S. degree in Physics from Shahid Beheshti University, Tehran, Iran in 2008 and her M.S. degree in Plasma Engineering from the Laser and Plasma Research Institute of Shahid Beheshti University in 2012. She joined Dr. Laroussi's group in the Plasma Engineering and Medicine Institute (PEMI) at Old Dominion University as a graduate assistant in 2012. She studied biomedical applications of low temperature plasma and cancer treatment for her Ph.D. research. She has authored and co-authored 7 papers in top peer-reviewed scientific journals and presented more than 10 oral and poster presentations in scientific conferences. She has been a member of IEEE and WIE (Woman in Engineering) since 2014. Soheila Mohades received the Engineering Dean's Graduate Fellowship Award for Excellence from the Batten College of Engineering and Technology of Old Dominion University in 2015. She was a recipient of Student Travel Award to present her work at the Gaseous Electronics Conference (GEC) held in Raleigh, North Carolina in 2014. She also received the best PhD researcher award of the year from the Electrical and Computer Engineering Department of Old Dominion University in 2017.